



Markus Gschiel, BSc

# **Quantitative analysis of pitch and its influence on paper properties**

**MASTER'S THESIS**

to achieve the university degree of

Diplom-Ingenieur

Master's degree programme: Chemical and Process Engineering

submitted to

**Graz University of Technology**

Supervisors:

DI Dr. techn. Jussi Lahti

Univ.-Prof. Dipl.-Ing. Dr. techn. Ulrich Hirn

Institute of Bioproducts and Paper Technology

Graz, October 2020

# Eidesstattliche Erklärung

Ich erkläre an Eides statt, dass ich die vorliegende Arbeit selbstständig verfasst, andere als die angegebenen Quellen/Hilfsmittel nicht benutzt, und die den benutzten Quellen wörtlich und inhaltlich entnommenen Stellen als solche kenntlich gemacht habe. Das in TUGRAZonline hochgeladene Textdokument ist mit der vorliegenden Masterarbeit identisch.

.....

Datum

.....

Unterschrift

# AFFIDAVIT

I declare that I have authored this thesis independently, that I have not used other than the declared sources/resources, and that I have explicitly indicated all material which has been quoted either literally or by content from the sources used. The text document uploaded to TUGRAZonline is identical to the present master's thesis dissertation.

.....

Date

.....

Signature

Never memorize something that you  
can look up.

---

ALBERT EINSTEIN (1879-1955)

# Acknowledgement

First, I would like to thank my supervisor Univ.-Prof. Ulrich Hirn, as he made it possible for me to work on this project. I also want to thank my co-supervisor Dr. Jussi Lahti and Dr. Werner Schlemmer, who have always been at my side with advice and action. Furthermore, a big thank you to Ms. Bakhshi Adelheid and her laboratory team, who helped me with practical work. I want to thank Dr. Walzl Andrea for evaluating the GCMS results. With regard to organization and bureaucracy, I would like to thank Ms. Bäumel and Ms. Schefzik and all the other employees of the institute. I would also like to thank all members of the APV and the Gaming League for the warm welcome and the unforgettable time together.

Another thank you goes to my friends and fellow students who were always there for me. Last but not least, I would like to thank my parents for their energetic emotional and financial support.

# Kurzfassung

Diese Masterarbeit behandelt zwei verschiedene Problemstellungen.

Im ersten Teil werden die Auswirkungen von schädlichen Holz-Extrakt Komponenten (Pitch), welche bei der Papierherstellung entstehen, in Bezug auf Papierfestigkeit untersucht. Es wurde erforscht, wie sich Additive (Stärke und Aluminiumsulfat) über deren Verweilzeit, auf die Stärke Retention und Zugfestigkeit auswirken. Der Einfluss von Soja-Protein auf die Zugfestigkeit und gegen Pitch wurde ebenfalls untersucht.

Im zweiten Teil wird eine Methode zur Pitch Analyse beschrieben, welche als Alternative zur Analyse mit Gaschromatographie Massenspektrometrie verwendet werden kann. Die Trennung der Pitch-Stoffgruppen erfolgt mit einer zweidimensionalen Dünnschichtchromatografie (2D-TLC). Durch Digitalisierung der Dünnschichtchromatographie-Platte und der Verwendung einer automatisierten Bildbearbeitungssoftware (MATLAB) werden die Spots in Messwerte umgewandelt. Über vorgefertigte Kalibrationsreihen, mit der Verwendung von Modellkomponenten der jeweiligen Stoffklasse, kann auf die Massen der industriellen Pitch Komponenten zurückgerechnet werden. In Summe wurden fünf verschiedene Pitch proben untersucht und ausgewertet. Beim Vergleich der relativen Mengen der Komponenten von GCMS und 2D-TLC Methode, konnten gute Korrespondenzen erzielt werden.

Sojaprotein erwies sich als potenzielles Additiv gegen Pitch, jedoch konnten die höchsten Zugfestigkeitswerte durch die Kombination von Sojaprotein mit Stärke im Verhältnis 1: 3 erzielt werden. Es wurde eine schnelle und einfache Methode entwickelt, um Pitch zu analysieren, die sich besonders gut für Prozesssteuerungszwecke eignet. Zwei Softwarevarianten wurden entwickelt, um einerseits den Auswertungsprozess der Pitch Analyse nahezu vollständig zu automatisieren und andererseits ein möglichst breites Anwendungsspektrum bereitzustellen.

# Abstract

This master thesis deals with two different problems.

In the first part the effects of wood extractive components (pitch), which arise during paper production, are examined in relation to paper strength. It was researched how additives (starch and aluminum sulfate) and their residence time affect the starch retention and the tensile index. The influence of soy protein on tensile strength and against pitch was also studied.

In the second part a pitch analysis method is described which can be used as an alternative to gas chromatography-mass spectrometry analysis. The groups of pitch substances are separated using two-dimensional thin-layer chromatography (2D-TLC). By digitizing the thin-layer-chromatography plate and using automated image processing software (MATLAB), the spots are converted into measured values. Using prefabricated calibration series, with the use of model components of the respective substance class, the masses of the industrial pitch components can be calculated back. In total, five different pitch samples were examined and evaluated. When comparing the relative amounts of the components of GCMS and 2D-TLC methods, good correspondence was achieved.

Soy protein turned out to be a potential additive against pitch, but the highest tensile values were achieved by combining soy protein with starch in a ratio of 1: 3. A quick and easy method was developed to analyse pitch which suits particularly well for process control purposes. Two software versions were created to almost completely automate the evaluation process of the pitch analysis on the one hand and to provide the broadest possible range of applications on the other.

# Table of Contents

<b>1</b>	<b>Introduction</b>	<b>1</b>
<b>2</b>	<b>Literature Review</b>	<b>2</b>
2.1	Wood structure . . . . .	2
2.2	Wood fractionation . . . . .	3
2.2.1	Mechanical pulping . . . . .	3
2.2.2	Chemical pulping . . . . .	3
2.3	Wood components and their properties . . . . .	4
2.3.1	Cellulose . . . . .	4
2.3.2	Hemicellulose . . . . .	5
2.3.3	Lignin . . . . .	6
2.3.4	Extractive substances . . . . .	6
2.3.5	Pitch . . . . .	6
2.3.6	Carryover pitch . . . . .	8
2.3.7	Important properties of the abundant carryover pitch compounds . . . . .	9
2.3.8	Carryover Pitch influence . . . . .	10
2.4	Kraft papers . . . . .	11
2.4.1	Influence on tensile strength . . . . .	11
2.5	Papermaking Additives for Kraft paper . . . . .	15
2.5.1	Starch . . . . .	15
2.5.2	Alum (Aluminum sulfate) . . . . .	16
2.5.3	Enzymes and Soy protein . . . . .	16
2.6	Analysis of the PITCH content via gas chromatography mass spectrometry (GCMS) . . . . .	17
2.7	Thin layer chromatography (principle) . . . . .	18
2.8	Explanation of the 2D-TLC . . . . .	20
2.9	Assignment of the spots via Peak method . . . . .	21

<b>3</b>	<b>Materials and Methods</b>	<b>22</b>
3.1	Chemicals and Samples . . . . .	22
3.2	Retention and papermaking experiments . . . . .	24
3.2.1	Preparation of starch, alum and soy protein solutions . . . . .	24
3.2.2	Sulfuric acid (H <sub>2</sub> SO <sub>4</sub> ) & Sodium hydroxide (NaOH) . . . . .	25
3.2.3	Pitch preparation . . . . .	25
3.2.4	Pulp preparation . . . . .	25
3.2.5	Drainage Freeness Retention (drainage freeness retention (DFR)) measurement & starch retention (acUV-Vis) . . . . .	26
3.2.6	Handsheet production . . . . .	27
3.2.7	Physical measurement of the laboratory paper sheets . . . . .	27
3.2.8	Tensile Index experiments . . . . .	28
3.3	2D-TLC experiments . . . . .	30
3.3.1	Class representatives . . . . .	30
3.3.2	Procedure . . . . .	31
3.3.3	TLC Calibration line Precautions . . . . .	33
3.3.4	Important integrated and developed MATLAB functions . . . . .	34
<b>4</b>	<b>Results</b>	<b>36</b>
4.1	Evaluation of starch retention experiments . . . . .	36
4.2	Influence of soy protein on paper strength . . . . .	37
4.3	MATLAB Program for evaluating pitch compounds . . . . .	38
4.3.1	Obstacles . . . . .	39
4.3.2	Large-scale digitalization . . . . .	41
4.3.3	Software versions (EXACT vs. EASY) . . . . .	42
4.3.4	Defining relevant areas . . . . .	43
4.3.5	EXACT version: Masking system . . . . .	46
4.3.6	EASY version: manual spot defining . . . . .	53
4.3.7	Background-Correction & Calculation . . . . .	54
4.4	Calibration results . . . . .	57
4.4.1	Offset error . . . . .	57
4.4.2	EXACT version . . . . .	58
4.4.3	EASY version . . . . .	60
4.4.4	Comparison (EXACT vs. EASY) . . . . .	63

4.4.5	Betulin (birch pitch sample) . . . . .	63
4.5	Industrial pitch analysis . . . . .	64
4.5.1	EXACT version (only for IP1 & IP2 sample) . . . . .	65
4.5.2	EASY version . . . . .	68
4.5.3	Comparison of the results of GCMS analysis and Thin layer chromatography (TLC) method . . . . .	70
4.6	Absolute Values & Yield . . . . .	73
<b>5</b>	<b>Conclusion</b>	<b>74</b>
<b>6</b>	<b>Appendix</b>	<b>76</b>
	<b>List of Figures</b>	<b>VI</b>
	<b>List of Tables</b>	<b>VII</b>
	<b>List of Abbreviations</b>	<b>VIII</b>
	<b>Bibliography</b>	<b>IX</b>

## Introduction

Pulp products and papers are indispensable in today's world. Especially since plastics from fossil resources should be reduced. Papers and cartons are frequently used in the packaging industry. For this reason, it is of great interest to optimize process steps and methods in this industry in order to achieve the best possible result economically and environmentally. One of the challenges here, however, lies in the various substances that are released during wood pulp production as accompanying substances in wood pulp production. One substance group is wood extractives (also called pitch) which has a strong impact on paper properties. [1]

In unbleached softwood kraft pulp, the proportion of extract substances is approx. 0.1% to 1%. This proportion is enough to strongly influence important properties. In the packaging industry, strength, hydrophobicity, air permeability and surface properties of the paper play a major role. [2] In this thesis the focus lies on the tensile strength of the papers. Pulp production depends very much on the type of wood used and its origin. Therefore, the composition and the amount of pitch can change over time.

In order to be able to react specifically to harmful substances, it is important to know their type and amount. A Gas chromatography-mass spectrometry (GCMS) analysis of the pitch is accurate but expensive, time consuming and difficult. Therefore, it is important to find a simple, quick and inexpensive alternative. [3]

## Literature Review

### 2.1 Wood structure

The main components of dry wood are cellulose, hemicellulose, lignin and organic extractives. [4] The composition of wood can vary depending on factors such as the type of wood, environmental influences and origin (table 2.1). [5] Due to the extreme weather influences in northern regions, woods tend to be more resinous. The type of wood influences the physical structure of the cellulose fibers. These are mainly divided into Softwood and Hardwood. Softwoods have long cellulose fibers, while hardwoods tend to have short cellulose fibers.

Furthermore, the seasons mainly affect water transport. This also affects the size of the vascular cells (trachea). In spring, the trachea has an increased diameter, as the water requirement is particularly great at this time of the year. In the later seasons, the temperature and water consumption decrease. The size of the newly formed vascular cells is therefore reduced. As a result, two different types of wood structures arise over the course of a year, which can be divided into early and late wood. Early wood has a rapid growth rate, but has a lower density. Late wood on the other hand, grows more slowly and thus has an increased density. [6]

**Table 2.1** Composition of the cell wall in Central European hardwood and softwood

<b>Fraction</b>	<b>Softwood</b>	<b>Hardwood</b>
Cellulose	42–49 %	42–51 %
Hemicellulose	24–30 %	27–40 %
Lignin	25–30 %	18–24 %
Extract substances (pitch)	2–9 %	1–10 %
Minerals	0.2–0.8 %	

## 2.2 Wood fractionation

In order to be able to make paper from wood, fibers should be separated from the wood matrix. For this purpose, various separation processes have been developed, which are briefly described below. In general, a distinction between mechanical and chemical pulping methods is made.

### 2.2.1 Mechanical pulping

With mechanical separation (groundwood pulp, thermomechanical wood pulp), the wood is split up into fibers by mechanically and thermally processes. [7]

#### Groundwood pulp

The debarked wood material (meter wood) is fed to rotating grinding stones and shredded with hot water. Spruce wood is mostly used for this, as it is long-fibrous and has a low density. [8]

#### Thermomechanical wood pulp

The wood material is further processed into wood chips and warmed up with hot steam for a few minutes. As a result of this heating, the fiber composite is weakened because the lignin softens. The defibration then takes place in a “refiner”. [8]

### 2.2.2 Chemical pulping

In contrast to mechanical pulping, chemicals are used to separate the wood fibers.

### **Sulfite process**

The wood is treated in the acid to neutral pH range. Lignin is converted into a water-soluble salt of the lignin sulfonic acid. Hemicelluloses are converted to sugars by acid hydrolysis. The cellulose fibers are also partly hydrolyzed, what weakens the pulp. This procedure can only be used for woods that are low in pitch and silica content. [9]

### **Sulfate process (Kraft-digestion)**

This process is the dominant method for producing pulp, as there are no restrictions regarding resin-rich woods. Contrary to the sulfite process, the shredded pieces of wood (wood chips) are treated in caustic soda for up to six hours in pressurized vessels under alkaline conditions. With cooking chemicals, the cooking liquor (white liquor) turns into black liquor (lignin residues, hemicellulose, and inorganic chemicals). Fibers are separated from the black liquor using washers and other dissolved substances. In the washing step the dissolved substances lignin, hemicelluloses, pectins, polysaccharides and pitch are removed. [10] Small amounts of pitch cannot be removed from the cellulose fibers and the process water and are referred to as carryover pitch or colloidal pitch. In the recovery process, the organic part of the black liquor is burned to generate energy and cooking chemicals are recovered for reuse. [11]

The cellulose fibers in the pulp are stronger than in the other manufacturing processes. After bleaching, this pulp is used for high quality papers. The most important requirements for such papers are high strength, resistance to yellowing and a high degree of whiteness. [12]

## **2.3 Wood components and their properties**

### **2.3.1 Cellulose**

Cellulose consists of chained anhydroglucose units. The units are linked to one another via a 1,4-b bond. The number of linked glucose units can go up to between 500-15000. Figure 2.1 shows a part of the chemical structure of cellulose. In wood cellulose acts as the scaffold building material of the cell walls. The structure is suitable for binding other molecules to one another by means of hydrogen bonds in in-plane direction. In out-of-plane direction,

the molecules are binding together via Van der Waals interaction. These bonds cause the molecules to form a board-like structure, which is also known as microfibrils. These lead to increased stability of the cell walls. [4] The main constituents of this molecule are carbon, oxygen and hydrogen and is therefore an important form of storage for carbon. Cellulose counts as a fiber basis for paper. It cannot be dissolved in most solvents, so cellulose fibers can be separated from the other present components. [13]

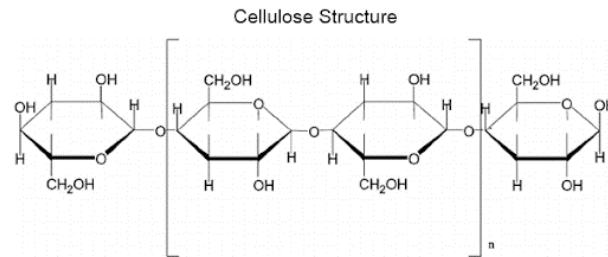


**Figure 2.1** Chemical structure of cellulose

### 2.3.2 Hemicellulose

Hemicellulose is a polysaccharide (figure 2.2), which is mainly composed of six different monosaccharides. The monosaccharides are glucose, mannose, galactose, xylose, arabinose and methylglucuronic acid. Due to the chirality of the monosaccharides, further specific subdivisions can be made, which are made clear by the naming. In the tree structure, hemicellulose acts as a transition link or "adhesive material" between cellulose and lignin. In the alkali, hemicelluloses are soluble and they can be hydrolyzed by acids and hence are removed in the washing step. [4]

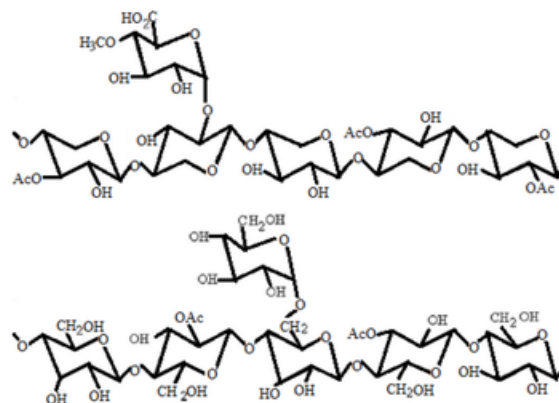


**Figure 2.2** Chemical structure of hemicellulose

### 2.3.3 Lignin

Lignin is a phenolic substance (figure 2.3) and consists of a variation of hydroxy and methoxy-replacing phenylpropane units. These polymers are responsible for lignification and thus contribute to avoiding the swelling of cellulose fibers due to the internal water transport. Lignin also binds and secures cellulose fiber in the wood matrix. Lignin has an influence on paper regarding browning and contributes to accelerated yellowing. In combination with oxygen, lignin can also lead to brittle paper. [14][4]

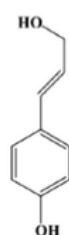


**Figure 2.3** Phenylpropane units are the building block of lignin

### 2.3.4 Extractive substances

These are also seen as accompanying components. These consist mainly of a complex mixture of ash, terpenes, fats, waxes, resin acids, fatty acids, phenols and tannins and esters (Triglyceride, Diglyceride, Monoglyceride, Stearyl ester). Small amounts of proteins, starches, sugars, salts and minerals also occur. Extractive substances are responsible for the chemical, biological and physical properties of the wood. These include light resistance and pest resistance. Additionally, some of these substances also contribute to the hydrophilization, which enables water to be transported within the cells. The Extractive substances can be further divided into inorganic and organic extract substances. Organic extractives include mainly pitch, terpenoids and small acids. [15][4] [16]

### 2.3.5 Pitch

The main groups of ingredients are fatty acids, fatty alcohols, sterols, resin acids, steryl esters, triglycerides, and terpenes (figure 2.4). [17] The composition depends to a large extent on the type of wood, the time of year in which it is deforested and from where the wood is collected. [18]

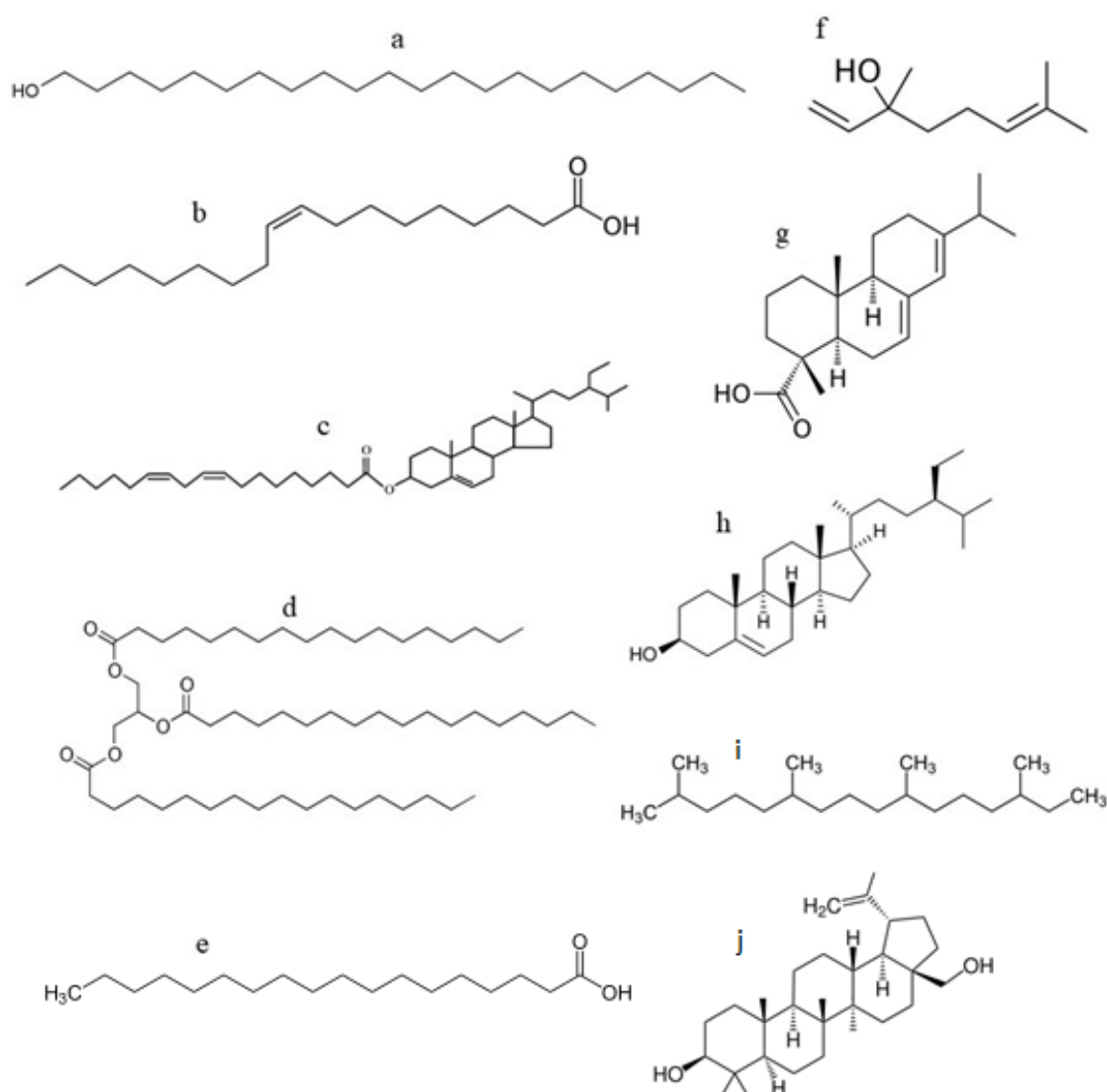


**Figure 2.4** Chemical structure of significant pitch compounds: a) docosanol (fatty alcohol); b) oleic acid (fatty acid); c) sitosteryl linoleate (steryl ester); d) tristearin (triglyceride); e) stearic acid (fatty acid); f) linalool (terpenoid); g) abietic acid (resin acid); h) beta-sitosterol (sterols); i) phytan (terpene); j) betulin (heavy sterols)

After the kraft cooking process, most of the pitch components are removed with the lignin, carbohydrate degradation products and inorganics (cooking chemicals) in the washing step. Steryl esters and glycerides are hydrolysed (alkaline hydrolysis) during kraft cooking to fatty acids, sterols and glycerol. The remaining content of pitch in the process water and on the fiber surface is described as carryover pitch. [19]

### 2.3.6 Carryover pitch

The term carryover pitch refers to the amount of pitch that cannot be removed in the washing process and is therefore carried along with the fiber and process water. [15] The main component classes of the Carryover pitch (colloidal pitch) are fatty acids, resin acids, terpenes and sterols. [17] Fatty acids and resin acids are partly hydrophilic and partly hydrophobic. The polar part (sphere) is a carboxylic acid group (figure 2.5). The rest of the carbon chain is shown as a linear hydrocarbon chain. [20] [17]

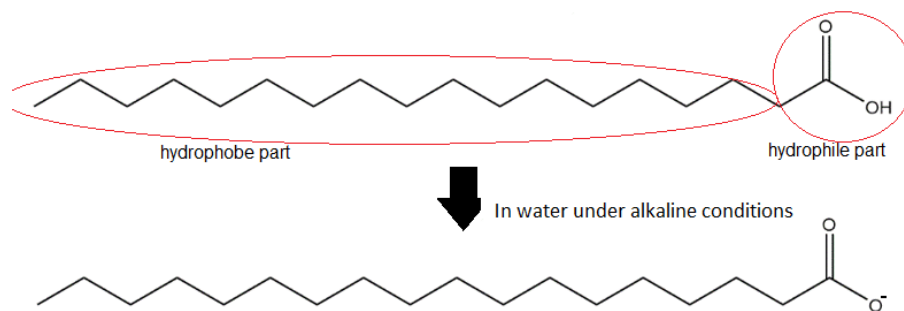


**Figure 2.5** Structure of fatty acids and their behavior in water

Fatty acids and resin acids tend to form micelles in water. (figure 2.6) Under alkaline conditions the carboxylic acid group releases a hydrogen atom, whereby the surface receives a negative charge. When micelles are formed, hydrophobic substances such as sterols and fatty alcohols are encapsulated. The diameter of these micelles ranges from approx. 50 nm to 100 nm. When two micelles come into contact, they fuse to form a larger micelle via capillary forces. The relative amount of fatty acids is much higher than resin acids. In that case, resin acids are not as harmful as fatty acids. [21][22]

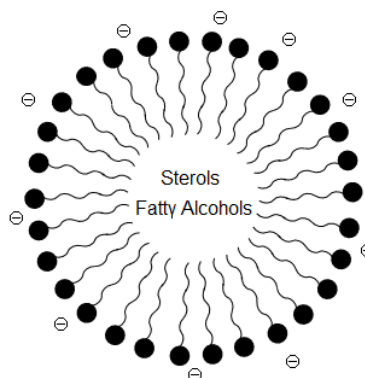


**Figure 2.6** Negatively charged fatty acid micelles with encapsulated sterols, resin acids and fatty alcohols

### 2.3.7 Important properties of the abundant carryover pitch compounds

according to: GESTIS-database; CosIng-database; SOFA-database; Encyclopædia Britannica; Data sheets from Sigma Aldrich

#### Stearic acid (S)

Occurrence: vegetable, animal oils and fats

Polarity: non-polar

soluble in alkalis and organic solvents such as: alkyl acetates, methyl formate, carbon tetrachloride, etc.

Molecular formula:  $C_{18}H_{36}O_2$

Molar mass: 284.48 g/mol

#### Oleic acid (OA)

Occurrence: vegetable, animal oils and fats

Polarity: non-polar

Soluble in methanol and alkalis

Molecular formula:  $C_{18}H_{34}O_2$

Molar mass: 282.46 g/mol

#### Abietic acid (A)

Occurrence: softwoods

Polarity: Non-polar

Soluble in alkalis, ethanol & diethyl ether

Molecular formula:  $C_{20}H_{30}O_2$

Molar mass: 302.46 g/mol

**beta-Sitosterol (beta-S)**

Occurrence: Vegetable oils

Polarity: Weakly non-polar

Soluble in acetic acid, ethanol and ether

Molecular formula:  $C_{29}H_{50}O$

Molar mass: 414.69 g/mol

**Docosanol (D)**

Occurrence: Plants, barks and leaf waxes

Polarity: Non-polar

Soluble in methanol & ethanol

Molecular formula:  $C_{22}H_{46}O$

Molar mass: 326.60 g/mol

**Betulin (B)**

Occurrence: birch bark

Polarity: Non-polar

Soluble in chloroform

Molecular formula:  $C_{30}H_{50}O_2$

Molar mass: 442.72 g/mol

**2.3.8 Carryover Pitch influence****Product (Paper)**

Pitch bonded to the surface of cellulose fibers reduces the possibility of fiber-to-fiber bonding. The consequence of this is that the tensile strength of the papers is reduced. Pitch agglomerates themselves can also be deposited on the product and lead to stains on the paper surface. [23][24][16][2]

## **Paper machine**

In the process water small amounts of carryover pitch can occur. For economic and environmental reasons, the process water is cycled. This can lead to accumulating of the carryover pitch over time and consequently parts of the system becoming dirty, clogged or in the worst case, destroyed. Agglomerated carryover pitch particles can also clog the wet press felts and impede drainage. Machine parts must be cleaned regularly, which is time-consuming and leads to long system downtimes. [23][1][16]

## **2.4 Kraft papers**

For kraft papers, less damaged cellulose fibers are preferred. Also, lignin should be extracted from cellulose fibers, because it influences yellowing and decreasing the bonding abilities. High strengths in papers are achieved by having good individual fiber strength, fiber quality and fiber-fiber bond. [25]

### **2.4.1 Influence on tensile strength**

The strength of papers depends on a variety of different influencing parameters. In the following section the most important influencing factors are briefly shown and briefly described.

#### **Cellulose fiber strength**

The strength of the individual fibers depends on the material used and on the stock preparation. The strength of the individual fibers differs depending on the type of wood, climatic conditions and the pulping process. Softwood tends to have long cellulose fibers, which are of great importance for strength. Long cellulose fibers can create multiple connections to other fibers. [26]

The properties of the fibers are changed by mechanical and chemical pre-treatments (refining, cooking process). On the one hand, fibrils are generated during the cooking and the refining process, which increase the surface area and the relative bonding area. There are two different types of fibrillation. External fibrils (figure 2.7) develop when subjected to shear stress. Squeezing creates fibrils inside of the fiber (figure 2.8). The whole cellulose

fiber is more flexible and generates more area, because the structure of the inner threads breaks open. [26][27][28]



**Figure 2.7** Milled cellulose fiber with outer fibrils

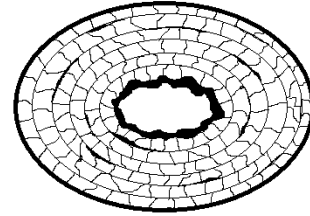


**Figure 2.8** Cellulose fiber in cross-section after the milling process - internal fibrillation

However, the refining process is associated with mechanical destruction of the fiber, which is noticeable through kinks (figure 2.9), curls (figure 2.10) and fiber breaks. If the fiber breaks, fine material is formed. Some of these are carried along with the process water. Since the process water is recycled, the fines are fed back and are therefore not lost in the process. Curls and kinks should be avoided. Therefore, kinked and curled fibers are straightened through low consistency refining before papermaking. The desired result is a flexible fiber that is still straight. Flexible fibers can be better incorporated into the structure and straight fibers ensure stability. The fiber bed becomes fixated after draining the water. During the drying process, liquid is evaporated from the swollen fibers. This leads to an increased stiffness of the fibers. This physiological change in the fibers offers a further increase in strength via entanglement friction between the fibers. [29]



**Figure 2.9** Curl - curvy cellulose fiber

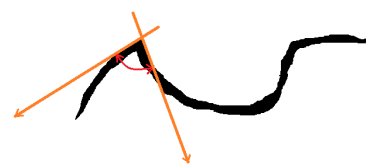


**Figure 2.10** Kink - drastic change of direction of the fiber

### Fiber constitution

The shape and nature of the fibers also play an important role in terms of the fiber-fiber bond strength. In order to achieve increased tensile strength, fibers with a small wall thickness are preferred (figure 2.11). Fibers with thin walls collapse and thus more of them

can be added to a certain volume, i.e. fibers are more densely packed with more bonds and larger bonded area. Also, fibers with a thin wall are more flexible and have larger area for fiber-fiber bonding as they are collapsed (flat, ribbon-like). [30]



**Figure 2.11** Cross-section of early and late wood fibers

### Fiber-fiber bond

When two fibers meet, there is a connection between the contacting surfaces (binding area) via several different binding mechanisms. In case of the binding area, a distinction is made between optically bound area and molecular contact area. In the case of the optically bound surface, it appears as if the fiber surfaces in contact lead to a complete binding surface (figure 2.12). However, the unevenness of the fiber surface can lead to cavities. The real bonding area is instead the summed contact area on a molecular level. [26]

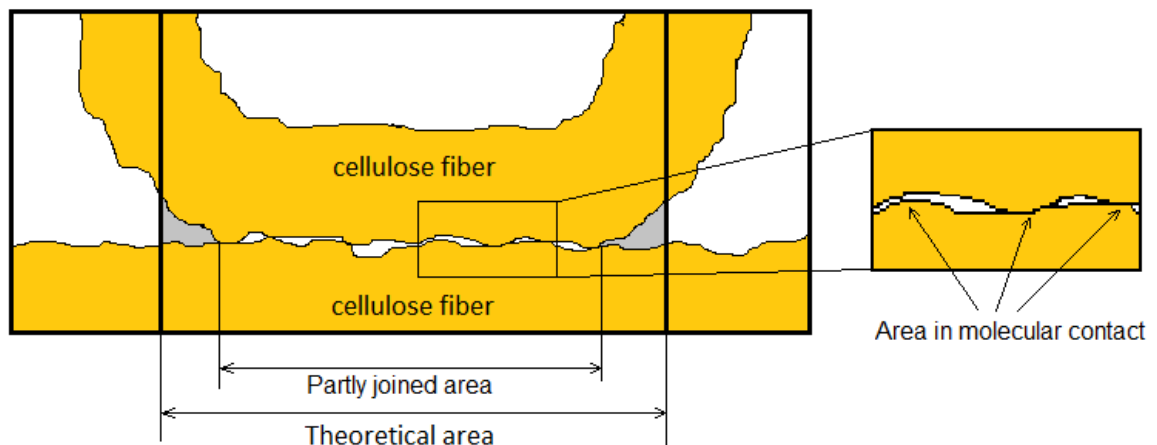


**Figure 2.12** Theoretical and real bonding area of cellulose fibers

The binding mechanism can be described by basic physical forces. Historically, the first model to describe the binding mechanism was based purely on hydrogen bonding (figure 2.13). When dewatering, water molecules remain between the fibers and form several

bridges that hold the fibers together. Over time, additional binding mechanisms could be determined. [31]

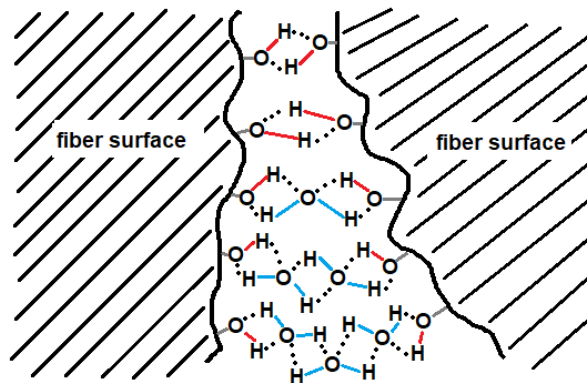


**Figure 2.13** Formation of hydrogen bonds between fibers - hydrogen atoms of the fiber (red); hydrogen atoms of water molecules (blue)

### Additional bonding types

Van der Waals forces (figure 2.16), coulomb forces (figure 2.14) and capillary bridges (figure 2.15) also play a role in molecular bonding. The coulomb force describes the force between two charged objects. Forces between charges of equal sign are repellant, while those of opposite sign are attractive. The effect of capillary bridges arises from molecular forces within a substance (water) and the interface between different phases (fiber surface). Van der Waals forces are intermolecular forces. The forces of attraction arise from formed dipoles. This leads to a charge shift in the atom/molecule. When two atoms/molecules meet with shifted but attracting charges, a bond occurs. The size of the contact area of the fibers (relative binding area (RBA)) and the strength of the bond are responsible for the strength of the fiber-fiber bond. A larger contact area leads to an increased probability of creating molecular connection possibilities. [32][26]

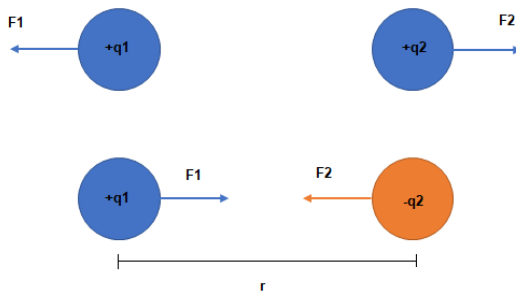


**Figure 2.14** Coulomb forces: Mechanism of attraction and repulsion [33]

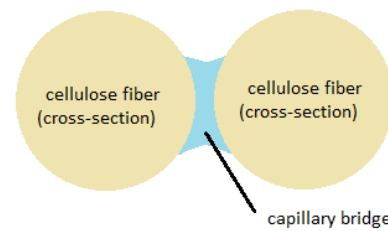


**Figure 2.15** Capillary bridging between fibers [21]

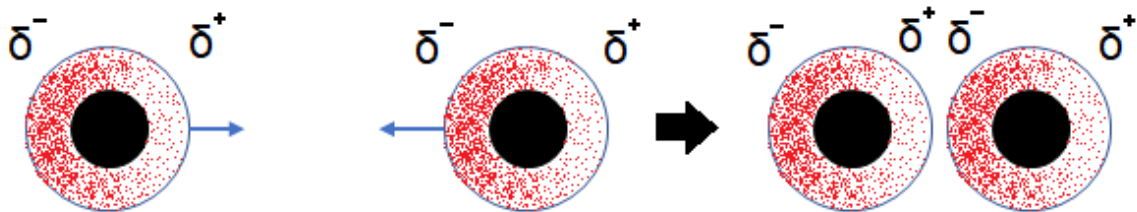


**Figure 2.16** Van der Waals forces - interaction of atoms or molecules with shifted charges (dipoles) [34]

## 2.5 Papermaking Additives for Kraft paper

In the paper industry, chemicals are added in the process to improve paper properties. The main focus lies on increasing strength properties, optical aspects and aging behavior. [35]

### 2.5.1 Starch

Starch is used in papermaking to achieve better product properties. The most important of these properties are increased strength, better retention, faster drainage and improved wastewater quality. Modified starches are used depending on the type of paper, type of raw material, manufacturing technology and required end properties. Starch acts as a binder and rheology modifier and replaces expensive synthetic chemicals, which also leads to a cost reduction. Figure 2.17 shows the molecular bond between cationic starch and cellulose fibers. The red regions show where they occur. [36][37][38]

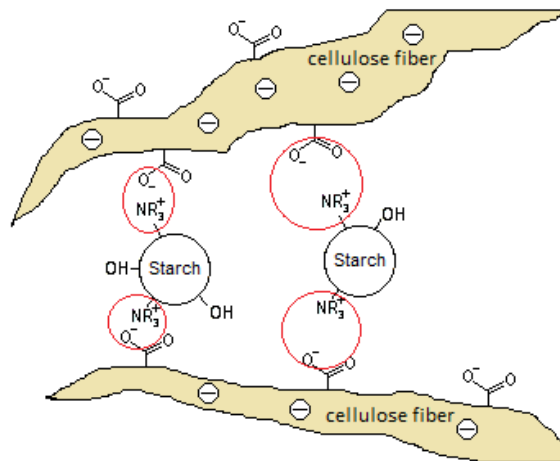


**Figure 2.17** Molecular bonding of cationic starch to cellulosic fibers; Acting coulomb forces (red marking)

### 2.5.2 Alum (Aluminum sulfate)

Alum is used as an additive in the paper industry. Since a 1 % alum solution has a low pH value of approximately 3, this substance serves as a cationic source and as an acidic buffer. The addition of alum improves drainage and is used in various retention programs. When alum meets pitch micelles, two different mechanisms can occur (figure 2.18). Alum adsorbs and fixes the colloidal pitch particles to the fiber. Also, pitch colloids that are already on the fiber surface get also fixed onto the fiber. This is the desired effect from the addition of alum. Alum also can connect unbound pitch colloids with one another. These agglomerations can be transported in the process water and lead to problems due to deposits in the plant. The agglomerated pitch colloids can also be fixed onto the fiber. If the agglomerations are too large, there is a high probability that these can become detached from the fiber again due to turbulent external influences. [37][39] [40][38]

### 2.5.3 Enzymes and Soy protein

In addition, pitch can also be eliminated by adding enzymes and microorganisms. However, enzymatic additives are only used when high resin contents occur. A basic distinction is made between hydrolytic enzymes (lipases, sterol esterases) and oxidative enzymes (laccases, lipoxygenases). Using lipases to catalyze the hydrolysis of fatty acid esters (triglycerides & steryl esters) of mechanical and sulphite pulps is well established. Otherwise the utilization of enzymes for pitch control is under development.

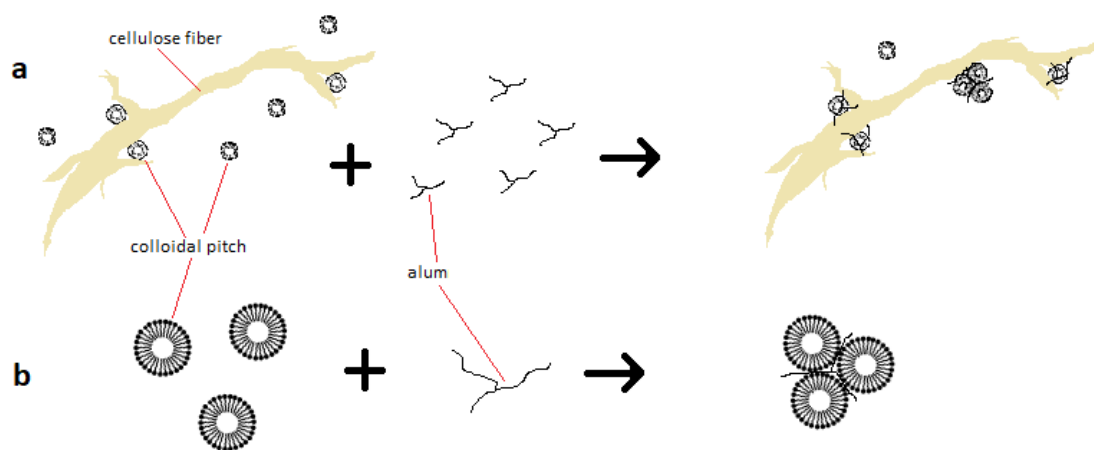


**Figure 2.18** Differences in effect when using alum: a) desired effect (pitch adsorbed and fixed to fiber); b) to be avoided (pitch agglomerated) [40]

In this thesis, soy protein is not an enzymatic additive itself. It is a source of lipoxygenases, i.e. it includes lipoxygenases which catalyzes the oxidation of unsaturated fatty acids and degrades them. Soy protein potentially improves bonding by making pitch less harmful for bonding and by working as a dry-strength agent. Soy protein can be bound to the cellulose fiber via a noncovalent hydrogen bond between protein amine groups and cellulose primary alcohols. A bonding also can take place via a weak ionic attraction between the ions of both systems. Also covalent imine bonds can occur between the protein primary amines and cellulose aldehydes. These binding mechanisms lead to an effective strengthening of the paper fiber web. [41][42][43][44]

## 2.6 Analysis of the PITCH content via GCMS

GCMS is a coupling of gas chromatography and mass spectrometry. Gas chromatography is responsible for the separation and mass spectrometry for the identification and quantification of the substance mixture to be examined. Only vaporizable substances with a relatively low molecular weight can be used for the GCMS. The separation principle is based on different boiling points and interaction of the substances with the material of the column (stationary phase). The stationary phase is a capillary through which an inert carrier gas (mobile phase) flows. The sample to be examined is then initiated into the carrier gas. The result is a different running speed of every component. After the components have passed through the capillary, they are ionized. The molecules are then separated in the

analyzer according to their mass and charge. The components and their masses can be determined in the detector using various electronic measuring methods. The GCMS analysis is an expensive, complicated, poisonous and time-consuming method. GCMS, when done correctly, is the most accurate and reliable method for pitch analysis.[45] Since a GCMS analysis cannot be carried out for every patch in paper production, an alternative, quick and simple method for the approximate determination of the amount of the substances must be developed. An attempt was therefore made to separate the pitch sample into its components by thin-layer chromatography. For the purpose of evaluating the alternative method, GCMS analyzes of the pitch samples were carried out. In the mass spectrometry chromatogram (figure 2.19) of the industrial pitch sample, 1255 different components were found. These were then divided into the classes of fatty acids, resin acids, sterols and fatty alcohols. [46]

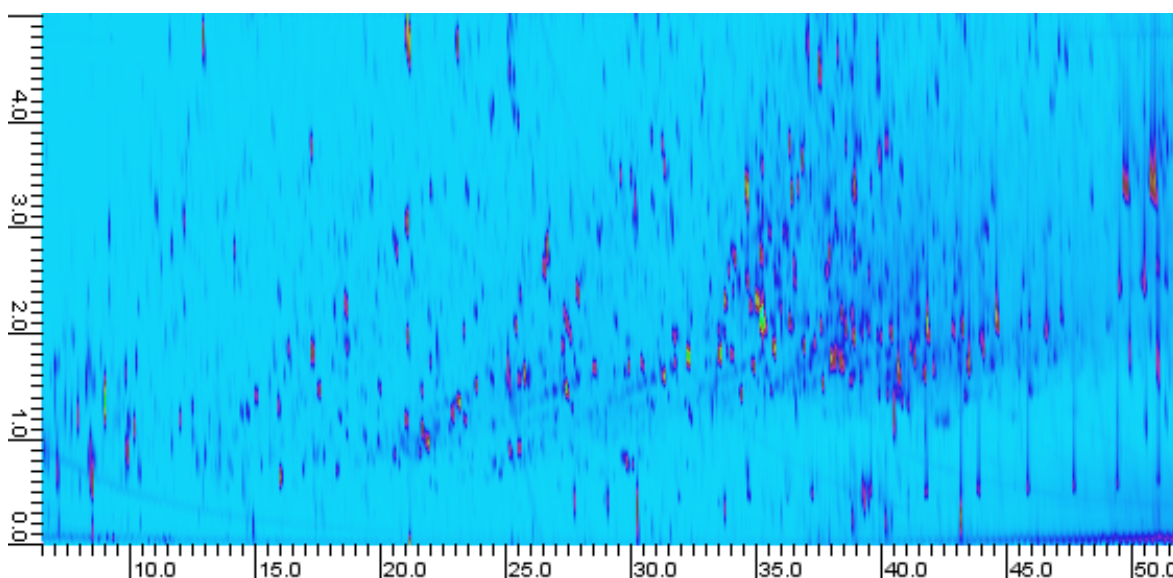


**Figure 2.19** MS chromatogram of industrial pitch with 1255 different components [3]

## 2.7 Thin layer chromatography (principle)

The principle of thin-layer chromatography (TLC) was used to separate the industrial pitch sample. In thin layer chromatography (figure 2.20), substances are separated from one another via an interaction between the solid material and the eluent. The solid material of the TLC plate is called stationary phase while the eluent is described as mobile phase. The stationary phase consists of a pebble-shaped, fine material which is evenly applied to a carrier plate. The mobile phase, on the other hand, is an eluent that flows over the

carrier plate by capillary forces. The more polar a substance is, the stronger the interaction with the stationary phase and the slower the substance moves on the plate. Non-polar substances dissolve more easily in non-polar eluents and change from the stationary phase to the mobile phase more frequently. Therefore, non-polar substances are transported much faster on the TLC plate than polar ones. [47]

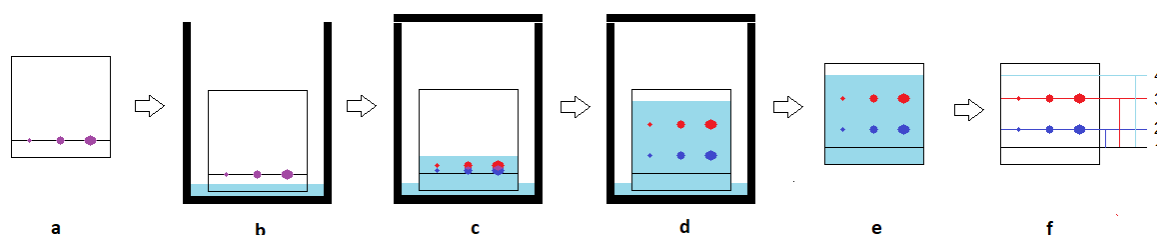


**Figure 2.20** Process of thin layer chromatography: a) Applying the mixture; b) put in eluent; c) start of substance separation; d) separation end; e) removing remaining eluent; f) evaluation

The applied sample is placed vertically in the TLC chamber and sealed so that a saturated atmosphere is established. This is done to prevent evaporation of the eluent, which can affect the results. Before the eluent reaches the upper end of the plate, the plate is removed from the chamber and dried as quickly as possible. Often the substance spots are not recognizable in visible light. When using ultraviolet scan (UV) light or with coloring methods, these can still be made visible. [48]

Usually the following regions are distinguished for the evaluation:

- 1 starting line (spot where the sample was applied)
- 2 substance spot A
- 3 substance spot B
- 4 eluent front (end point of the eluent when removing the plate)

Retarding front (Rf) values can be determined from the traveled distances of the spots and the traveled distance of the eluent. These values contain information of the spot regions in order to make comparisons with other TLC results. [49] These values were determined with the formula: 2.1

$$Rf[] = \frac{\text{traveled distance of substance spot}[cm](2;3)}{\text{traveled distance of eluent}[cm](4)} \quad (2.1)$$

## 2.8 Explanation of the 2D-TLC

In our case, a simple thin layer chromatography can't manage the separation of such a high multi-component substance. Therefore a 2D thin-layer chromatography was carried out (figure 2.21). It is a special case of thin-layer chromatography and is often used for multi-component mixtures. The difference to the ordinary TLC procedure is, that after running through the first eluent, the plate is dried (removing eluent), rotated by 90 ° and placed in the second eluent. After the second drying, the spots of the separated substances can rarely be seen with the naked eye. With suitable coloring it is possible to make the spots visible. An alternative would be to display the TLC plate in UV light. Depending on the wavelength, the spots can also be displayed visibly without coloring agent. [3]

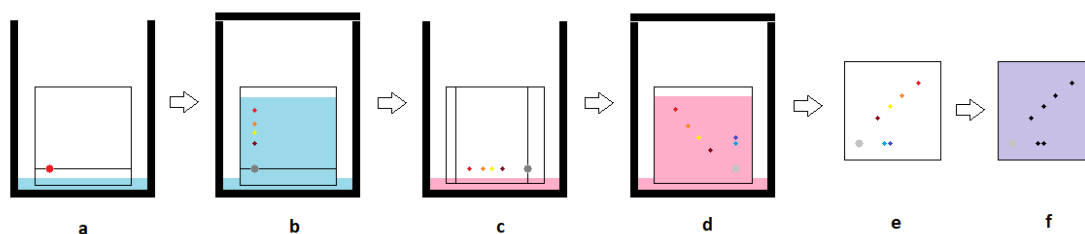


**Figure 2.21** Flow chart of 2D thin-layer chromatography with industrial pitch a) Apply pitch and starting with alkaline eluent b) end of the first round c) removing remaining eluent and restarting with acidic eluent and a 90 degree turn d) end of the second separation process e) removing remaining eluent f) coloring & evaluation

In the following figure 2.22 the images of traveled distance of the components is shown in the acidic and alkaline region. Also the corresponding relative travelling distances ( $R_f$  values) of each class are shown in table 2.2.

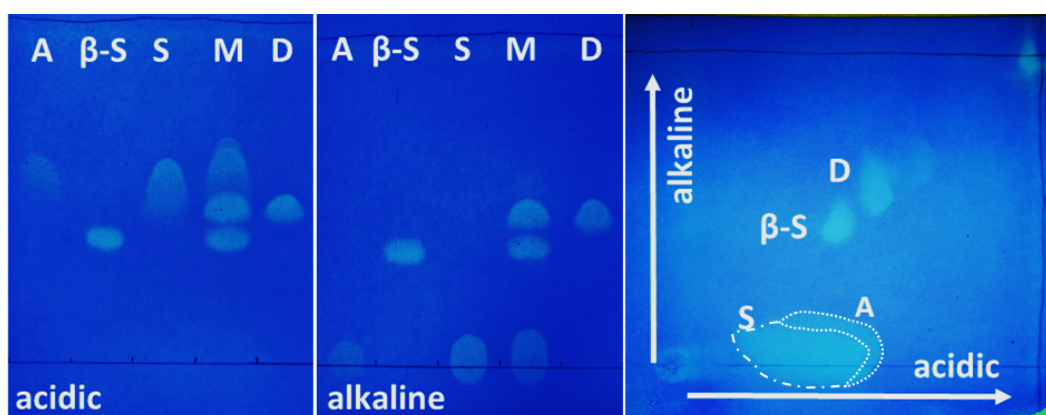


**Figure 2.22** Left: 1-dimensional TLC (top left and center) of the class components: abietic acid (A); beta-sitosterol (beta-S); stearic acid (S); mixture of compounds (mixture (M)); docosanol (D). Right: 2D-TLC of all class components. [3]

**Table 2.2** R<sub>f</sub> values in both directions from the 2D-TLC method of the substance classes [3]

Substance	Class	R <sub>f</sub> acidic []	R <sub>f</sub> alkaline []
abietic acid (A)	resin acids	0.63	0.01
beta-Sitosterol ( <b>beat-S!</b> ( <b>beat-S!</b> ))	sterols	0.37	0.37
stearic acid (S)	fatty acids	0.52	0.02
1-docosanol (D)	fatty alcohols	0.45	0.45

## 2.9 Assignment of the spots via Peak method

The regions of the substance classes on the TLC plate were determined using a PEAK method, which is described in the following. A TLC plate was created on which the mixture of model compounds was added. This plate is used as a reference after using 2D thin-layer chromatography. Further, new plates were created where the amount of a single substance was increased. In comparison with the reference, it was possible to determine which substances are associated with the spots on the TLC plate via the increase in the size of the dots and the increase in intensity. In figure 2.23 a TLC plate of the model compounds and an according TLC plate with industrial Pitch sample is shown in figure 2.24. The spot regions of the model compounds are identical with the regions of the pitch sample. [3]

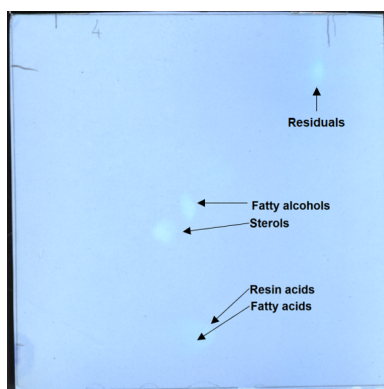


**Figure 2.23** Determined regions of the component classes via peak method using model components

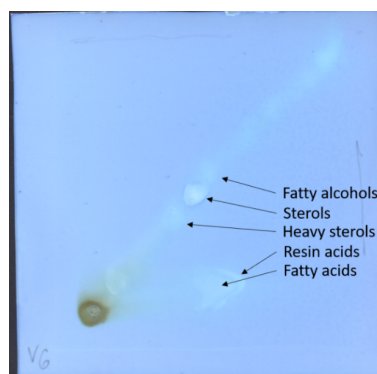


**Figure 2.24** Transfer of the spots from the PEAK tests to the industrial pitch sample

## Materials and Methods

This section of the thesis provides an insight into used chemicals, equipment and software. Physical paper properties, starch retention and the pitch composition was analysed.

### 3.1 Chemicals and Samples

In the further course the term pitch is used as the definition of industrial carryover pitch. For the paper tests, the unbleached softwood kraft pulp (unbleached softwood kraft pulp (UBSK)), alum (aluminium sulfate) and the pitch samples were provided by an industrial pulp mill. A Soxhlet extraction according to ISO standard 14453:1997(E) was carried out after the last pulp washing step to obtain the pitch. The organic phase was extracted with acetone in at least 16 cycles and then dried at 105 °C. for 2 hours. The sample had to be protected from light in order to avoid a change in the composition. To keep aging effects low, the sample must be examined as quickly as possible within a month. In total, 5 different pitch samples were provided:

- industrial 1 pitch (industrial pitch number 1 (IP1))
- industrial 2 pitch (industrial pitch number 2 (IP2))
- softwood pitch
- hardwood pitch
- birch pitch

Sulfuric acid (99.8 %) and sodium hydroxide (99.8 %) from VWR International (Stříbrná

Skalice, Czech Republic) were used to adjust the pH value. In order to be able to assess the influence of pitch and the effectiveness of auxiliaries in paper production, laboratory tests were carried out in which relevant parameters were varied. The following substances and chemicals were included in the papermaking experiments:

- UBSK
- Deionized and tap water
- Cationic starch (Fibraffin K75; Südstärke GmbH; dry content: 82.8 %)
- Aluminium sulfate
- Soy protein (SoBind™ Clarity 5 Soy Polymer; DuPont; dry content: 92.39 %)
- IP2 sample
- Sulfuric acid (H<sub>2</sub>SO<sub>4</sub>)
- Sodium hydroxide (NaOH)

In the two dimensional thin layer chromatography (2D-TLC) experiments the creation of calibration lines was performed with model compounds. The compounds stearic acid (fatty acid, 95 %), abietic acid (resin acid, 75 %), beta-sitosterol (sterols, 70 %), 1-docosanol (fatty alcohols, 98 %) from Merc Millipore (Burlington, MA, USA) and betulin (betulin, 97.5 %) from Sigma-Aldrich INC. were used. Since oleic acid is a very sticky substance and difficult to dissolve, it was removed from the calibration tests.

High performance thin layer chromatography (HPTLC) silica gel with aluminum base plates with 60F 254 (Merk Millipore, Borlington, USA) were used for the TLC experiments and glass ringcap capillaries (Hirschmann, Eberstadt, Germany) were used for the application of the substances. Cyclohexane (99.5 % TCI chemicals, Tokyo, Japan), ethyl acetate (98.0 % TCI chemicals, Tokyo, Japan), formic acid (99 % Sigma Aldrich, St. Louis, USA) and aqueous ammonium hydroxide solution (28-30 % Sigma Aldrich, St. Louis, USA) were used for the mobile phase as eluents. Nile blue A-sulfate (80 %, Carl Roth, Germany) was used to stain the TLC plates. In addition, ethanol (99 %) and isopropanol (99.5 %) were purchased from TCI chemicals (Tokyo, Japan) to dissolve the solids. A TLC sprayer from CAMAG (Berlin, Germany) was used to apply the coloring agent to the TLC plate.

The calculation and evaluation of the TLC plates was carried out with the MATLAB software using graphic image processing.

## 3.2 Retention and papermaking experiments

The aim of the papermaking and retention experiments is to determine which process settings can be used to achieve the highest proportion of starch retained in the product 3.2.5. For this purpose, three test series were planned in which the focus was on the pH value and the stirring time. [11] Furthermore, the auxiliaries and their order were varied. In order to investigate the effects of these parameters on the tensile index, hand sheets were created in addition to the DFR (Drainage Freeness Retention) measurements. A double measurement was carried out for each parameter setting. The experimental setup was schematically listed in table 3.1.

**Table 3.1** Starch retention trial setup

Trial	Chemical order		Additional settings
	Setup 1	Setup 2	
1	H <sub>2</sub> SO <sub>4</sub> ->Starch	Alum ->H <sub>2</sub> SO <sub>4</sub> ->Starch	Mixing time: ~1 min pH value: 6.8 ± 0.3
2	Starch ->H <sub>2</sub> SO <sub>4</sub>	Starch ->Alum ->H <sub>2</sub> SO <sub>4</sub>	Mixing time: ~15-20 min pH value: 6.8 ±0.016
3	Starch ->H <sub>2</sub> SO <sub>4</sub>	Starch ->Alum ->H <sub>2</sub> SO <sub>4</sub>	Mixing time: 15-20 sec pH value: no measurement

### 3.2.1 Preparation of starch, alum and soy protein solutions

Since the auxiliaries cannot simply be added in their original form, they must first be dissolved in deionized water. A 1 % solution was prepared for each substance. To increase the binding capacity of starch and soy protein, they had to be stirred at increased temperature. The respective substance first had to be mixed in cold water and then heated to 93 °C with constant stirring. In the case of cationic starch it had to be considered that the gelling process starts at a temperature of 55.4 °C and the viscosity increases significantly. To avoid solidification, the speed of the stirrer must be increased in order to maintain a homogeneous consistency. After the temperature of 93 °C has been reached, it was stirred for another 15 minutes. In the case of starch and soy, the solution was then cooled to 40 °C and then mixed with a hand blender. This was done to make sure that no agglomerations had formed within the solution. The result of the solutions was a clear, viscous liquid

without any agglomerations. The dissolved substances were stored temporarily at approx. 10 °C for preservation.

### 3.2.2 Sulfuric acid (H<sub>2</sub>SO<sub>4</sub>) & Sodium hydroxide (NaOH)

Sulfuric acid and sodium hydroxide solution were used to adjust the pH value. The addition of sodium hydroxide increased the pH value. Sulfuric acid was added if the pH value was too high or if the pH value needed to be reduced during the process.

### 3.2.3 Pitch preparation

The pitch samples were delivered in dry state and weighed in total only a few grams (figure 3.1). In order to achieve a satisfactory result, the solvent toluene was used, which transfers the dried pitch residues back into a liquid state. The estimated concentration of the pitch was 5.1 mg/ml.



**Figure 3.1** Dried pitch sample from industrial paper mill

### 3.2.4 Pulp preparation

The unbleached softwood kraft pulp had to be prepared to be used in the experiments. Since it was delivered in a dry state, it had to be soaked in deionized water for about 24 hours. After the swelling process, the material was stirred with deionized water for 3 minutes (30 g of solid in 300 ml of deionized water). Afterwards the fiber material was ground in a PFI mill for 3000 rev according to ISO 5264-2 standard. The result was a Schopper Riegler degree of 15 (°SR). After that, the ground material was whipped again for 3 minutes (30 g of solid in 300 ml of tap water), to re-homogenize the milled fibers in tap water. The substance was then placed in a distributor and filled to 10 liters with tap

water. A consistency check was then carried out by taking a certain volume (approx. 800 ml) from the distributor and creating a test sheet from it. After the drying process, the test sheet was placed in the drying cabinet for approx. 10 min and the weight of the test sheet was determined using an integrated balance. The exact amount of fiber material per liter can be calculated using the weight and the used volume.

### 3.2.5 Drainage Freeness Retention (DFR) measurement & starch retention (acUV-Vis)

In order to be able to measure the amount of starch that is not bound to the fibers, the filtrate had to be collected during sheet production. Since the filtrate could not be collected during the Rapid Köhten sheet production, a DFR device was used instead. With a DFR measuring device, it is possible to simulate the drainage during sheet formation and to measure the retention. About 1 L of pulp from the distributor was filled into the chamber of the DFR device. A rotor located inside the chamber ensured turbulent flow behavior and prevented sedimentation of the fiber material. The speed of the rotor and the addition of chemicals via transferpette pipette can be controlled via a pre-definable program. After the program has ended, a channel is opened and drained through an 80 $\mu$  sieve. In order not to falsify the results, the first 50 ml of the filtrate are automatically discarded in order to prevent contamination from preliminary tests. 2.7 ml of the collected filtrate were mixed with 0.3 ml Lugol and transferred to a cuvette. The sample was measured with UV and visible light in the spectrophotometer. The wavelength of the light in the measurement was 550 nm. In addition, a calibration series (figure 3.2) with known starch concentrations was made. This enabled the starch content in the sample to be calculated back. [50]

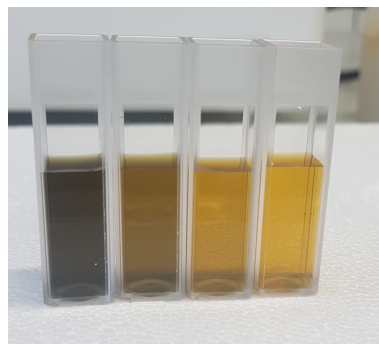


**Figure 3.2** Calibration cuvettes with different lugol filtrate concentrations - striking yellow color (dark = high concentration; light = low concentration)

### 3.2.6 Handsheet production

In addition to the DFR measurement test, laboratory sheets were prepared from the pulp using the Rapid-Köthen apparatus according to ISO 5269-2 standard. As indicated in table 3.1 two different parameter settings were treated for the test series. In the first trial, the amount of fiber per liter of pulp was set at 3 g for test purposes. From the consistency check, the required volume (approx. 1000 ml) of pulp for the 3 g of fiber material could be calculated. 4.5 ml of the 1 % alum solution and the 1 % starch solution were added according to the experimental design. The necessary amount of H<sub>2</sub>SO<sub>4</sub> had to be determined via a continuous measurement of the pH value. Since the pulp in the distributor was constantly stirred, there was an exchange of CO<sub>2</sub> via the air. As a result, the concentration of CO<sub>2</sub> in the pulp causes the pH to drop steadily. Throughout the experiment it could be observed that, in the case of long-lasting test series, smaller amounts of H<sub>2</sub>SO<sub>4</sub> were required to reach a pH value of 6.8. For the following two trials, a fiber amount of 2.4 g per paper sheet (oven-dry basis) was set. The amount of the 1 % alum solution and the 1 % starch solution was reduced to 3.6 ml. The quantities for H<sub>2</sub>SO<sub>4</sub> were determined dynamically. In the third test series stirring times of 15 to 20 seconds were set. No measurement of the pH value was performed, due to lack of time. The required amounts of sulfuric acid were taken from the previous experiments.

The laboratory paper sheets were stored in the climatic room for 24 hours. The conditions in the climatic room are standardized to the ISO 187 standard with under 50 % relative humidity and 23 °C.

### 3.2.7 Physical measurement of the laboratory paper sheets

Tensile strength and sheet density are closely related. Since more fiber-fiber bonds occur with a higher sheet density, the sheet strength is consequently also increased. For this reason, it is necessary to obtain a uniform measurement of the samples. In order to determine the sheet density, which is important for calculating the tensile strength, the average weight per unit area had to be determined. The laboratory sheets were individually weighed in accordance with the ISO 536 standard and their thickness measured in accordance with ISO 534. The defined area of a laboratory sheets is 0.0317 m<sup>2</sup>. The medium basis weight was calculated via the formula 3.1. The tensile index is calculated by using the formulas 3.2 and 3.3.

$$\text{medium basis weight}[\text{g}/\text{m}^2] = \frac{\text{measured paper sheet weight}[\text{g}]}{0.0317(\text{paper sheet area})[\text{m}^2]} \quad (3.1)$$

$$\text{tensile strength}[\text{kN}/\text{m}] = \frac{\text{measured force (until sample breaks)}[\text{kN}]}{\text{sample width}[\text{m}]} \quad (3.2)$$

$$\text{tensile index}[\text{N m}/\text{g}] = \frac{\text{tensile strength}[\text{N}/\text{m}]}{\text{medium basis weight}[\text{g}/\text{m}^2]} \quad (3.3)$$

The tensile strength was automatically measured on a L&W (Lorentzen & Wettre) measuring device according to the ISO 1924-3 standard. Many different property values are measured and provided by the L&W measuring device. Only the tensile index was important for the further investigations. In the table 3.2 all values of the test series for determining the tensile strength are summarized.

**Table 3.2** Physical property measurements of the starch retention experiments

<b>Trial 1</b>	<b>Medium basis weight [g/m<sup>2</sup>]</b>	<b>Medium thickness [μm]</b>
Starch	84.363	132.08
Starch + Alum	83.945	126.3
<b>Trial 2</b>		
Starch	79.898	121.6
Starch + Alum	80.258	123.3
<b>Trial 3</b>		
Starch	82.745	125.9
Starch + Alum	82.208	129.3

### 3.2.8 Tensile Index experiments

The aim of this trial was to study the influence of soy protein and starch on paper strength and its efficiency against pitch. In this experimental setup no starch retention experiments were performed via DFR measurement. The trial setting is shown schematically in table 3.3. The pitch (IP1 sample) was used in this experiment. Soy protein served as a starch substitute. Alum was used as an auxiliary reagent in all settings. Starch, alum and soy protein were added as a 1 % solution with the amounts from table 3.4 For the experiment, 3.12 mg pitch (dry) should be added per 2.4 g fiber material in order to achieve a pitch proportion of 0.13 %. With a pitch solution concentration of 2.622 mg/ml, an amount of 1.2 ml had to be added to achieve the desired pitch percentage. A pH value of 6.8±0.045 could be set using continuous pH measurement and dynamic addition of sulfuric acid.

**Table 3.3** Tensile index trial setup

Trial	Substance order
1	Alum ->H <sub>2</sub> SO <sub>4</sub>
2	Soy ->Alum ->H <sub>2</sub> SO <sub>4</sub>
3	pitch ->Alum ->H <sub>2</sub> SO <sub>4</sub>
4	pitch ->Soy ->Alum ->H <sub>2</sub> SO <sub>4</sub>
5	Alum ->H <sub>2</sub> SO <sub>4</sub>
6	Starch ->Alum ->H <sub>2</sub> SO <sub>4</sub>
7	pitch ->Starch ->Alum ->H <sub>2</sub> SO <sub>4</sub>
8	Soy ->Starch ->Alum ->H <sub>2</sub> SO <sub>4</sub>
9	pitch ->Soy ->Starch ->Alum ->H <sub>2</sub> SO <sub>4</sub>

The quantities of used chemical solutions are listed in table 3.4. The stirring time for pitch and soy was set to 30 minutes each. For the remaining chemicals, the stirring time was set to 30 seconds each. After the addition of sulfuric acid, stirring was continued for a minute and then the sheet-forming process was initiated immediately. Few laboratory paper sheets had white spots on their surface (figure 3.3). These were created by sedimented agglomerations of pitch and alum on the paper surface.

**Figure 3.3** Produced laboratory sheet with over 30 agglomeration stains

The laboratory sheet data of the individual sheets for determining the tensile index from the pitch tests is listed in table 3.5.

The tensile strength was measured on a L&W measuring device according to the ISO 1924-3 standard. The data obtained was processed in EXCEL. Outlier in the data were removed with a Dixon-Grubbs outlier test. For the reference test, twice the amount of paper in relation to the other test settings was produced and measured.

**Table 3.4** Amounts of chemicals in soy protein trials

IP2 2.622 mg/ml	Soy protein 10 mg/ml	kat. Starch 10 mg/ml	Alum 10 mg/ml	H <sub>2</sub> SO <sub>4</sub> 1 mg/ml (0.01 M)	Agglomeration stains on the paper surface
			3.6 ml	1.65 ml	0
	3.6 ml		3.6 ml	1.45 ml	0
1.2 ml			3.6 ml	1.45 ml	15-30
1.2 ml	3.6 ml		3.6 ml	1.4 ml	15-30
			3.6 ml	1.3 ml	0
		3.6 ml	3.6 ml	1.3 ml	0
1.2 ml		3.6 ml	3.6 ml	1.25 ml	30+
	0.9 ml	2.7 ml	3.6 ml	1.2 ml	0-15
1.2 ml	0.9 ml	2.7 ml	3.6 ml	1.2 ml	0-15

**Table 3.5** Physical property measurements of the soy protein trials

Trial setting	Med. basis Weight [g/m <sup>2</sup> ]	Med. Thickness [μm]
Alum ->H <sub>2</sub> SO <sub>4</sub>	77.89	123.15
Soy ->Alum ->H <sub>2</sub> SO <sub>4</sub>	80.47	127
pitch ->Alum ->H <sub>2</sub> SO <sub>4</sub>	78.72	125.66
pitch ->Soy ->Alum ->H <sub>2</sub> SO <sub>4</sub>	80.16	125.83
Alum ->H <sub>2</sub> SO <sub>4</sub>	79.21	125
Starch ->Alum ->H <sub>2</sub> SO <sub>4</sub>	81.68	127.66
pitch ->Starch ->Alum ->H <sub>2</sub> SO <sub>4</sub>	82.34	130.55
Soy ->Starch ->Alum ->H <sub>2</sub> SO <sub>4</sub>	84.08	130.24
pitch ->Soy ->Starch ->Alum ->H <sub>2</sub> SO <sub>4</sub>	83.79	129.91

### 3.3 2D-TLC experiments

Industrial pitch is a complex substance made up of many different components. The separation takes place via the differences in the polarities of the compounds. The R<sub>f</sub> value of fatty acids and resin acids is close to zero at low pH values. Fatty acids and resin acids travel under alkaline conditions when having negative charges. Sterols and fatty alcohols act as neutral compounds, which are not effected by the pH value. The R<sub>f</sub> values of both directions are roughly the same which means, that their spots are on the diagonal. [51]

#### 3.3.1 Class representatives

In order to be able to measure the quantities of industrial pitch components, it was necessary to create calibration lines with the same substances. However, since some components are very difficult to obtain in their pure form and are therefore expensive, cheaper alterna-

tives with identical properties were used. In table 3.6 a list with the main substance classes in the pitch and their associated representatives was created. [3]

**Table 3.6** Pitch classes with associated model components

<b>pitch compound</b>	<b>model compound</b>
Fatty acids	Stearic acid / Oleic Acid
Resin acid	Abietic acid
Sterols	beta-Sitosterol
Fatty alcohols	Docosanol
Betulin	Betulin

### 3.3.2 Procedure

The following preparations had to be made for the separation of the pitch components via 2D-TLC.

#### Eluent preparation

Two different eluents were required in order to be able to separate components with different properties from one another. An alkaline eluent and an acidic eluent were prepared. With the eluents it was possible to separate the substances from one another by means of interaction between silica gel and the respective eluent. As an alkaline eluent, cyclohexane (99.5 % TCI chemicals, Tokyo, Japan) was mixed with ethyl acetate (98.0 % TCI chemicals, Tokyo, Japan) in a ratio of 4:1. Formic acid (99 % Sigma Aldrich, St. Louis, USA) was used for the acidic eluent.

#### Process sequence

In these experiments it is important to keep the experimental process as constant as possible. The substance to be applied had to be converted into dissolved form before application. Since not every substance can be dissolved with the same solvent, specific selections had to be made. Acetone was used as solvent for the model compounds of the calibration line. The industrial pitch samples were dissolved with toluene in order to achieve a better sample yield. The spot was applied to a HPTLC plate with the dimensions 6.5 cm \* 6.5 cm. Changing the size of the TLC plate can lead to significant deviations in the results. The initial point should be in a corner, approx. 1 cm apart from both edges (figure 3.4).

To avoid interference with the environment, TLC chambers were used. The two eluents were added to the respective chambers (approx. 3 ml) and left to stand for a short time (3-5 min) in order to equilibrate the environment within the chamber (figure 3.5).



**Figure 3.4** Location of the initial spot of the industrial pitch sample on the TLC plate (6.5cm \* 6.5cm) for the 2D-TLC method (red circle)

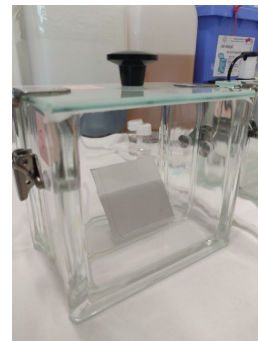


**Figure 3.5** TLC experiment: TLC chamber with TLC plate inserted

The alkaline eluent was used to start. After a waiting time of approx. 5 min, the eluent should be approx. 1 to 0.5 cm from the edge of the TLC plate. The TLC plate is removed from the chamber and the end spot of the eluent on the plate is marked. Subsequently, residues of the eluent on the plate must be removed in order not to have any interference with the following eluent. Since the eluent has a high volatility, it is possible to let it evaporate more quickly using compressed air. After the plate has been dried, it is rotated by 90 ° and placed in the TLC chamber with the acidic mobile phase. The further process for the plate in the acidic eluent is carried out in the same way as the alkaline one.

### Colorants

Since the separated spots can only be seen very weakly or not at all on the white TLC plate, it must be colored to highlight the spots (figure 3.7). A solution of 10 mg Nile blue (figure 3.6), 100 ml ethanol and 0.1 ml acetic acid was mixed for the purpose of coloring. This was applied evenly by hand onto the TLC plate using a sprayer.

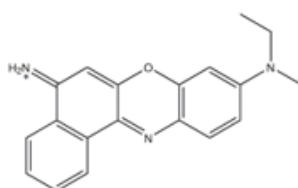


**Figure 3.6** Chemical structure of Nile blue

After the coloring process, the plate was dried again, by using compressed air. Afterwards the plate was digitized immediately 4.3.1. In the next step the plate was placed in the drying cabinet (100 °C), for about one hour in order to remove the last residues of eluent and to set the colorant. After the drying process, the plates were digitized again. The residual amount of eluent can affect the visibility of the spots and further the results of the analysis.

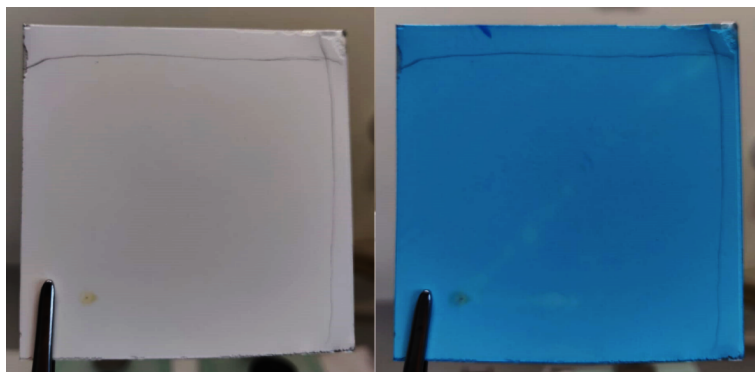


**Figure 3.7** Finished TLC plate before coloring (left) and after applying the coloring agent (right)

### 3.3.3 TLC Calibration line Precautions

Care was taken to ensure that the quantity range was within the limit of detection (limit of detection (LOD)). If the amount was too small, no spot was visible on the plate and couldn't be evaluated (figure 3.9). Excessive amounts will overload the initial spot and will lead to tailing in the separation process. No distinction can be made between the spot and the starting point (figure 3.8).



**Figure 3.8** Upper LOD: Overfilling of the initial spot with sample - Tailing effect



**Figure 3.9** Lower LOD: too little sample applied - no visible spot recognizable

### 3.3.4 Important integrated and developed MATLAB functions

In the following, the most important functions and how they work for graphic image processing and evaluation of the digitized spots are listed and briefly explained.

#### IMFILL (integrated function)

This integrated MATLAB function detects all black pixels that were surrounded by white pixels and changes their colour to white. This important function was used when "spaces" inside the structure need to be filled. The working procedure of the function is shown in figure 3.10.

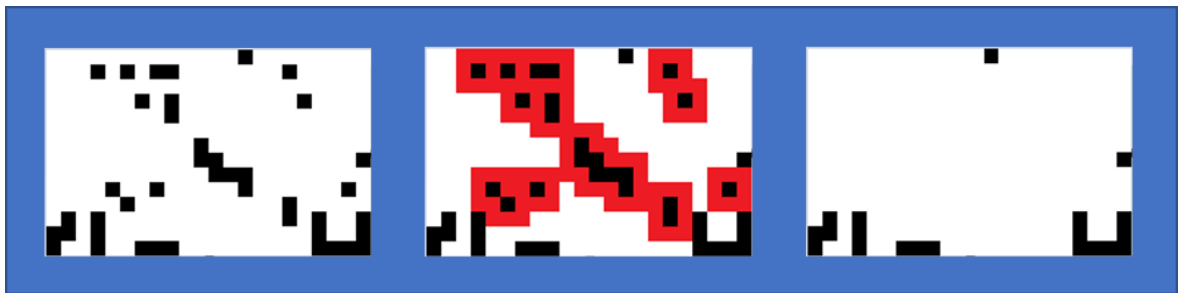


**Figure 3.10** Steps from the "IMFILL" function (Background: white pixel): Start screen (left); Procedure (center); Result (right);

#### CLUSTERFILTER (developed function)

The function (figure 3.11) is developed to filter out the largest, coherent structure. Therefore, all pixel structures are divided into a separate class. The pixel number and its indices are retained in every structure. The structure classes are then sorted according to their number of pixels. The class with the highest number of pixels is searched for and reinserted using the indices of the pixels inside the class.

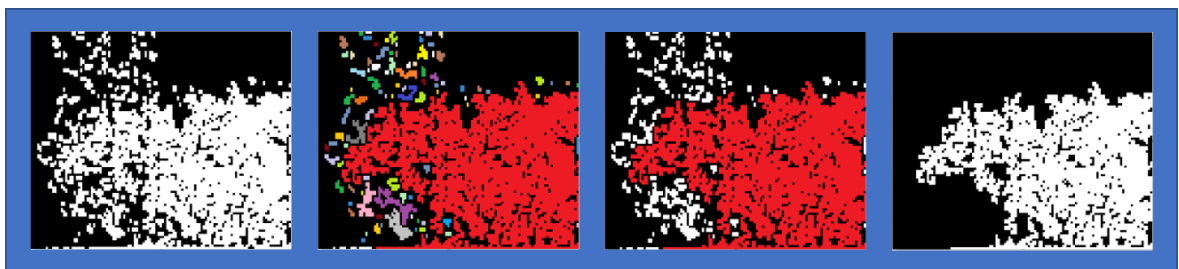


**Figure 3.11** Steps of the "CLUSTERFILTER" function (Background: black pixel): Start picture (left); Classification (center-left); Filter step (center-right); Result (right);

### PIXELKILL (developed function)

The function (figure 3.12) is developed to separate pixel connections which only consist of one pixel. For this purpose, each black pixel is examined in the horizontal plane for opposite, neighboring, white pixels. The same process is also carried out in the vertical plane. If black pixels are found to which this condition applies, they are removed by changing their colour from black to white.



**Figure 3.12** Steps from the "PIXELKILL" function (Background: white pixel): Start picture (left); horizontal and vertical pixel detection (center-left); Elimination (center-right); Result (right)

### GAPFILLER (developed function)

The last function (figure 3.13) is used to remove indentations and notches in a structure. It is checked whether a predetermined length of pixels (50) can connect two free-standing pixels in one plane. If this is the case, a "bridge" is built and the spaces below are filled in with a modified version of "IMFILL".

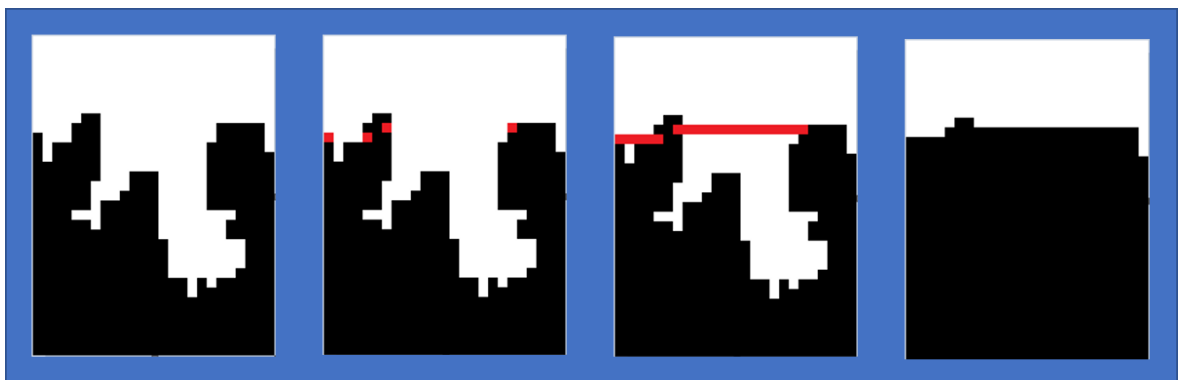


**Figure 3.13** Steps from the "GAP FILLER" function (Background: white pixel): Start screen (left); Pixel search within a defined distance and in the same plane (center-left); Bridging and filling (center-right); Result (right)

## Results

In this part of the thesis results are discussed. The papermaking experiments and the pitch component analysis are considered separately. Furthermore, the creation and the results of the graphic image evaluation are discussed in more detail. In addition, the options and limitations of the software are explained.

### 4.1 Evaluation of starch retention experiments

In the experiments, the duration of the residence time of the individual auxiliary chemicals was varied. For this, starch alone or starch in combination with alum was used. With the stirring time of one to two minutes of each chemical, a pH value of  $6.8 \pm 0.3$  could be achieved. A precise pH value of  $6.800 \pm 0.016$  could only be reached with stirring times of 15 to 20 minutes. It was found that with long stirring times, the cardboard covers stuck onto the paper after the papermaking process and caused slight damage to the paper surface when they were removed. The reason for this could be a faulty product batch of the cover boards. Also, an increased high concentration of starch on the fiber mat surface could lead to a bond between the cover board and the paper. It is assumed that the sticky coverboards only have a minor influence on the tensile and are therefore neglected. Figure 4.1 shows the results of the tensile and starch retention tests.

A comparison of the stirring times showed that very low strength values regarding tensile index, were achieved with short duration. The highest tensile index value was achieved with a stirring time of 15 to 20 minutes using only starch as an aid. The lowest tensile index

value was achieved with a stirring time of 15 to 20 seconds. Starch in combination with alum was used in this setup. Regardless of the stirring time, it was found that the tensile index was lower when using starch combined with alum than with starch alone. This means that alum can also agglomerate starch molecules with one another, thus reducing the ability of the cellulose fiber to bind. Summarized, the presence of alum has a negative influence according to the tensile strength. Short stirring times and the addition of alum lead to a decreased starch retention. It turned out to be unusual that with increased stirring time and the presence of alum, a high starch retention could be achieved. It is assumed that the longer residence times of the chemicals lead to a precipitation of alum and starch together to the fibers. This means that a higher number of starch molecules are bound to the fibers, which results in increased starch retention.

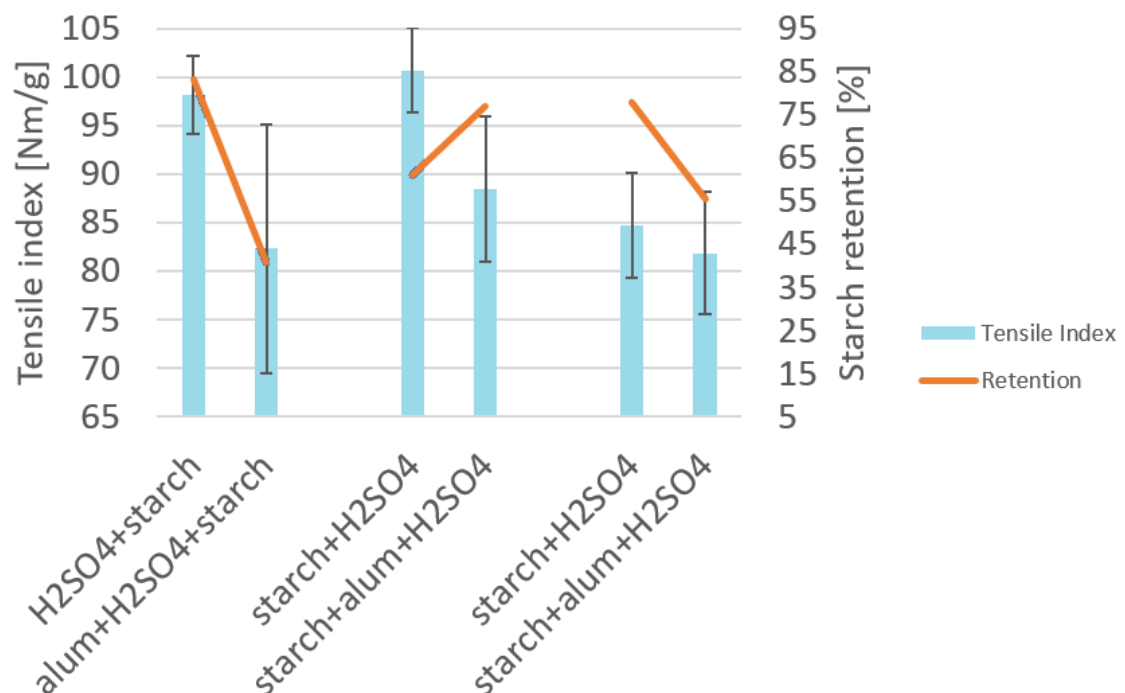


**Figure 4.1** Starch retention experiments: mixing time: 1-2 min (two columns left); mixing time: 15-20 min (two columns center); mixing time: 15-20 sec (two columns right)

## 4.2 Influence of soy protein on paper strength

In figure 4.2 the various trial settings were compared to each other. The trial with only alum and sulfuric acid as auxiliary aid acts as reference setting. In most cases pitch had the influence of reducing strength. The only exception was the setting of pitch combined with

alum. Here a slight increase in strength could be achieved by adding pitch. The reason for this surprising result is unknown, because pitch and alum have a negative influence on the tensile strength. Earlier results have shown, that pitch has a negative influence on paper strength when adsorbed/precipitated on the fibers with a fixative.

The highest tensile strength could be achieved with the combination of soy protein and starch in a ratio of 1:3. In relation to the reference results, an increase in strength of up to 21 % could be achieved with the presence of pitch as in the case of [43]. The addition of only starch and soy protein, respectively, to the papermaking trials yielded similar results. Starting from the reference setting an increase of 11 % was achieved for both cases with pitch included in terms of tensile strength.

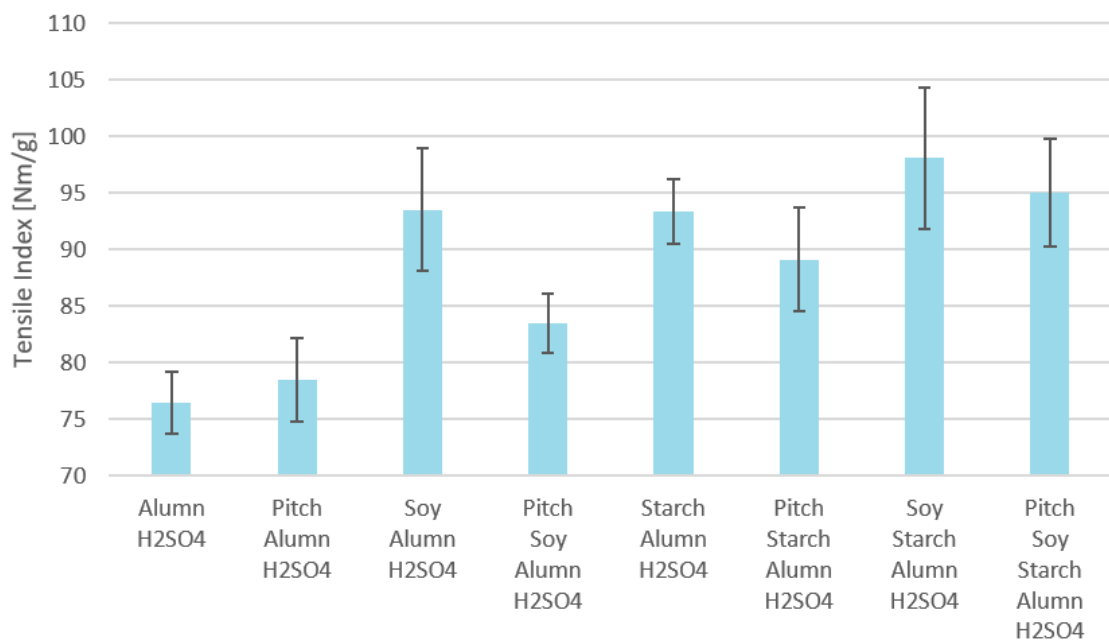


**Figure 4.2** Tensile index experiments: Comparison of aid substance combinations

### 4.3 MATLAB Program for evaluating pitch compounds

The MATLAB software was used for the graphic image evaluation. Images can be quickly and easily modified and processed in MATLAB, which thus serves as the basis for the evaluation. [52] Regarding the evaluation of the digitized spots, the pixel intensity of the colour channels is used. The intensity values in the z coordinate can be plotted over the dimensions of the entire image. To calculate the volume of the generated body (figure 4.3), the intensity values of the pixels are integrated over the area of the image. The volume of

the resulting body can be equated with the applied amount of substance on the TLC plate.  
[53]

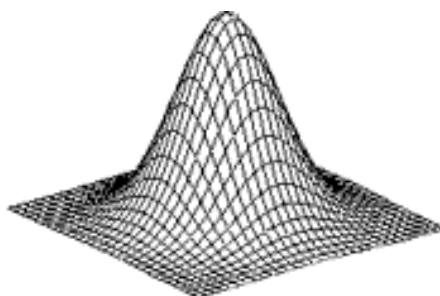


**Figure 4.3** 3D presentation principle to evaluate TLC spots

### 4.3.1 Obstacles

When starting the project, problems and hurdles were identified. The problems that have arisen are described below and subsequently resolved or circumvented.

#### **Spraying problems in staining process**

The spraying of the TLC plates with the colorant was necessary to make the dots visible. Sometimes the slightest spray errors and stains occurred (figure 4.4). These mistakes can occur when dried-up paint residue sticks to the spray head and clogs the exit hole or the colourant is too old and starts to agglomerate. For the evaluation it was necessary to separate the area of the dots as well as possible from impurities. It should be avoided that impurities manifest themselves as consequential errors. To solve the problem, colourants that were more than two weeks old were discarded and newly produced.

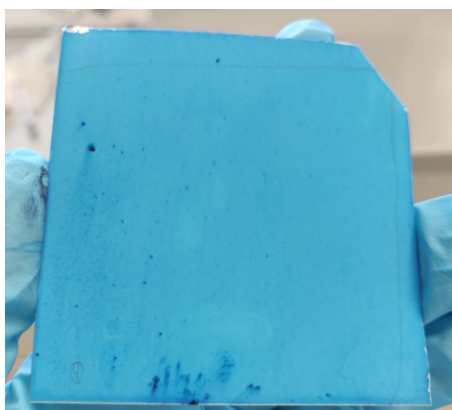


**Figure 4.4** TLC plate with sprayer stains

### Upshifting of fatty acids

During the production of the TLC plates, an upshifting of the fatty acids was found (figure 4.5). This phenomenon only occurred in the IP1 experiments. It is assumed that the silica surface of the TLC plate was slightly damaged when the pitch sample was applied with the capillary tube. As a result of this damage, a detaching flow process of the solvent may have been initiated. Another reason could be an error in the deprotonation of the carboxyl groups. Fatty acids and resin acids in the alkaline running agent are not stuck to their current location on the TLC plate. As a result, they are transported upwards with the sterols and fatty alcohols with a delay. No problem solution could be found for this phenomenon. With the manual spot marking of the second version of the evaluation software (EASY version 4.3.6), it was possible to evaluate also these kind of samples.

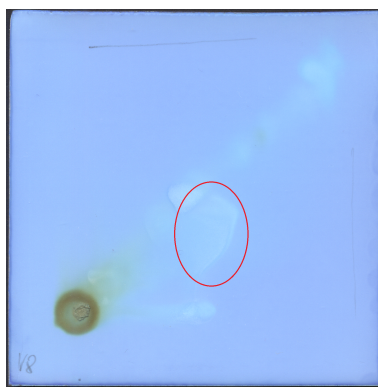


**Figure 4.5** TLC plate with a shifted fatty acid spot (red mark)

### Scanning

The TLC plates were digitized with a UV /VIS scanner (CHROMIMAGE AR2i flatbed scanner; 4800x2400 DPI CCD; 48-BIT COLOR). [52] First the image was saved in the data format joint photographic group (JPG) (figure 4.6), due to data storage space. Later this was changed into tagged image file (TIF) format (figure 4.7). The reason was a error caused by JPG compression. Compression leads to information being lost and leads to a deviation in the measured values. The difference between the TIF format and the JPG format can be clearly seen in the pixel structure of the enlarged area. In JPG format the picture is divided into 8x8 block sections. The compression is carried out by means of color model conversion, low-pass filtering, a discrete cosine transformation and other process steps. [54]



**Figure 4.6** Spot excerpt in JPG format



**Figure 4.7** Spot excerpt in TIF format

In order to avoid reflections and changes in contrast at the edge of the panels due to the light background during the scanning process, a black cardboard was placed over the scanning surface. It was also found that scanning an image often led to strong changes in contrast one after the other (figure 4.8). The explanation for this is that the lamp needs a certain time for the scanning process to level off its intensity. The starting current for electrical components is many times higher than in standard operation, which explains the increased contrast in the first images. Therefore, as a precaution, each image was scanned twice in a row. The first version was discarded and the second used for the evaluation.



**Figure 4.8** Image from the first scan - scanning lamp not yet balanced (left); Image of the subsequent scanning process - intensity of the scanning lamp constant (right)

### 4.3.2 Large-scale digitalization

Several TLC plates were prepared for this analysis. Since the scanning time is relatively long due to the high number of dots per inch (DPI), an attempt is made to convey as many plates as possible, onto a digital image. It should be noted that the TLC plates should be placed in ascending or descending order. Automated separation of the TLC plates turned

out to be problematic, due to impurities (spray errors, scratches,...) and writings on the TLC plate.

To solve this problem, a manual marking method was developed to define relevant areas. The marking procedure and the associated specifications are explained in detail in chapter 4.3.4.

### 4.3.3 Software versions (EXACT vs. EASY)

Two different versions of the program were created for this problem. One specializes exclusively in the present spot configuration. Only fatty acids, sterols and fatty alcohols are analyzed. The version is easy to use and has a high degree of automation. Since in this version the spots are determined and separated pixel by pixel, this version is referred to as the "EXACT" version. In the case that the constellation of the spots and their intensity changes, a second version was created. The focus of this version was simplicity and universal application. This version is referred to as the "EASY" version. For an overview, a rough schematic sequence of the working methods of both versions is attached in the appendix (figure 6.4).

#### Advantages & disadvantages

The advantage of the EXACT version is that the spots are analyzed quickly and precisely and evaluated fully automatically. The negative aspect of the EXACT software was that it could only be specifically applied to the existing problem. In the event of a deviation from the usual spot area, the determination of further substances or a change in the mean intensities of the spots, the automated mask generation reaches its limits.

The EASY version is preferred when new additional substances are to be analysed. Independent of the location, intensity, size and shape of the spots, evaluations can be carried out by means of manual spot definition. The downside of this version is that the results are prone to contamination on the TLC plate. Furthermore, a loss of information must be accepted in the case of spots that are difficult to recognize. Since the spots are marked by the user, the results can vary depending on the marked area. Reproducibility is therefore only possible if the user and its marking pattern remain the same.

#### 4.3.4 Defining relevant areas

Since the spots to be analyzed on the TLC plate are only of small size in relation to the total area, an attempt was also made to narrow down the relevant area. The advantage was that the storage capacity required for the evaluation itself is drastically reduced and consequently leads to less calculation and processing time. For further treatment, these marked areas are cut out and saved automatically using a predefined name. The direction of the sequence is queried in the software. Before the analysis can be carried out, a certain type of marking must be determined. It was decided that by means of PAINT, white, rectangular frames with a width of 3 pixels should be placed.

The reason for the white colour of the frame is that this type of intensity (255) only occurs when the light from the scanner is fully reflected. Other levels of intensity occur more frequently due to the black cover cardboard.

In rare cases some TLC plates had damaged edges (figure 4.9). Silica gel has partially peeled off and the exposed aluminum plate completely reflects the light from the scanner. The consequence of this is that the intensity values occur up the range of 255. To avoid further marking problems, a special function was developed for recognizing clear white frames with a thickness of three Pixel. This made it possible to filter out the marked regions in the visible light scan (VIS) and the UV versions.

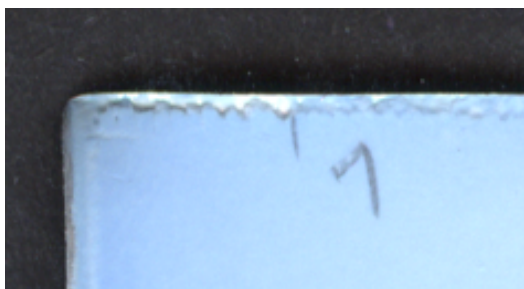


**Figure 4.9** TLC plate: peeling of the silica gel at the edges - caused by damage

In order to exclude contaminations and other disruptive factors on the TLC plates, the automated frame search is guaranteed with the subroutines (bordercheck & bordercheckin). The division into two subroutines was made to save computing time on the one hand and to ensure an error-free search mechanism. Areas will be investigated to ensure the presence of a set frame. The subroutine "bordercheck" (figure 4.10) was used to quickly find potential borders in the whole image via four reviews. All pixel in green, orange and grey are needed to have a value of 255 (white). The two yellow pixels should have an intensity value less

than 250. Are all these conditions met, the next subroutine “bordercheckin” (figure 4.11) starts for verification. All four areas must have an intensity value less than 250. If the conditions of this query have been met, the location of a set frame is guaranteed.

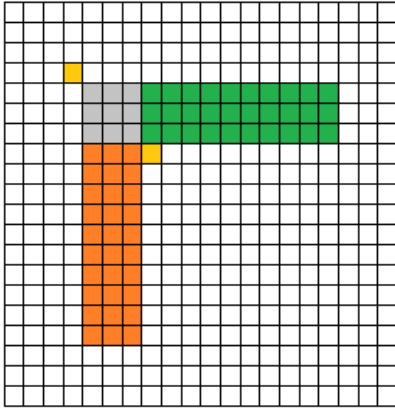


**Figure 4.10** Review sections for a set, white frame; Division into 4 different queries (green, orange and gray must have a value of 255; yellow must have a value less than 250)

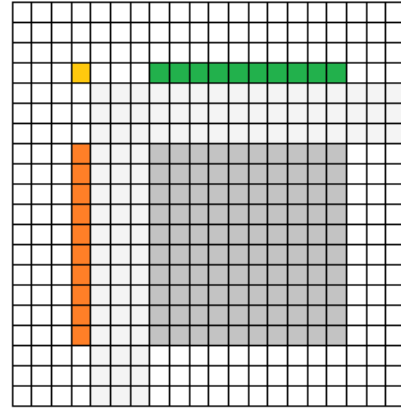


**Figure 4.11** Additional review sections for confirmation; Division into 4 different queries (green, orange, gray and yellow must have a value less than 250)

As the working methods of the two versions differ, different marking processes had to be carried out.

#### TLC Marking steps (EXACT version)

In the EXACT version, the spots themselves were marked with the frames. Unfortunately, it was not possible to mark all spots individually. Some spots were too close to each other. Marking them anyway as single spots, would result in an overlay of the frames. When determining the regions, parts of the neighboring spots influence the calculation of the background intensity values and thus make automated segmentation impossible (figure 4.12). For this reason, it was decided to place the marking region over all spots (two in total) that are too close to one another. The separation of them will be done mathematically via software functions. [55]

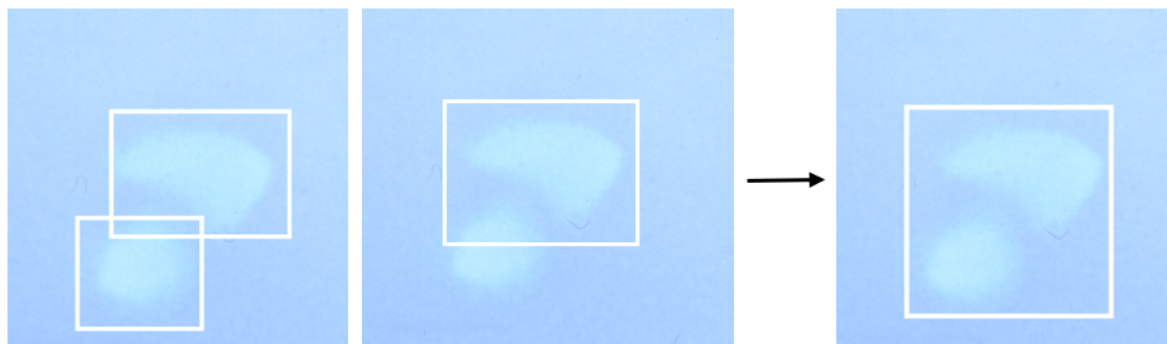


**Figure 4.12** Marking problem: overlapping of the set frames (left) and intensity falsification of the background by the second spot (center); Remedy: summarized marking (right)

### TLC Marking steps (EASY version)

In this version, relevant areas must first be manually marked in the original scan (figure 4.13). In order to retain as many automation steps as possible, new preparations had to be made. A rectangular, white frame with a thickness of three pixels must be placed around the entire relevant detection area of a TLC plate. This means that each marked area can be automatically distinguished from one another using a newly integrated border detection function. This division was always carried out for both image versions (UV and VIS) and is saved with automatic numbering. An additional function has been integrated, to examine different amounts of the same substance on a single TLC plate. These TLC plates correspond to the 1D TLC version. It must be ensured that only one TLC-plate is existing in the entire scanned image. The marking properties of the relevant areas are the same as in the previous version.

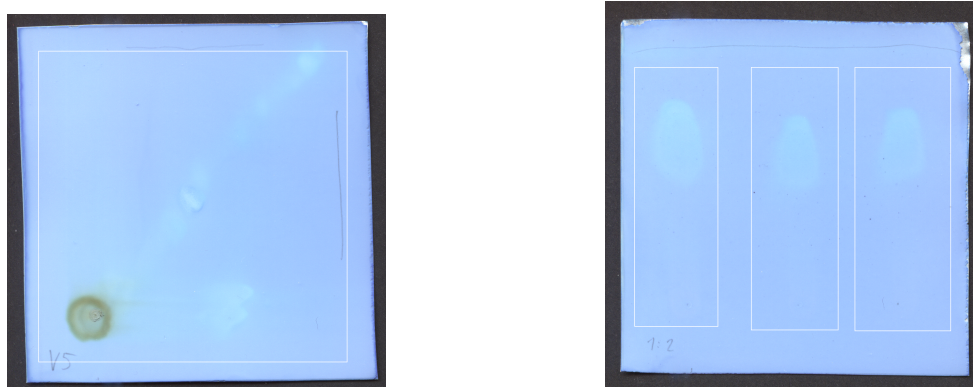


**Figure 4.13** Marking process for two different thin-layer chromatography results: 2D-TLC - marking of the relevant area of the TLC plate - evaluation of multiple TLC plates possible (left); 1D-TLC - separate markings - same substance - only one TLC plate can be evaluated at the same time (right)

After the automated cut-out process the separated pictures were saved automatically in a self-generated folder with their correct names in both versions.

### 4.3.5 EXACT version: Masking system

In this version, so-called "masks" are created for automated spot detection. The masks define the spots on the TLC plates with pixel accuracy, while the entire process stays automated.

#### Color manipulation

The separated images behave like a three-dimensional matrix. The first two dimensions reflect length and width of the image. The third dimension is for the three-color layers (RGB) which add up to the original colour image. The intensity values of a layer give information how strong the appropriate colour is displayed. The spectrum of intensities goes from 0 (no contribution) to 255 (complete contribution).

In order to be able to treat the image mathematically, it must be simplified to a single layer. With gray-scale conversion (figure 4.14), the pixel of the three-color layer can be converted into a single layer with the same value range (0 to 255). The gray values are determined using the formula 4.1 [56].

$$\text{Gray value } (b) = 0.299 \text{ red channel } (c) + 0.587 \text{ green channel } (d) + 0.114 \text{ blue channel } (e) \quad (4.1)$$

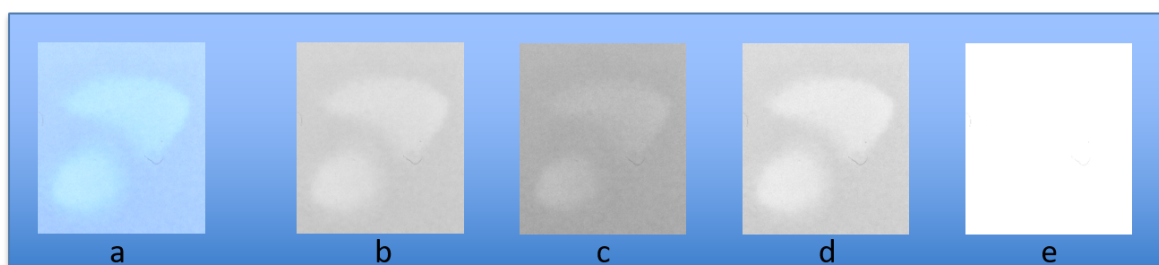


**Figure 4.14** Original image (a) with grayscale image (b) and the individual color channels (c = red; d = green; e = blue)

In terms of contrast, for the spots to be recognized, the grayscale image delivered no satisfying results. When looking at the images in their individual color channels, it was found

that in all cases the green channel could best differ the spots from the background (figure 4.15). This assumption was confirmed by the creation of histograms (figure 4.16) and a binarization of the gray value images using Otsu's method. [57][58]

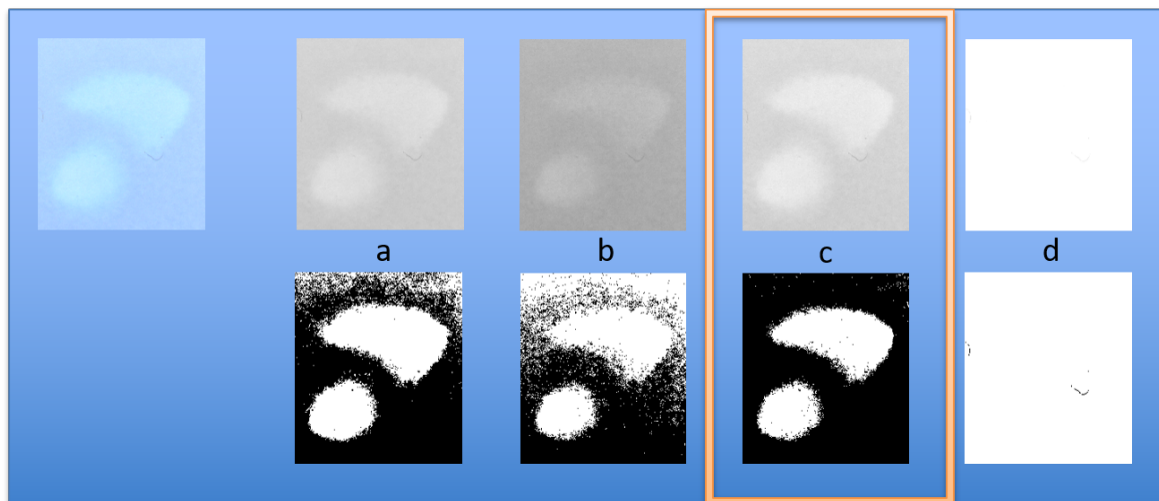


**Figure 4.15** Binarization of the images using Otsu's method (a = grey; b = red; c = green; d = blue) of beta-sitosterol and docosanol: best result - green color channel (c)

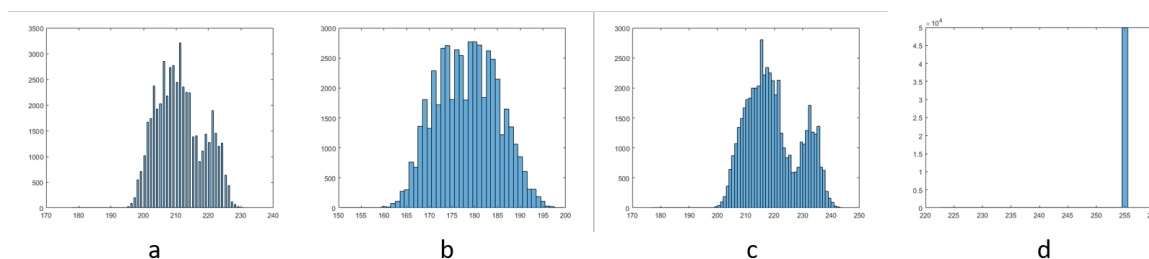


**Figure 4.16** Histograms of the color channels and the grayscale image (a = gray; b = red; c = green; d = blue) of beta-sitosterol and docosanol: Confirms that the green channel is the best choice

### Steps for masking of D&beta-S

In order to be able to determine the exact area of the spots, mathematical operations were developed that could determine these automatically pixel by pixel. However, since the intensity and the spot shape of the various substances varied, a uniform method for a spot detection was difficult or even impossible. A detection model was developed for the following substances: stearic acid, docosanol and beta-sitosterol. The calculation methods for docosanol and beta-sitosterol were kept identical, since these substances were in the same image file and their average intensity was in the same range. For abietic acid a fully automated detection model wasn't possible, because the spot area was way too small.

According to that, all following TLC plates for the calibration were created without resin acids.

Since the spots of beta-sitosterol and docosanol appeared in general with high intensities, the dots can be determined with few operations. In order to be able to assess the result better later, the production of masks was used. A comparison with the original image can then be used to decide how good the automated spot finding was.

The first step of the method was a binarization of the green channel using Otsu's method. All black pixels that were framed by white pixel were turned into white pixel with the "imfill" function. The result was a complete structure and a rough template for both spot areas. To avoid possible impurities from the background a filter system for the two largest pixel clusters was necessary. This was performed by the existing function "clusterfilter". These function sorts all coherent structures, of the entire picture, into classes. The two classes with the highest amount of pixel got filtered out. To differentiate between the two substances, the position in which the dots were located was used. Docosanol was sure to be always above the dot of beta-sitosterol, therefore a vertical check was carried out from top to bottom to ensure that the spots were correctly assigned. Finally, a 5-pixel wide border was added around both structures (figure 4.17) to compensate for possible binarization errors in the edge-region.



**Figure 4.17** Created masks: beta-sitosterol (left); docosanol (right); red frame for security against pixel loss through Otsu's method

The black region in the image (Mask) represents the final area of the substance spots. These will be later used for the calculation of the total intensity amount. The remaining white area, without the areas of both spots was set as the mask of the background.

A comparison of the mask with the spot of the original image shows that the automated spot recognition achieves good results. After the spots were cut out using the masks, they were displayed as a 3D image to illustrate the influence of the background (figure 4.18). Even small surveys in the background can lead to a serious change in the result. By using

the masks, only areas related to the spot can be used for mass calculation. In addition, a third one can be created for the background using the two existing masks. This mask is only required for the contrast correction in the later process.

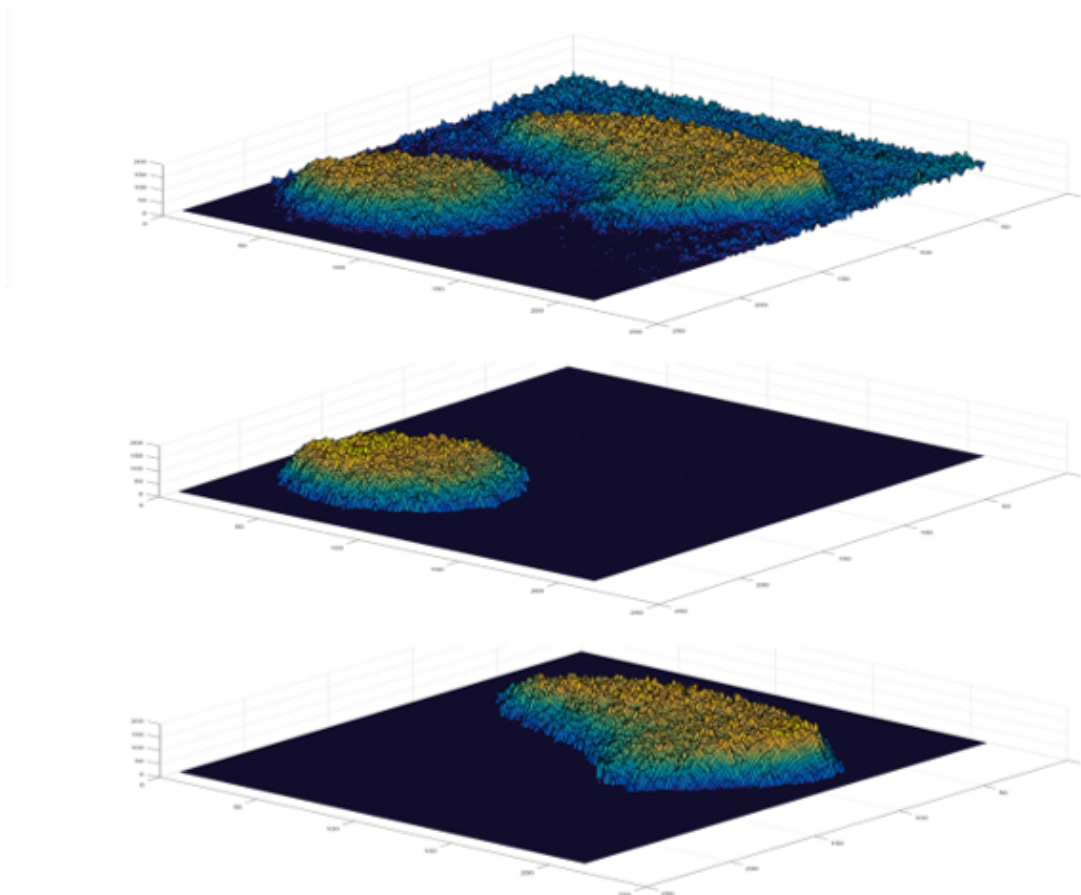


**Figure 4.18** 3D view of the evaluation (EXACT version): initial image (top); beta-sitosterol spot (middle); Docosanol spot (bottom); separation via masks

These steps were carried out for all created TLC plates of the calibration lines identically.

#### Steps for masking of fatty acid (FA)

The mask generation for fatty acids turned out to be difficult because the intensities of the spot differ only slightly from its background (figure 4.19). It was not possible to binarize the entire green channel image using Otsu's method, as a slight unevenness of the background emerged due to the manual coloring of the TLC plate. [58] Even with the check by creating histograms (figure 4.20), it was not possible to generate a simple contrast difference between the spot and the background, which would provide a sufficiently satisfactory result. Therefore, additional operations had to be added to be able to create masks.

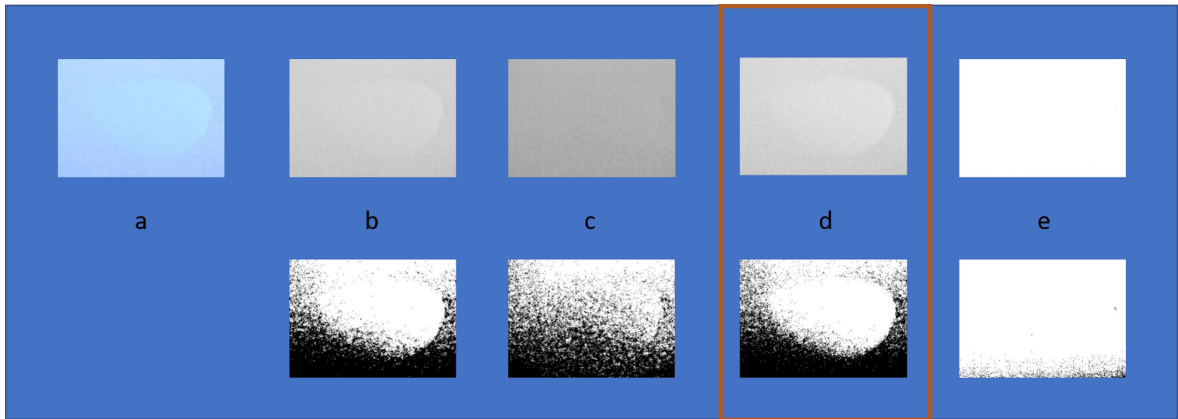


**Figure 4.19** Binarization of the images using Otsu’s method (a = original; b = grey; c = red; d = green; e = blue) of fatty acids: best result - still green color channel (c)

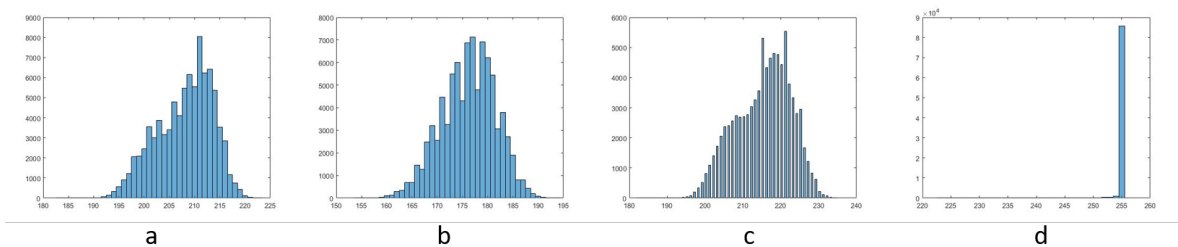


**Figure 4.20** Histograms of the color channels and the grayscale image (a = gray; b = red; c = green; d = blue) of fatty acids: green channel is the best choice for further operations

With the following steps it was possible to automatically generate masks from the spots of fatty acid. In the first step (figure 4.21) the green channel of the image was divided into four quadrants. These were then binarized separately using Otsu’s method and reassembled into one image. This picture was used as the starting point.

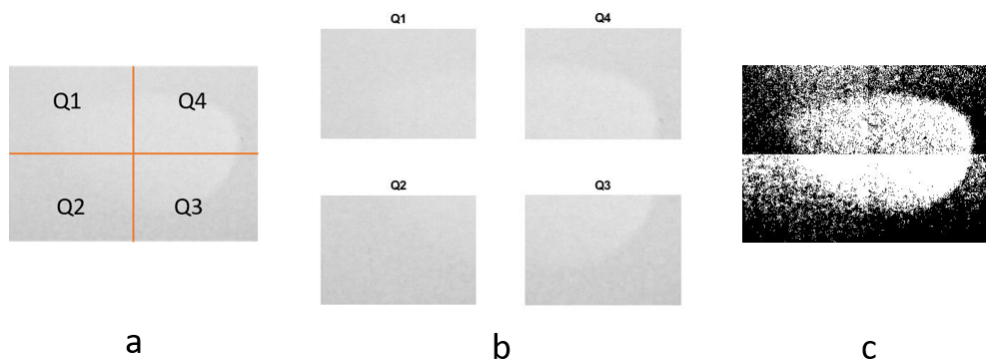


**Figure 4.21** Operation 1 to improve contrast: division into 4 quadrants (left); separate binarization of the squares (middle); re-assembling (right)

One can see immediately that the transitions between the quadrants are quite uneven. To avoid this, new sections (figure 4.22) of the original image were cut out. The image was divided into nine even parts. The new sections, that cover the problematic transitions of the Quadrants were binarized again.

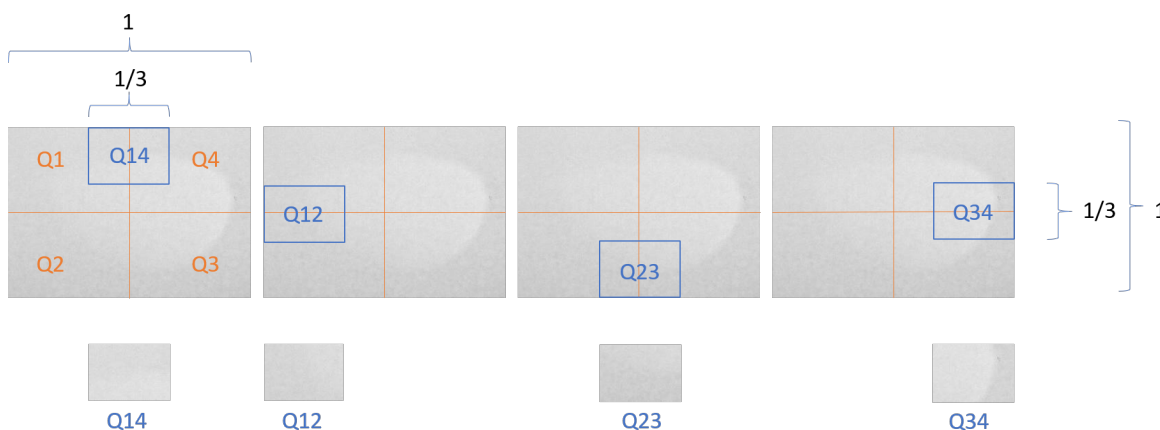


**Figure 4.22** Operation 2 for contrast enhancement: improvement of the transitions; division into 9 segments; again separate binarization of the transition segments

Subsequently, these parts were also inserted back into the already combined picture. In the next step, the gaps within the structure were filled with the function "imfill" (figure 4.23 a). Now that there was a solid structure, impurities in the background had to be removed. For this purpose, all white, continuous contiguous, interconnected pixel were listed and sorted according to area by the function "clusterfilter". The largest area (highest amount) of connected pixels was filtered out (figure 4.23 b). Still there were parts of the background connected to the structure. These parts do not match parts of the spot area. To get rid of those further improvement steps were necessary.

All black pixels from the original image of the first step were reinserted (figure 4.23 c). A step was developed, to sort out all single connections (pixelkill). This was necessary to delimit interfering regions which were bound to the main structure by just a few pixels (figure 4.23 d). This problem got solved by using two queries. The first query checked if a white pixel was adjacent with two white and two black pixels. The next query it was checked whether the white neighboring pixels are opposite. If that was the case, the white pixel was changed to black. Once again, all pixel clusters were divided into classes and filtered out via the function "clusterfilter" (figure 4.23 e). The black regions inside the structure were removed again with the function "imfill" (figure 4.23 f). A rough version of the spot structure was getting visible. As with the mask system of docosanol and beta-

sitosterol, a frame with a width of 5 pixel was added around the existing structure in order to compensate for information losses near the edge (figure 4.23 g). Empty spaces inside the structure (figure 4.23 h) were removed and channels that got protruded into the interior of the structure were closed with the function “gapfiller” (figure 4.23 f). In the final image the black area has been defined as mask for the fatty acid spot. The remaining white pixels in the image were used as a mask for the background, which is used for later calculations.

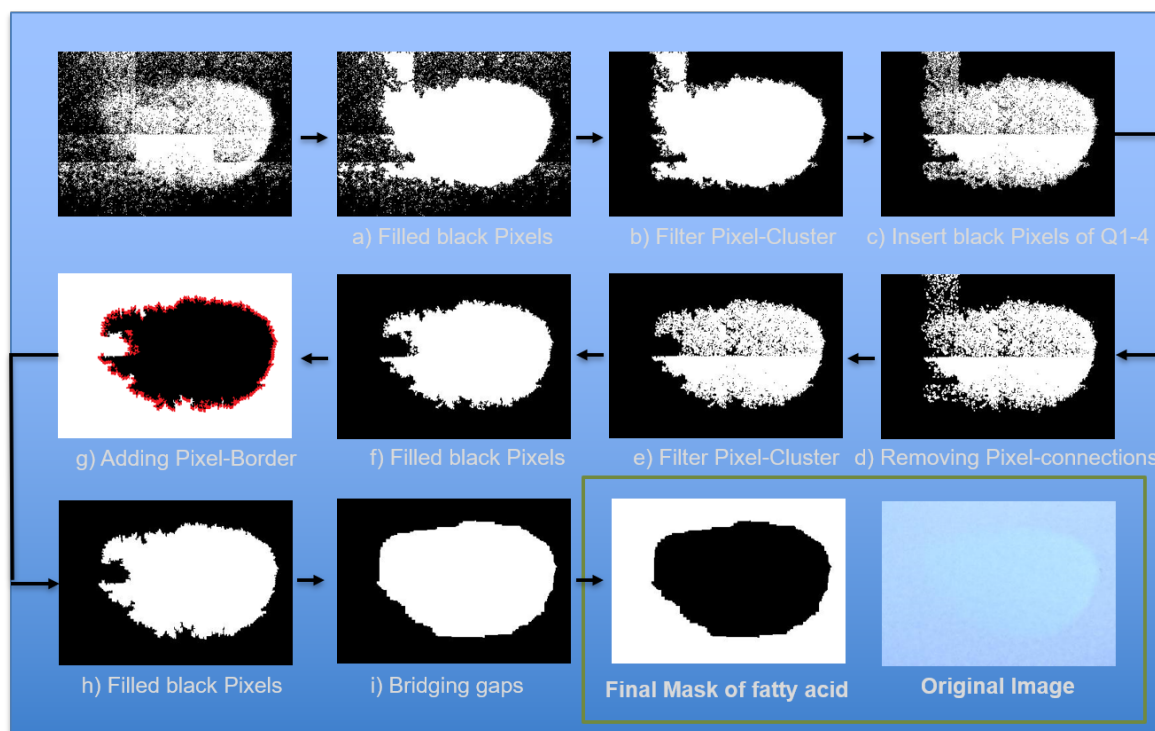


**Figure 4.23** Operation 3 for contrast enhancement: removal of the internal voids (a); Removing the surrounding collections of pixels (b); Reintroduction of the black pixels from operation 1 (c); application of Pixelkill (d); application of cluster filter (e); Application of Imfill (f); Adding border around the structure (g); Application of Imfill (h); Application of Gapfill (i); Comparison of the original image with the mask created for fatty acids

The use of masks is particularly beneficial for this group of substances. Since these stand out only very slightly from the background, it is important to determine the exact boundaries of the spot for the calculation. From the comparison of the 3D versions (figure 4.24), the influence of the background noise can be seen. This noise can further lead to high deviations in the results.

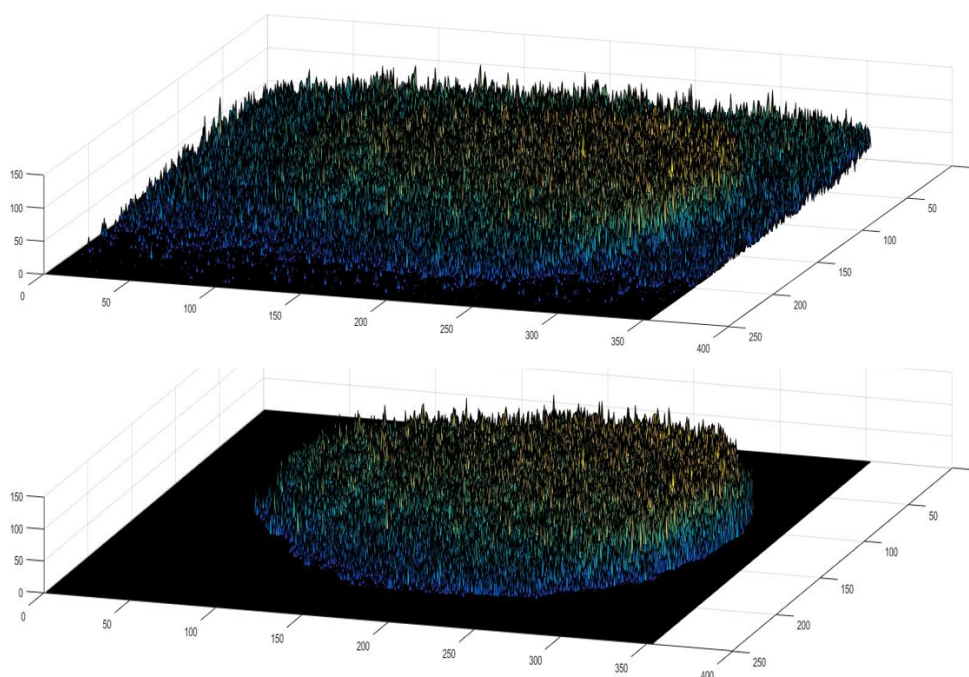


**Figure 4.24** 3D view of the evaluation (EXACT version): initial image (top); fatty acid spot (bottom); separation via mask

### 4.3.6 EASY version: manual spot defining

As already mentioned, the focus of this version is easy usage and a wide range of applications. Therefore, as in the previous version, specifications must be made to classify the problem. These specifications are defined in the main program (SimpleMain). A list of the specific input options is shown in the table (4.1).

**Table 4.1** Questions about the definition of the problem definition of the EASY version

Question	Input options	Standard input
Measuring Pitch or Calibration?	[P/C]	Pitch
Main Measurement in VIS-Pics? (else UV)	[Y/N]	Yes
Creating new Data?	[Y/N]	Yes
What resolution was scanned at?	Number	600
How many TLC plates will be measured?	Number	1
Number of measuring Components?	Number	1
Order and Names of Component	Name	Retry
Data from Excel file? (Otherwise manual input)	[Y/N]	Yes
Measurement of VIS-versions and UV-versions?	[Y/N]	Yes
Is the spot darker than the background?	[Y/N]	Yes

The first function (Picgen\_2D\_white\_TLC and Picgen\_2D\_black\_TLC) is used to separate the marked regions of the original image. The frame inserted in Paint is automatically found, cut out and saved with correct numbering. The respective process is used depending

on the type of image (UV / VIS). When analyzing a calibration line, it is possible to choose between the selection of a ready-made EXCEL table and the manual entry of the associated mass values. The recommended format in the case of an EXCEL table is shown in table 4.2.

**Table 4.2** Format template for pre-defined mass integration via EXCEL tables

	1	2	3	4	5	6	7
Unit	$\mu\text{g}$						
Stearic Acid	184.7	118.3	82.8	59.1	37.8	21.3	10.7
Abietic Acid	39.2	25.1	17.6	12.6	8.0	4.5	2.3
beta-Sitosterol	143.6	92.0	64.4	45.9	29.4	16.6	8.3
Docosanol	46.4	29.8	20.8	14.9	9.5	5.4	2.7

In contrast to the previous version, this one requires individual marking of the spots. For this, a polygon can be drawn manually around the spot with the sub-program “drawpolygons”. As shown in figure 4.25 it is necessary that a small part of the background of the spot is included in the delimitation. The drawn border is used in the later process to calculate the mean intensity of the background. It is recommended to keep parts of neighboring spots as far away as possible from the marking.

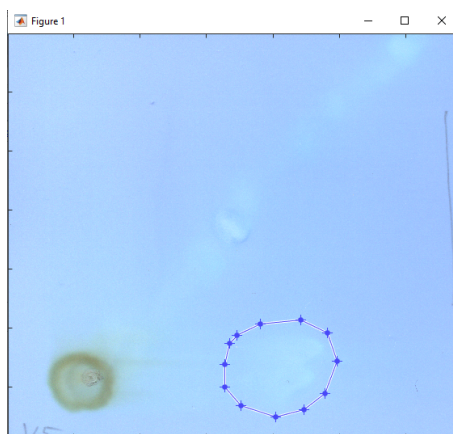


**Figure 4.25** TLC plate with manual polygon spot selection of the EASY version

Depending on the entered number of substances to be examined and the number of TLC plates that have been read in, the polygon marking is automatically called up. If manual marking is unsatisfactory, it is possible to carry out the marking process again. The manually selected areas are saved individually and numbered for verification purposes.

### 4.3.7 Background-Correction & Calculation

The determination of the intensity can be equated with an integration over the entire image area. Only with a white, homogeneous background is it possible to perform a simple

integration to determine the summed intensity of the spot. Since the entire TLC plate was sprayed with a dye to make the dots visible, a uniform background had to be created first. When the TLC plates were compared with one another, a constant deviation in the background coloration could be confirmed. These differences have a great influence on the result and would consequently lead to deviations as a consequential error. Therefore, mathematical precautions were taken which standardized the background of each image. In equation 4.2, 4.3 and 4.4) all gray values are 8-bit values between 0 and 255 and have a dimensionless unit. Following steps were performed to generate a uniform background in the EXACT version (figure 4.26):

1. Inverting the grayscale image (spot needs to be darker than the background in the EXACT version)

$$\text{Inverted image}[\ ] = 255 - \text{gray value image}[\ ] \quad (4.2)$$

2. Contrast correction

$$\text{New contrast}[\ ] = \text{Inverted image}[\ ] * \frac{255}{\text{mean gray value (Background)}[\ ]} \quad (4.3)$$

3. Re-inverting

$$\text{Re - inverted image}[\ ] = 255 - \text{New contrast}[\ ] \quad (4.4)$$

The combination of these steps results in the formula 4.5. The constant

$$c = 1.792 * 10^{-3} [\text{mm}^2 * \text{pixel}^{-1}]$$

is used as a correction factor to make the result independent of the resolution during the scanning process.  $GV_P$  represents the gray value of each individual pixel in the image, where  $GV_{BG}$  is the mean gray value of the background of the spot.

The result is calculated by summation of all modified pixel intensities over the entire image area. Image intensities are represented with 8 bits and range from 0 to 255. Calculated, negative intensities are set to zero and floating point numbers are rounded to whole numbers during the evaluation.  $I_s$  is the corrected, nominated intensity signal from the spot and has the unit  $[1 * \text{mm}^2]$ .

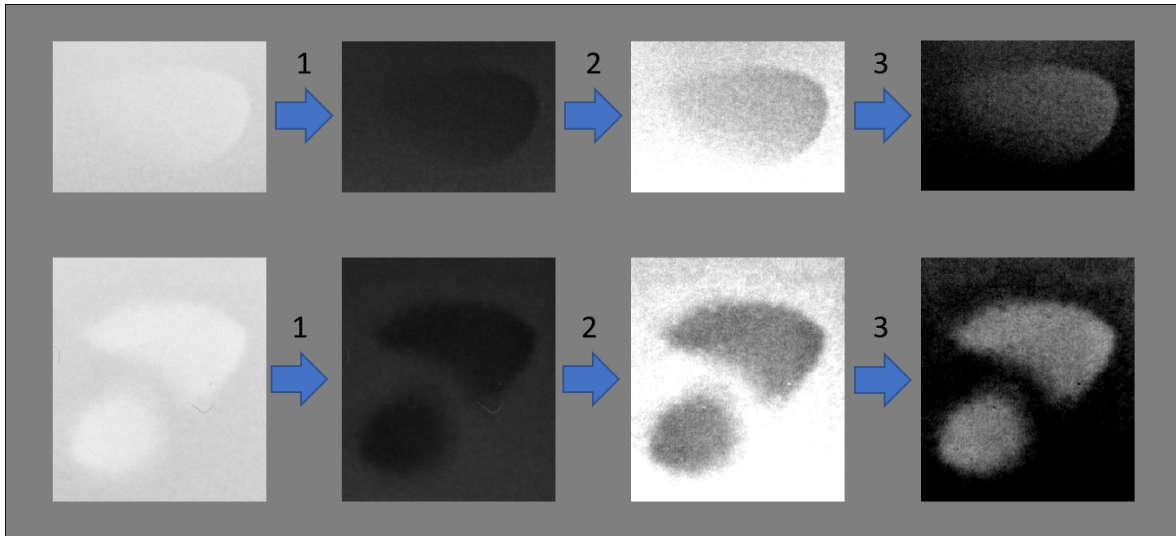


**Figure 4.26** Contrast manipulation: Steps to transform the image for easier calculation: Inversion (1); Contrast correction (2); Re-inversion (3)

$$I_s [1 * mm^2] = 255 * c [mm^2/pixel] * \sum^{all\ pixel} \left( 1 - \frac{255 - GV_{pixel}}{GV_{BG}} \right) \quad (4.5)$$

By a comparison of the original and the standardized image in 3D, a clear difference could be determined in the results.

In the EASY version the contrast of each polygon marked is corrected by using an averaged intensity value of the background, as in the “EXACT” version (figure 4.26) chapter 4.3.7. The difference of this version is that the average intensity of the background is determined via the border pixels of the drawn polygon. After each contrast correction, an image preview is created in which the user can decide to carry out further manual contrast corrections. These subsequent corrections are changed by a percentage input value (figure 4.27).

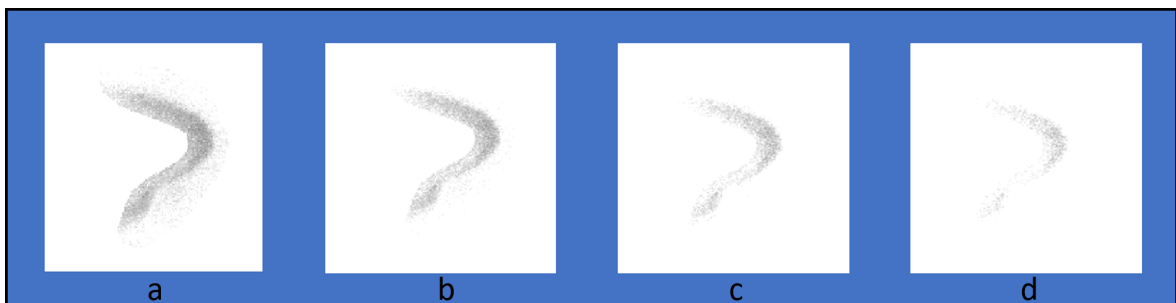


**Figure 4.27** Manual contrast correction of the EASY version: original result (a); 10 % contrast correction (recommended) (b); 20 % contrast correction (c); 30 % contrast correction (d)

After the contrast corrections of all images have been completed, the collected data is automatically sorted and saved in an EXCEL file. Additional information such as the selected order of the components and the associated mass values in the case of a calibration are also noted. The graphical evaluation of the measured values and the creation of the regression line were carried out in EXCEL, since problematic values (outliers) could be removed quickly and easily.

## 4.4 Calibration results

This part summarizes the results from the calibration tests. The results of the EXACT version and the EASY version are dealt with separately.

### 4.4.1 Offset error

In general, the regression lines show a small offset error (figure 4.28). This occurs because at low amounts the software can't differentiate between spot and background noise. With very low amounts of substance, no spot is visible on a TLC plate. Due to the spot finding process the biggest connected cluster of the TLC plate (noise) is filtered out and evaluated. For prevention, the calibration line was forced through the zero point. The side effect is a decrease of the coefficient of determination.

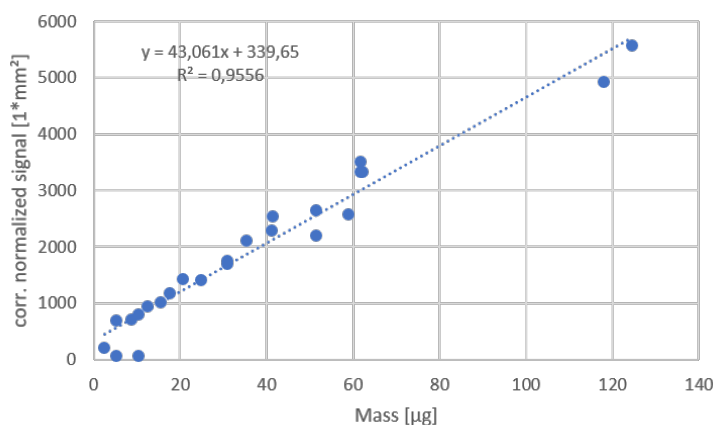


**Figure 4.28** Calibration line with offset error in the small quantity range: stearic acid (EXACT version)

#### 4.4.2 EXACT version

In the graphical evaluation, it could be seen that the calibrations created for the fatty alcohols and the sterols fit well together. In the case of the fatty acids, it was noticeable that calibration 1 differed from the others (figure 4.29). The reason for this was that in addition to stearic acid, abietic acid was added (figure 4.30).

Hence, calibration 1 was excluded in the fatty acid calibration line (figure 4.31). Individual regression lines were created for each substance from the data collected. The associated equation and the coefficient of determination were also given using the EXCEL function.

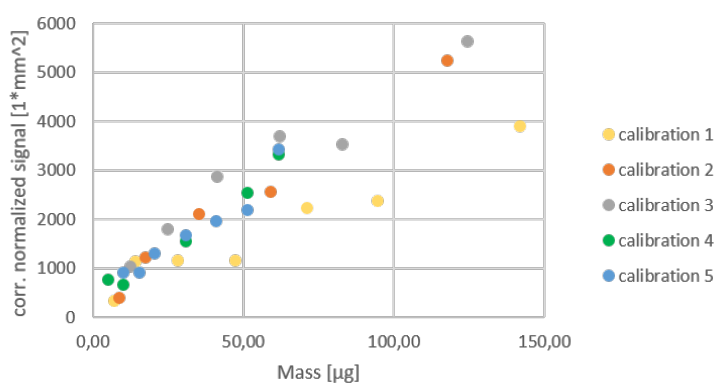


**Figure 4.29** Calibration line: stearic acid - comparison of all calibration attempts (EXACT version)



**Figure 4.30** UV scan: pure stearic acid spot (left); spot with stearic acid and abietic acid (right)

When creating the calibration line for fatty alcohols (figure 4.32) and sterols (figure 4.33), calibration 1 did not have to be removed because the measured values of this calibration matched the values of the other calibrations very well. The reason for this is that there were no other interfering substances in these areas. After inserting the regression line, a small offset error could also be found for these substances. As well as with fatty acid, the calibration line of sterols and fatty alcohols was forced through zero.

The results of the calibrations confirm that the automated graphical evaluation system works particularly well with pure, good separated substances. Especially in the case of sterols and

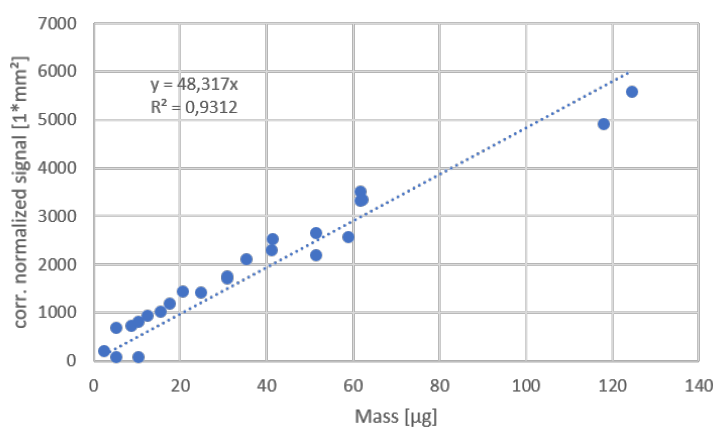


**Figure 4.31** Calibration line: pure stearic acid - exclusion of the first calibration attempt (EXACT version)

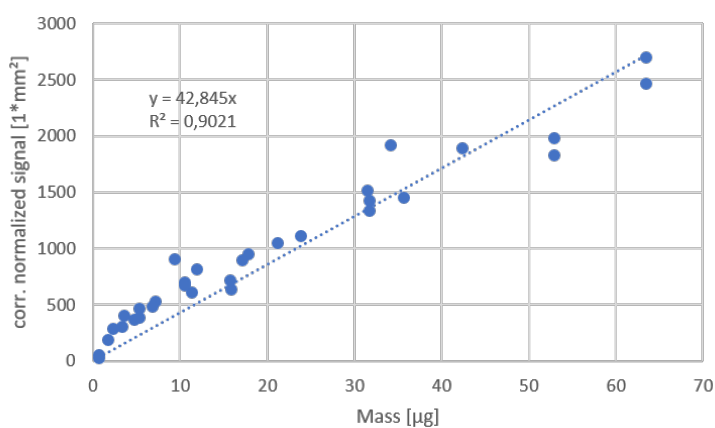


**Figure 4.32** Calibration line: beta-sitosterol (EXACT version)

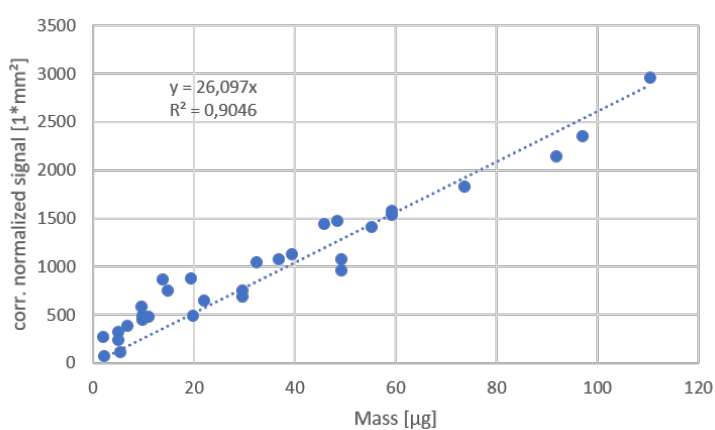


**Figure 4.33** Calibration line: docosanol (EXACT version)

fatty alcohols, linear calibration lines could be achieved thanks to the precise separation of substances.

### 4.4.3 EASY version

As in the EXACT version, good results of the calibration lines for sterols (figure 4.34) and fatty alcohols (figure 4.35) could be achieved in this version. However, it was noted that the slopes of the calibration line were in both cases slightly lower than in the EXACT version. A reduction in the coefficient of determination was also found for both substances.

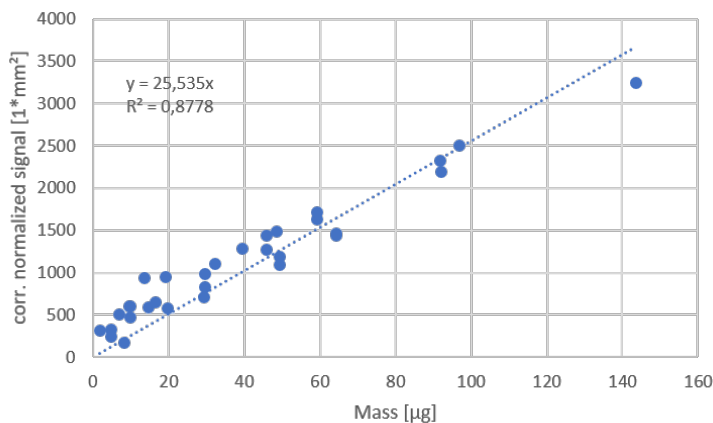


**Figure 4.34** Calibration line: beta-sitosterol (EASY version)

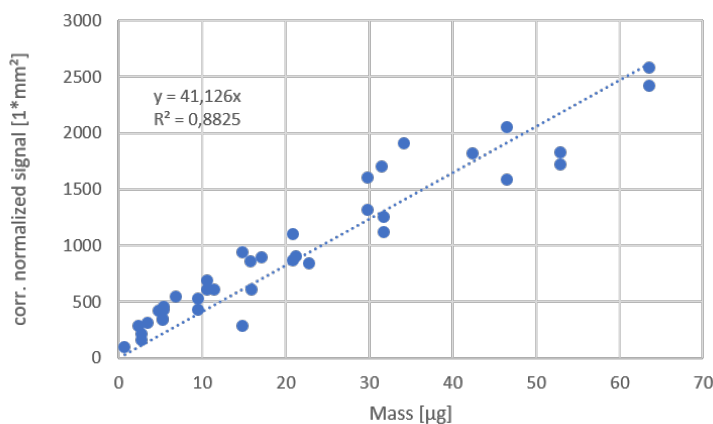


**Figure 4.35** Calibration line: docosanol (EASY version)

In the EASY version, the problem of fatty acids and resin acids was looked at again. Additional tests for the calibration line were carried out, in which fatty acids and resin acids were treated separately from one another (figure 4.36). The results of the combined and separated tests showed that the slopes of the calibration lines had large deviations. This shows that the two substances interact with each other during the separation process.

The calibration data for pure stearic acids was used for evaluations of pitch samples in which no resin acids were present. Further, it was decided to calibrate the fatty acids only

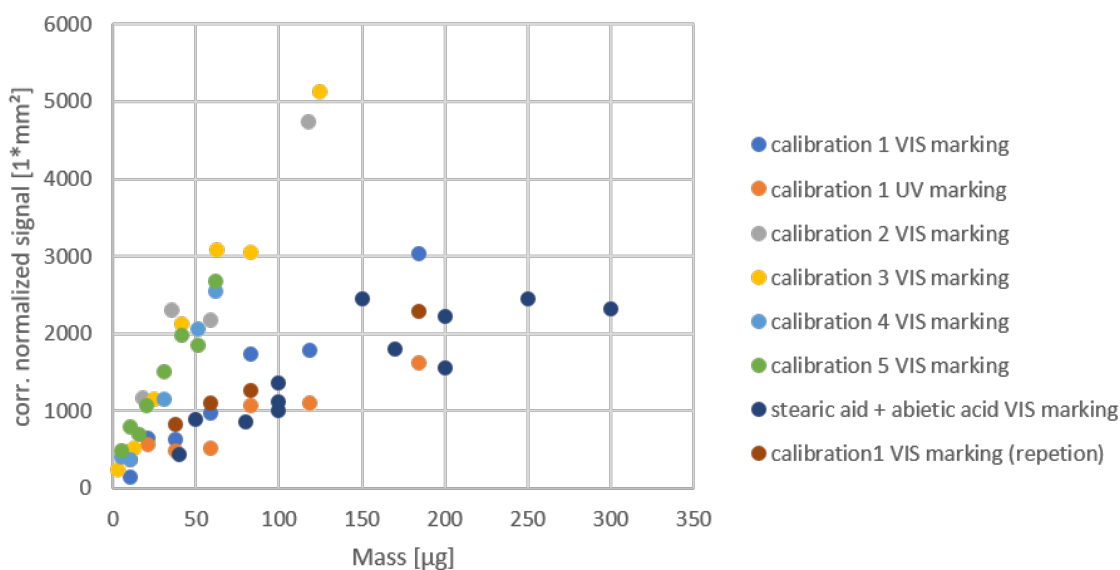


**Figure 4.36** Calibration line: data from all stearic acid experiments (EASY version)

in the presence of resin acids for pitch samples, where both substances occurred. Due to the fact that the spots of both components overlap and are very difficult to separate from each other in manual marking, a new system for the type of marking was developed (figure 4.37). Calculation errors based on background errors caused by the existing problematic marking system should be avoided as far as possible. In the first step of the new method, the entire region spots of both substances was marked together in the VIS version. The region of the resin acids could be defined precisely and evaluated in the UV images. With the option to calculate both versions, it is possible to set markings in the UV version and get a corresponding result of the VIS version. In the last step, the value of the resin acids obtained (VIS version) was subtracted from the total value of both substances (VIS version). The new calibration values show linear progressions. Similar slope values could also be determined for both substances. When evaluating the data, the degree of certainty is more than 10 % higher for abietic acid than for searic acid. The data is clearly shown in the figures 4.38 and 4.39. In the abietic acid calibration curve, the presence of stearic acid did not affect the result. The reason for this is that abietic acid has a much higher intensity compared to stearic acid and the influence of stearic acid is negligible.

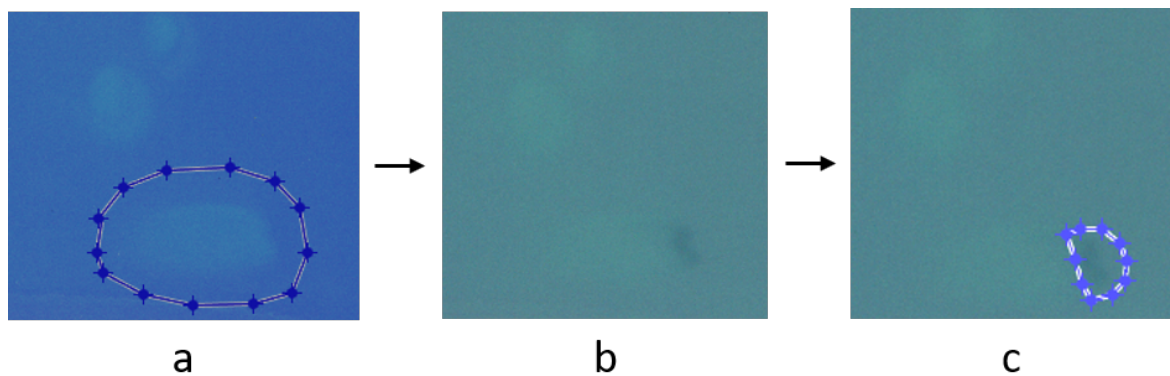


**Figure 4.37** new process for determining the spots of stearic acid in combination with abietic acid: marking both spots together in the VIS image (a); switch to UV image (b); Marking of the abietic acid (dark spot) in the UV image (c); determination of the stearic acid signal by subtracting the abietic acid spot from the total spot

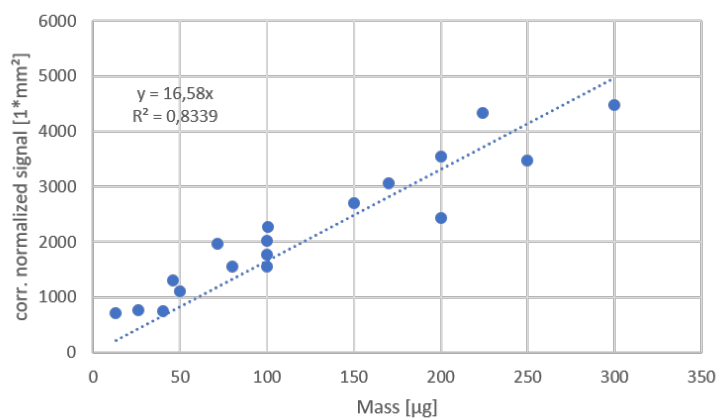


**Figure 4.38** Calibration line: stearic acid in the presence of abietic acid (EASY version)

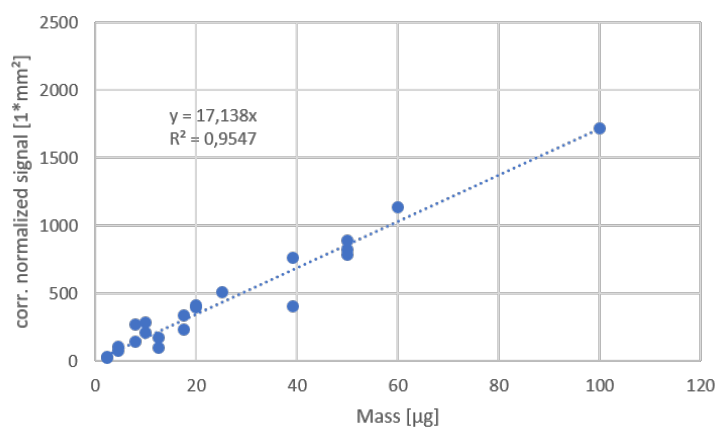


**Figure 4.39** Calibration line: abietic acid with and without the presence of stearic acid (EASY version)

#### 4.4.4 Comparison (EXACT vs. EASY)

When comparing the new evaluation method to the old one, some similar results could be achieved. In general, it was found that the slope values of the calibration lines are higher in the EXACT version than in the EASY one. It is assumed that parts of the spots are neglected with the simplified marking method. A drop in values of 2.2 % to 4 % was found for Docosanol, beta-sitosterol and fatty acid. In the evaluation of fatty acid combined with resin acid, the value drops were increased by 10 %. Calibration 1 was not taken into account here because the resin acids could not be evaluated in the EXACT version. For a clear comparison, the gradient values of the calibration lines and their associated coefficient of determination of both software versions are shown in table 4.3.

**Table 4.3** Comparison of the gradient values of the EXACT and EASY version

	EXACT slope	R <sup>2</sup>	EASY slope	R <sup>2</sup>
Stearic Acid	48.317	0.9312	41.945	0.948
beta-Sitosterol	26.097	0.9046	25.535	0.8778
Docosanol	42.845	0.9021	41.126	0.8825

#### 4.4.5 Betulin (birch pitch sample)

In addition to the substances mentioned above, it was decided to create another calibration series for betulin. It appears mainly in the bark of birch woods. To create a calibration line, the position of the spot on the TLC plate first had to be determined again (figure 4.40). The location of betulin was just below the sterol spot.

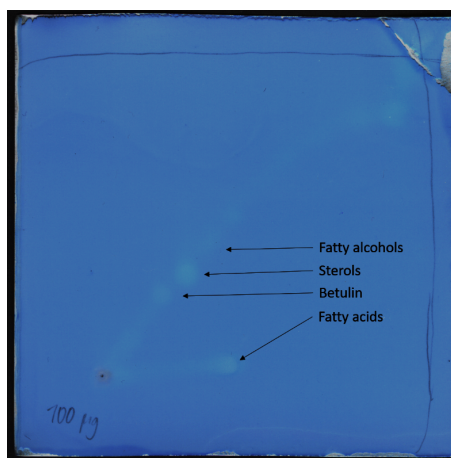


**Figure 4.40** TLC plate: with assigned substances to the spots

Various tests were also carried out in which, in addition to betulin, beta-sitosterol was

applied to the same TLC plate at the same time. The reason for this was that these substances generally have similar properties and their spots are very close to one another. The graphical evaluation of the data for a calibration line yielded good results (figure 4.41).

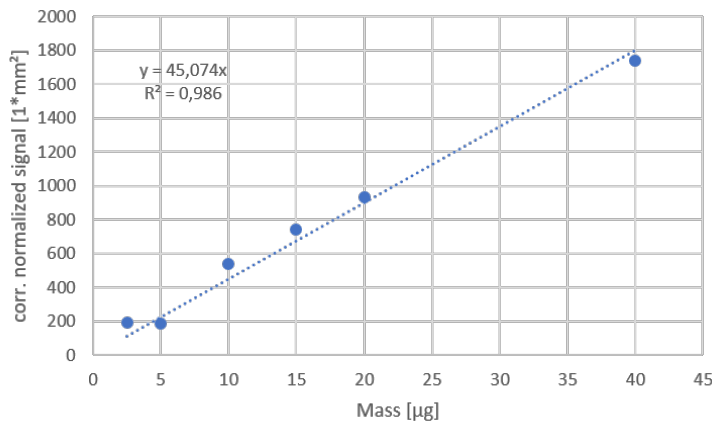


**Figure 4.41** Calibration line: betulin (EASY version)

The following table (4.4) summarizes the used values of the equation from the regression lines for further investigations of the industrial pitch samples.

**Table 4.4** Summarized slope values for further evaluation (EASY version)

	<b>slope</b>	<b>R<sup>2</sup></b>
Stearic Acid (only S)	41.95	0.948
Stearic Acid (S+A)	16.58	0.8339
beta-Sitosterol (beta-S)	25.54	0.8778
Docosanol (D)	41.13	0.8825
Abietic Acid (A)	17.14	0.9547
Betulin (B)	45.07	0.986

## 4.5 Industrial pitch analysis

In the following section, the evaluations of the five different pitch samples are discussed. Most of the evaluations were carried out with the EASY version, as the EXACT version was specially tailored to the constellation of the IP1 and the IP2 sample and therefore could not be used on other samples. The results of the 2D-TLC method were also compared with the results from GCMS analysis. Sample images of the TLC plates and their spot evaluation of the five different pitch samples are attached in the appendix (figure 6.1, 6.2 and 6.3). In addition, the relative quantities of the individual TLC plates for all different pitch samples

were summarized and statistically evaluated in tables 6.1, 6.2, 6.3, 6.4, 6.5, 6.6 and 6.7 in the appendix.

#### 4.5.1 EXACT version (only for IP1 & IP2 sample)

In total 21 TLC plates were created with the IP1 sample, but only 9 of them could be evaluated via EXACT version. TLC plates with upshifting fatty acid spots could not be used in the EXACT version, since in these cases an automated mask creation was not possible. From the IP2 sample, 12 TLC plates were produced. All TLC plates of the IP2 sample could be evaluated with the EXACT version.

The spots for fatty acids and resin acids of the industrial pitch samples couldn't be separated with the same result as sterols and fatty alcohols (figure 4.42). Even after the contrast correction, these spots couldn't be separated from each other.

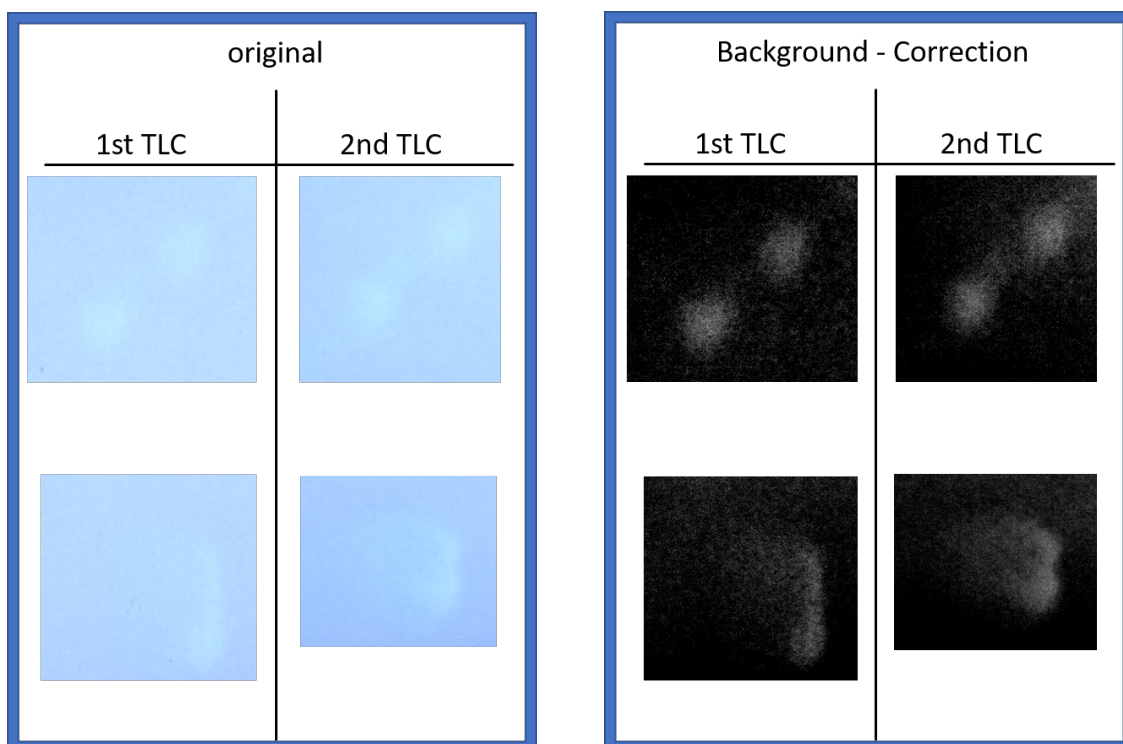


**Figure 4.42** Separation of the IP1 sample using 2D-TLC: original image (left); after contrast correction (right); Identification of fatty acids (lower images), sterols and fatty alcohols (upper images)

Since the EXACT version is not able to determine resin acids separately, the spots of both substances were merged in this case and viewed as uniform. When comparing the values of the 2D-TLC method with the GCMS analysis, good results could be achieved. The results show only slight differences from the analytical values. For the reason, that the values of the IP2 sample just differ slightly from the values of the IP1, both pitch samples were

compared with the GCMS analysis of the IP1 as shown in figure 4.43. In figure 4.44 it can be seen that in the IP2 sample the sterols spot is more intense than in the IP1 sample. The same result was achieved in the comparison of the pitch samples (figure 4.43). This shows, that the composition of the second pitch sample changes slightly from the first pitch sample.

It must be noted, that this result could only be achieved from a statistical point of view. In the case of a non-homogeneous, complex sample, it is advantageous to prepare a larger number of TLC plates and to add up the results to counteract segregation and component clusters.

The relative amounts of fatty acids and resin acids from the GCMS analysis were also added up, to compare them to the relative values from the EXACT version.

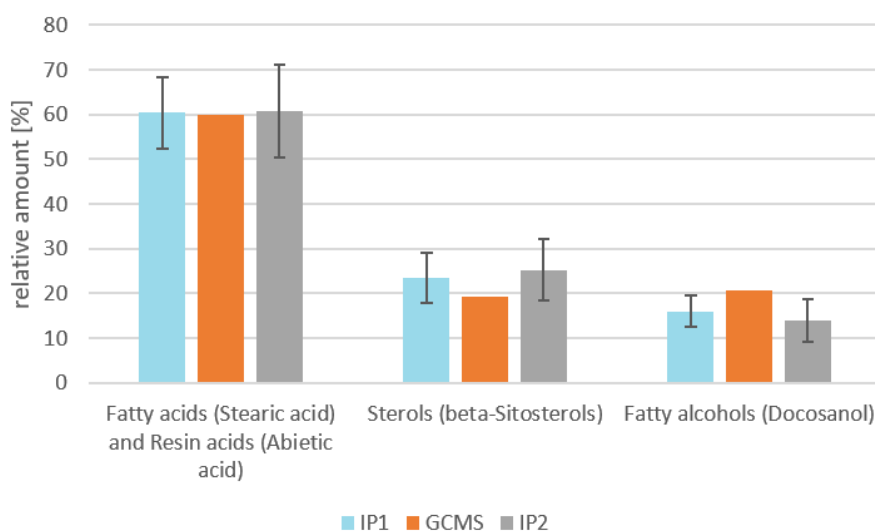


**Figure 4.43** Comparison: EXACT version vs. GCMS analysis (IP1 sample)

With summation, correction and normalization of all evaluated TLC plate spot-values, similar results from the GCMS analysis could be achieved. When investigating individual plates, very strong deviations were found. It is assumed that the reason for this is due to an insufficiently mixed sample. Since when the sample was applied, even after using an ultrasonic bath for about five minutes, streaks of the substance could be found in the sample vial. When applied, certain components are more present than others and produce different results. This shows that the location, from where the sample was taken in the vial, does play an important role. By creating several TLC plates of the same sample and summing up the results, it is possible to lower the occurring deviation.

The evaluation of the absolute values for the IP1 sample turned out to be impossible,

because the concentration of the first pitch sample was unknown. The remaining amount of the sample was too small for an analysis of the concentration. Therefore, a new pitch sample (IP2 sample) was requested from an industrial paper mill, which was analyzed in addition to the previous one (figure 4.44). The IP2 sample was dissolved with toluene. The concentration of this solution was 5 mg/ml. With this information it was possible to make statements about the absolute quantities.

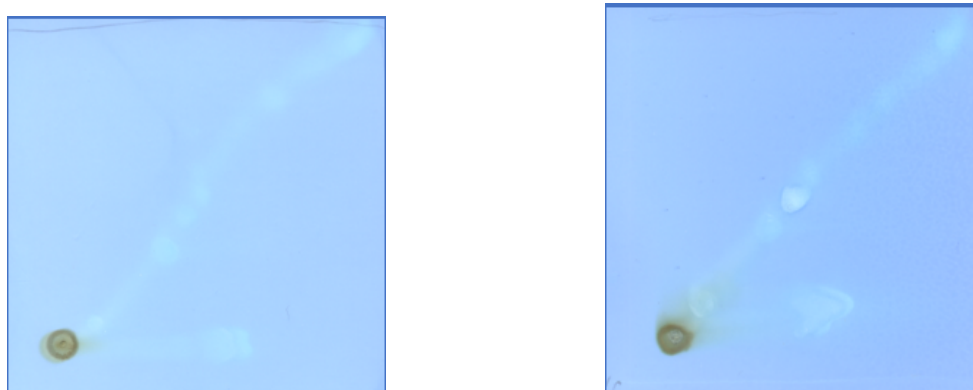


**Figure 4.44** Separate substances on TLC plate: IP1 sample (left); IP2 sample (right)

In some TLC plates of the IP1 sample an upshifting of the fatty acids occurred. These plates could not be evaluated with the EXACT version. With the EASY version, however, it was possible to examine TLC plates with a fatty acid upshift, because in this version a manual spot selection can be carried out. For this reason, all plates produced were analyzed and evaluated again using the EASY version.

In order to compare the two versions with each other, scatterplots were created for the pitch samples IP1 and IP2 (figure 4.45 & figure 4.46). EXACT values were plotted on the abscissa and the associated EASY values on the ordinate. Deviations between the two versions can be clearly shown with the inserted 45 degree line. The further the points are away from the line, the higher is the deviation of the determined values of both versions. Points that are above the 45 degree line show that a higher estimated value was determined in the EASY version. For points below the 45 degree line, a higher estimated value of the same TLC plate was determined in the EXACT version.

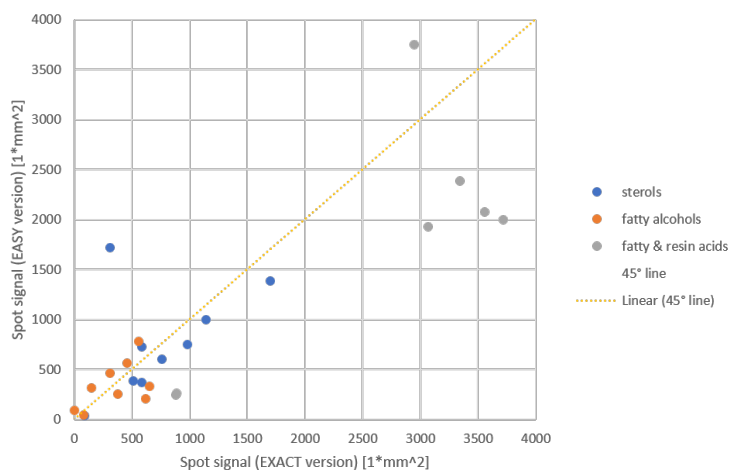


**Figure 4.45** Scatterplot of EASY and EXACT version (IP1): Fatty alcohols, sterols and fatty acids combined with resin acids of 9 TLC plates are shown

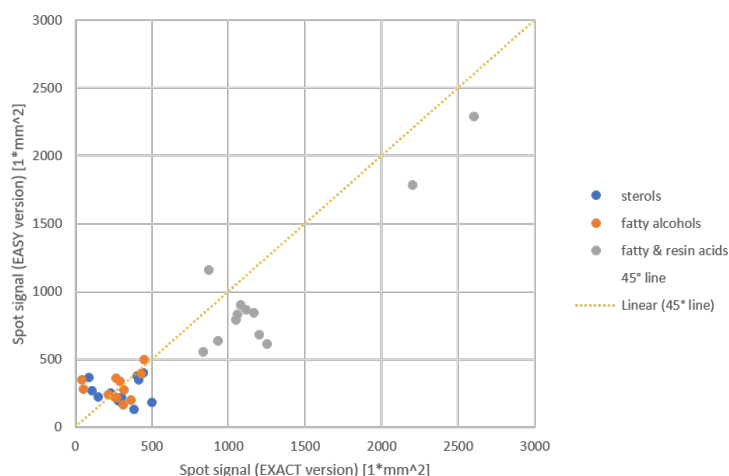


**Figure 4.46** Scatterplot of EASY and EXACT version (IP2): Fatty alcohols, sterols and fatty acids combined with resin acids of 12 TLC plates are shown

#### 4.5.2 EASY version

Same as in the EXACT version, when comparing the evaluations of the industrial pitch sample, strong fluctuations in the measured values were found (figure 4.47). The coefficient of variation shows that the results of the individual TLC plates differ greatly with up to 48 % of the averaged value (table 6.1). These deviations occur due to insufficient mixing of the pitch sample, as streaks appeared on closer inspection. Even after the sample was placed in the ultrasonic bath for mixing, segregation occurred in the sample vial when the sample was applied to the TLC plate.

For this reason, the sum of the measured values of all prepared TLC plates was used for the

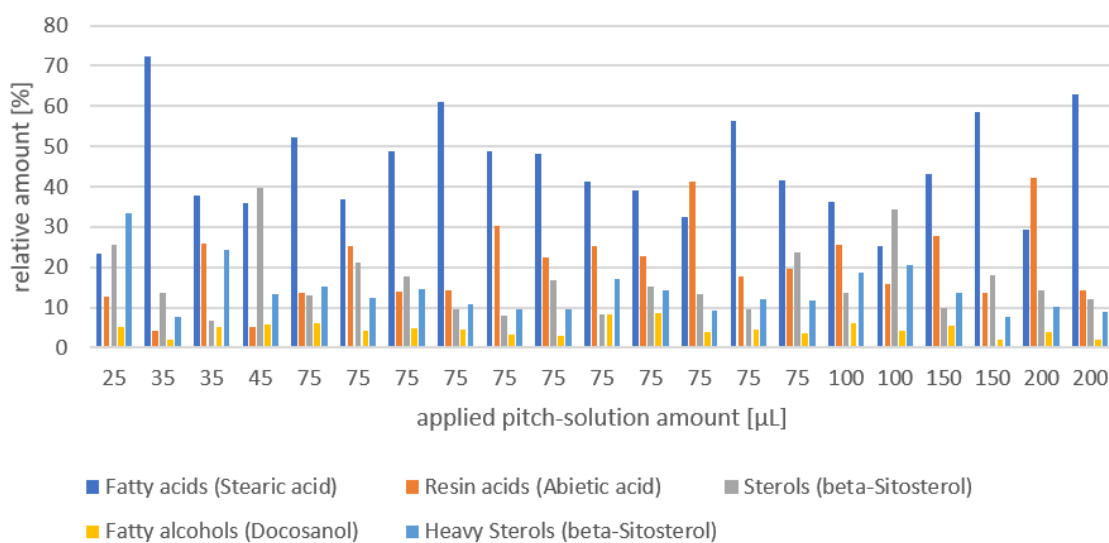


**Figure 4.47** Comparison of all 2D-TLC results of the masses: 21 prepared TLC plates (IP1 sample)

evaluation again. With a high number of TLC plates, the error caused by the segregation is kept low. The relative amounts of the IP1 and IP2 sample are shown in figure 4.48.

For the evaluation of the heavy sterols, the calibration value of beta-sitosterol was used, as these have very similar properties. The comparison of the two pitch samples show, that the relative amounts of fatty acids and fatty alcohols stays almost the same. The relative amount of resin acids is higher in the IP1 sample, while the relative sterols amount is higher in the IP2 sample.

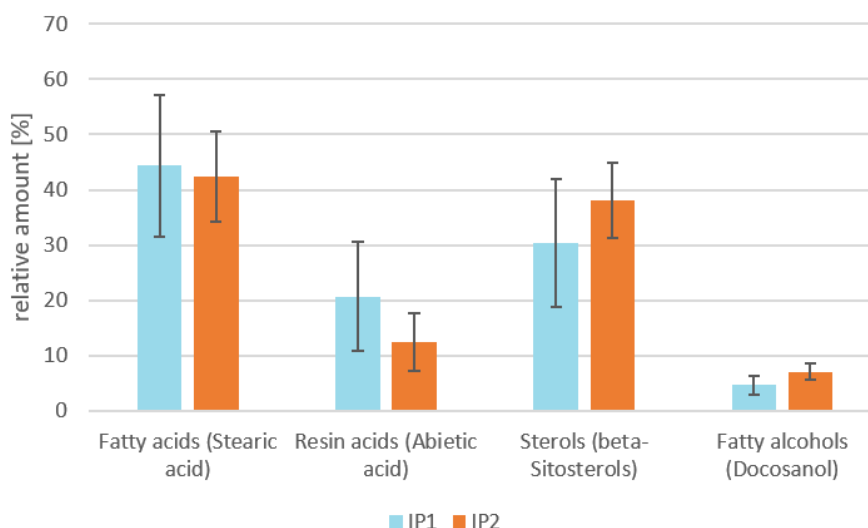


**Figure 4.48** Comparison of IP1 and IP2 sample

### 4.5.3 Comparison of the results of GCMS analysis and TLC method

For the samples: IP1, birch pitch, softwood pitch and hardwood pitch, GCMS analyzes were carried out in order to be able to evaluate the results of the 2D-TLC method.

#### IP1 & IP2 sample

In total, 21 TLC plates were produced from the IP1 sample and 12 TLC plates from the IP2 sample. After applying the calibration equations to the industrial pitch, the following relative values could be achieved. When comparing the values from the GCMS analysis with the values from the TLC method, good results were obtained (figure 4.49).

The results from the TLC method were slightly lower for fatty acids and sterols. In the case of resin acids the relative amount was for IP1 higher than in the GCMS analysis. Since no specific GCMS analysis was carried out for the IP2 sample, the GCMS analysis of the IP1 sample was taken for a comparison. The substance classes of IP1 and IP2 don't differ from one another with a few exceptions. Good results could also be achieved in this comparison. The differences between the two different pitch samples are not so pronounced in comparison to the GCMS analysis, since the GCMS values are similar to the values of the two pitch samples.

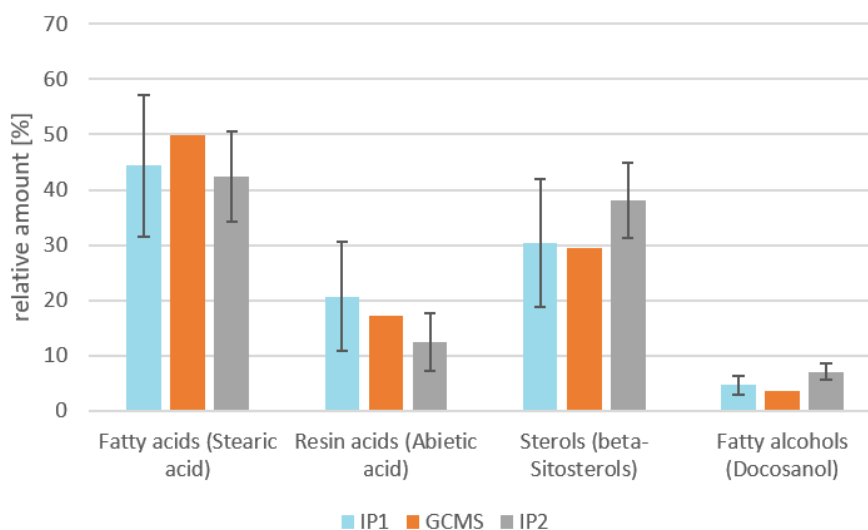


**Figure 4.49** Comparison: (EASY version) IP1 and IP2 vs. GCMS analysis

### Birch pitch sample

Three TLC plates were produced from this sample. A comparison of the quantities determined with the TLC method and with the analytical values shows that good results could be achieved in the case of betulin and fatty alcohols (figure 4.50). For sterols and fatty acids, however, strong deviations from the analytical values were found. It is assumed that a large part of the betulin was carried over into the spot of sterols. Also, it is possible that the values of the GCMS analysis could be faulty, since the assignment of the components to the substance groups proved to be difficult. Resin acids were also found in the GCMS analysis, which should actually only be very low or nonexistent in hardwood.

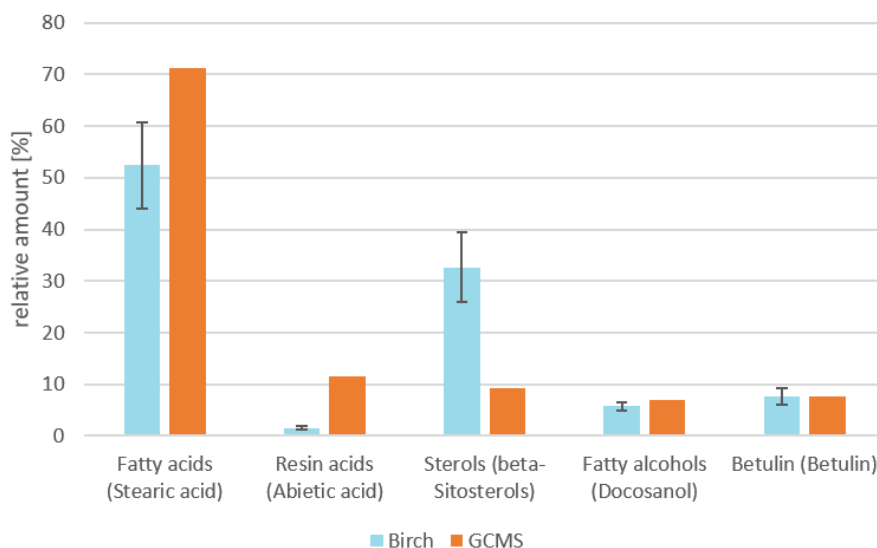


**Figure 4.50** Comparison: EASY version vs. GCMS analysis (birch pitch sample)

### hardwood & softwood pitch sample

Also, 2D-TLC experiments of hardwood and softwood pitch samples were carried out. For each sample three TLC plates were produced and evaluated. The calibration equations for the respective substances were used for the evaluation (table 4.4). Results of the two pitch samples were compared graphically in figure 4.51 and 4.52. In the hardwood sample, mainly fatty acids and sterols are represented and as expected, nearly no resin acids could be detected. The comparison with the GCMS analysis shows that accurate results were achieved. In the case of softwood, on the other hand, the proportion of fatty acids dominates, while the other substances were present in moderate amounts. A comparison with the results of the GCMS analysis showed that the 2D-TLC method was able to determine

fewer fatty acids and more resin acids. It is assumed that, on the one hand, because of the small number of TLC plates, an error occurred that could otherwise be removed with more data. On the other hand, inaccurate marking of the spots due to poor spot separation during the test can also lead to this result. This means that some of the fatty acids were identified as resin acids in the TLC measurements. A comparison with the GCMS analysis confirms this assumption, since the missing amount of fatty acids is too much in the resin acids. In addition to the conventional substances, a new group of substances was included. These are "heavy sterols" and belong to the group of sterols. The separation of these two substances in the 2D-TLC method is attributed to their molecular structure. The spot of sterols and heavy sterols were each evaluated with the EASY version. Since both belong to the same group of substances, their results are added together and evaluated as sterols.

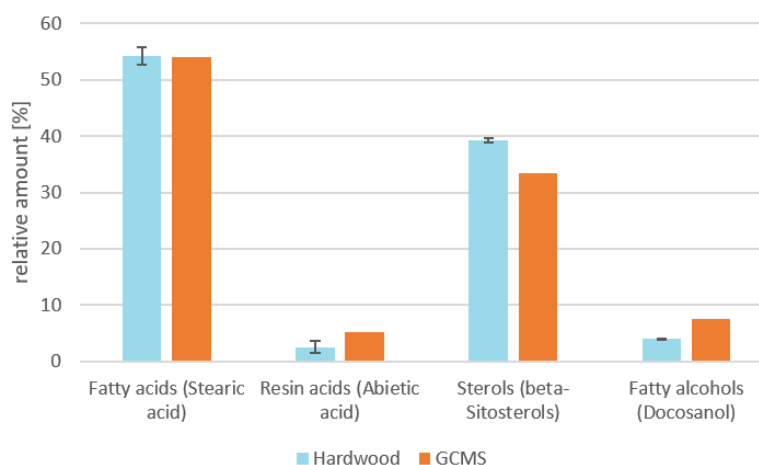


**Figure 4.51** Comparison: EASY version vs. GCMS analysis (hardwood pitch sample)

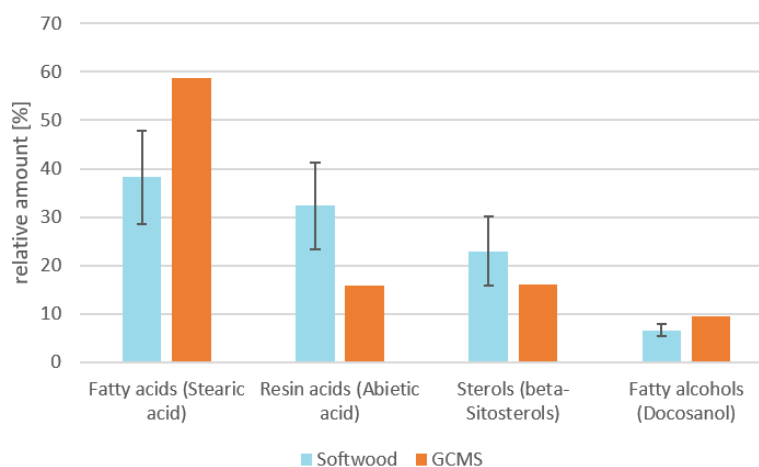


**Figure 4.52** Comparison: EASY version vs. GCMS analysis (softwood pitch sample)

## 4.6 Absolute Values & Yield

To determine the absolute values, the amount applied to the TLC plate had to be calculated back to the real amount of pitch in the solution. Based on the comparison of the results of the relative amounts from GCMS analysis and 2D-TLC method, it was possible to calculate back to the absolute amounts of the IP1 sample. Accordingly, the following amounts of the respective substance groups were found and determined (table 4.5).

The yield of the substances found could also be calculated from the 2D-TLC experiments. These are listed in table 4.6 for all pitch samples. The remaining percent of the detection yield are unknown substances, e.g. terpenes.

In the case of the GCMS analysis the detection yield was also around 50 %, i.e. there were also about 50 % of unknown substances.

**Table 4.5** Determined mass values of the pitch classes from all experiments

Pitch sample	Fatty acids	Resin acids	Sterols	Fatty alc.	Heavy Sterols	Betulin
	$\mu\text{g}$	$\mu\text{g}$	$\mu\text{g}$	$\mu\text{g}$	$\mu\text{g}$	$\mu\text{g}$
IP1	1468.11	737.36	504.22	137.00	392.52	
IP2	543.27	171.92	124.42	86.21	343.73	
birch	76.74		47.11	8.29		11.03
softwood	138.18	106.54	28.61	22.08	47.26	
hardwood	334.34		25.49	9.31	67.96	

**Table 4.6** Yield of the analyzed spots compared to the amount applied

	analysed amount	applied amount	detection yield	produced TLC plates
	$\mu\text{g}$	$\mu\text{g}$	%	#
IP1	3239.21	7460.00	43.42	21
IP2	1269.55	2550.00	49.79	12
brich	143.19	350.00	40.91	3
softwood	342.68	820.00	41.79	3
hardwood	437.10	840.00	52.04	3

## Conclusion

The residence time of the chemicals mainly affects the tensile index. Increased stirring times led to higher tensile strengths. In terms of retention, the combination of starch and alum plays a bigger role. Apart from long stirring times, adding alum led to a reduction in starch retention. The negative influence of pitch could be proven in the laboratory tests. Surprisingly a low positive strength effect on fiber in combination with alum could be achieved. It could not be clarified if this was a faulty sample or unknown bonding forces were involved. The addition of soy protein and starch in a mass ratio of 1:3 proved to be the best parameter setting. With this setting, a strength-increase of 21 % could be achieved with the presence of pitch. Without adding pitch, a further increase of up to 26 % in total was possible.

The results of the TLC tests show that it is possible to roughly estimate small amounts of a substance using 2D-TLC. This method works particularly well with pure substances. Also, this process is applicable to mixtures of substances, if these can be separated from one another via thin layer chromatography. Furthermore, reasonable model components must be used as representatives for substance groups. With a precise and careful way of working, most potential errors can be avoided. In order to avoid unavoidable sources of error (no ideal mixture of the pitch sample), additional measures must be taken (statistical evaluation).

Soy protein turned out to be a potential additive against pitch and a quick and easy method was developed to analyse pitch which suits particularly well for process control purposes. Furthermore, two software variants were created to almost completely automate the eval-

uation process of the pitch analysis on the one hand and to provide the broadest possible range of applications on the other.

## Appendix

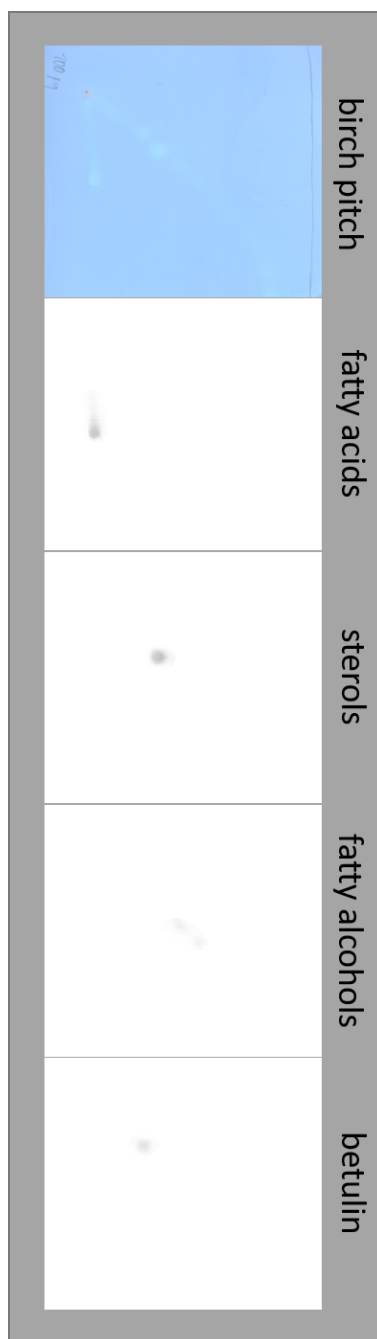


**Figure 6.1** TLC plate sample (birch) with evaluated individual spots

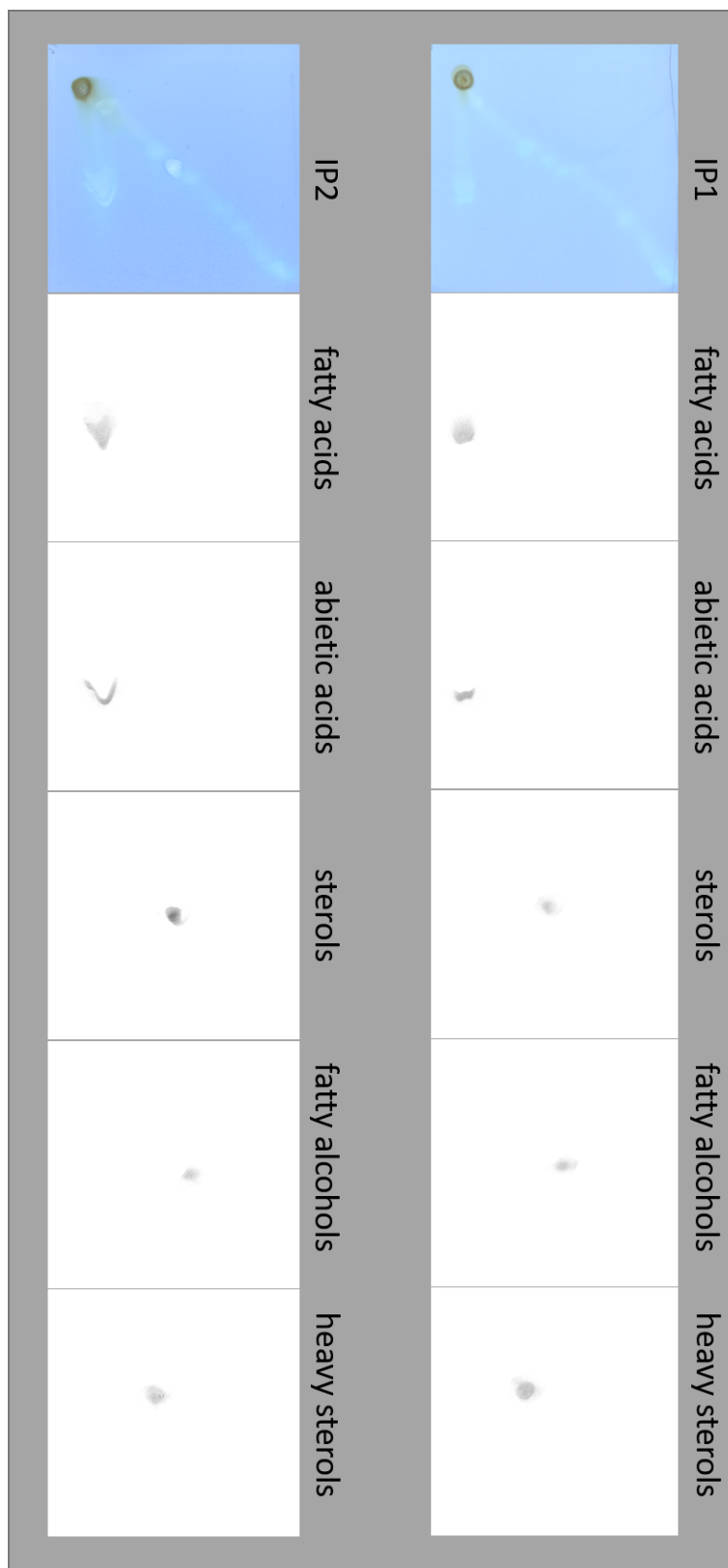


**Figure 6.2** TLC plate sample (IP1 & IP2) with evaluated individual spots

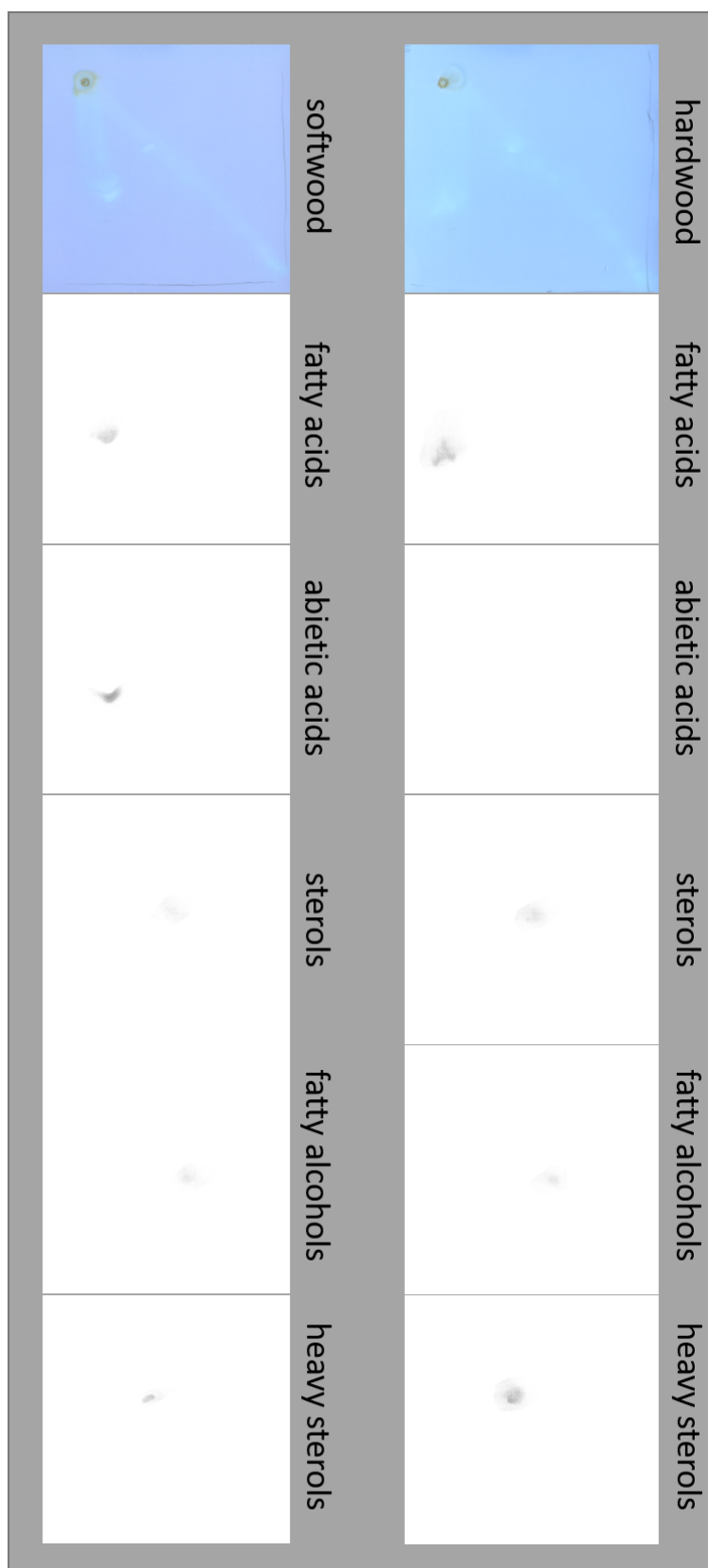


**Figure 6.3** TLC plate sample (softwood & hardwood) with evaluated individual spots

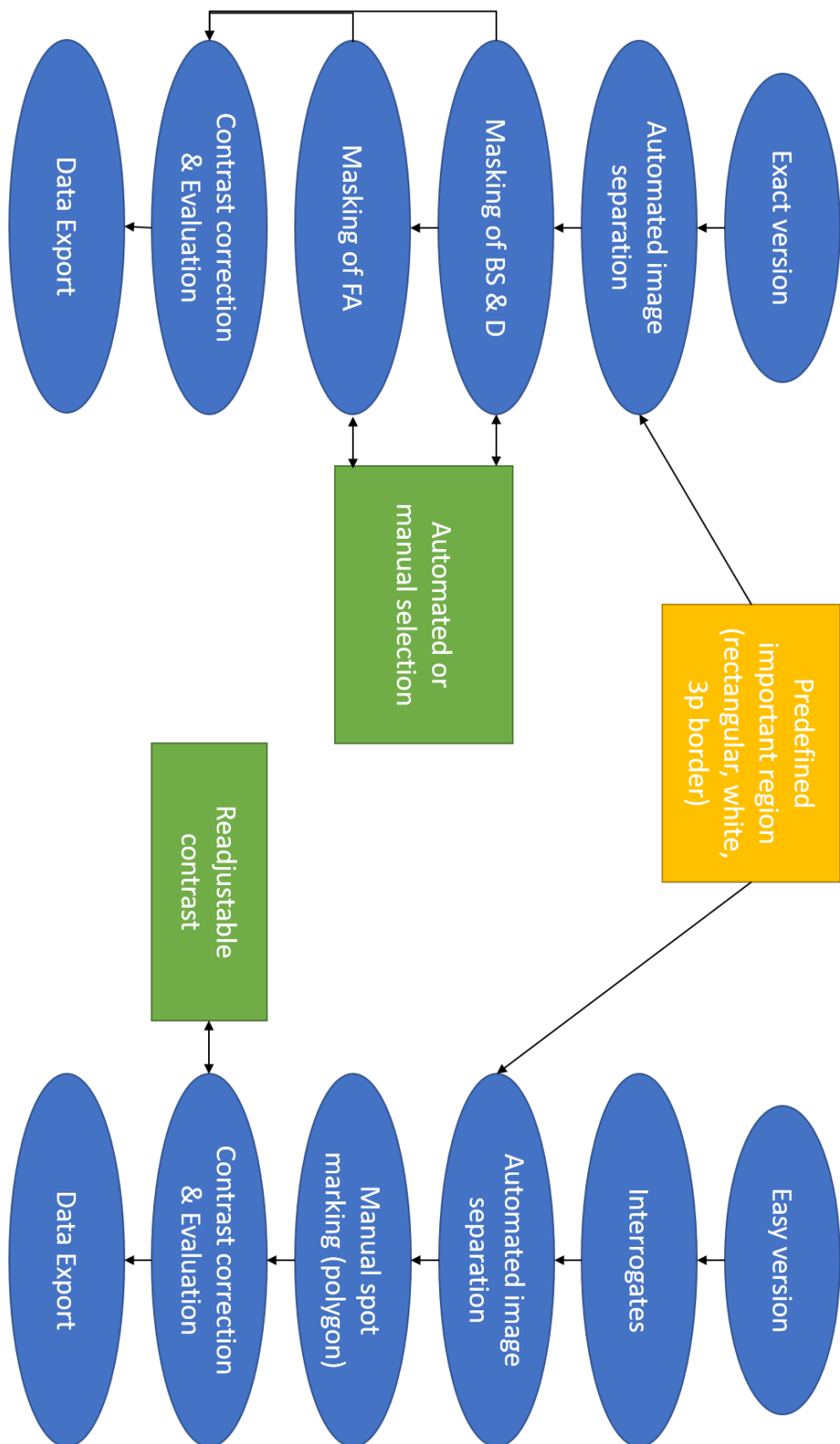


**Figure 6.4** Schematic flow diagram for a clear representation of the software operation of both versions

**Table 6.1** Summary and statistical evaluation of all produced TLC plates. (IP1; EASY version)

<b>IP1 TLC plates</b>	<b>Fatty acids</b>	<b>Resin acids</b>	<b>Sterols</b>	<b>Fatty alcohols</b>
<i>Unit</i>	%	%	%	%
1	23.42	12.69	58.83	5.07
2	72.32	4.30	21.41	1.97
3	37.91	25.79	31.17	5.13
4	35.91	5.21	53.06	5.82
5	52.13	13.54	28.14	6.19
6	36.92	25.34	33.54	4.20
7	48.95	14.00	32.22	4.83
8	60.95	14.12	20.29	4.63
9	48.72	30.14	17.76	3.38
10	48.31	22.54	26.31	2.84
11	41.26	25.11	25.35	8.27
12	39.22	22.76	29.49	8.53
13	32.43	41.23	22.57	3.77
14	56.20	17.69	21.60	4.51
15	41.61	19.49	35.41	3.49
16	36.09	25.49	32.16	6.27
17	25.18	15.82	54.89	4.12
18	43.06	27.72	23.75	5.47
19	58.68	13.58	25.73	2.01
20	29.42	42.16	24.60	3.82
21	62.82	14.16	20.96	2.05
<b>Mean</b>	44.36	20.61	30.44	4.59
<b>Standard deviation</b>	12.87	9.89	11.58	1.80
<b>Coefficient of variation</b>	0.29	0.48	0.38	0.39
<b>Confidence interval (95%)</b>	5.86	4.50	5.27	0.82
<b>GCMS result</b>	49.82	17.27	29.37	3.54

**Table 6.2** Summary and statistical evaluation of all produced TLC plates. (IP2; EASY version)

<b>IP2 TLC plates</b>	<b>Fatty acids</b>	<b>Resin acids</b>	<b>Sterols</b>	<b>Fatty alcohols</b>
<i>Unit</i>	%	%	%	%
1	25.06	17.80	49.51	7.64
2	35.33	14.40	42.38	7.89
3	38.01	8.92	42.27	10.79
4	41.74	17.48	32.98	7.80
5	44.26	9.18	40.70	5.85
6	52.82	8.48	31.31	7.40
7	48.30	8.24	37.36	6.11
8	53.83	3.71	36.09	6.37
9	42.60	11.47	39.35	6.58
10	36.01	10.48	47.58	5.93
11	42.68	20.98	30.60	5.74
12	49.07	18.04	26.93	5.96
<b>Mean</b>	42.48	12.43	38.09	7.01
<b>Standard deviation</b>	8.16	5.22	6.89	1.44
<b>Coefficient of variation</b>	0.19	0.42	0.18	0.21
<b>Confidence interval (95%)</b>	5.19	3.32	4.38	0.92
<b>GCMS result</b>	49.82	17.27	29.37	3.54

**Table 6.3** Summary and statistical evaluation of all produced TLC plates. (IP1; EXACT version)

<b>IP1 TLC plates</b>	<b>Fatty acids and Resin acids</b>	<b>Sterols</b>	<b>Fatty alcohols</b>
<i>Unit</i>	%	%	%
1	14.35	8.12	77.52
2	31.16	20.93	47.91
3	26.49	14.83	58.68
4	23.96	15.42	60.62
5	25.81	18.21	55.98
6	24.81	16.13	59.07
7	14.95	19.27	65.78
8	22.77	15.46	61.77
9	27.87	15.83	56.30
<b>Mean</b>	60.40	23.57	16.02
<b>Standard deviation</b>	8.07	5.60	3.61
<b>Coefficient of variation</b>	0.13	0.24	0.23
<b>Confidence interval (95%)</b>	6.20	4.31	2.77
<b>GCMS result</b>	60.02	19.35	20.63

**Table 6.4** Summary and statistical evaluation of all produced TLC plates. (IP2; EXACT version)

<b>IP2 TLC plates</b>	<b>Fatty acids and Resin acids</b>	<b>Sterols</b>	<b>Fatty alcohols</b>
<i>Unit</i>	%	%	%
1	20.24	17.96	61.80
2	34.61	14.86	50.53
3	25.75	17.96	56.29
4	25.61	17.42	56.96
5	36.52	13.95	49.53
6	30.51	17.66	51.83
7	27.55	15.47	56.99
8	28.96	16.14	54.90
9	15.27	4.34	80.39
10	15.27	4.48	80.25
11	21.80	14.09	64.11
12	20.88	12.85	66.27
<b>Mean</b>	60.82	25.25	13.93
<b>Standard deviation</b>	10.45	6.86	4.76
<b>Coefficient of variation</b>	0.17	0.27	0.34
<b>Confidence interval (95%)</b>	6.64	4.36	3.02
<b>GCMS result</b>	60.02	19.35	20.63

**Table 6.5** Summary and statistical evaluation of all produced TLC plates. (Birch; EASY version)

<b>Birch TLC plates</b>	<b>Fatty acids</b>	<b>Resin acids</b>	<b>Sterols</b>	<b>Fatty alcohols</b>	<b>Betulin</b>
<i>Unit</i>	%	%	%	%	%
1	50.13	1.55	34.34	5.14	8.83
2	45.42	1.34	38.44	6.69	8.12
3	61.56	1.86	25.27	5.40	5.91
<b>Mean</b>	52.37	1.58	32.68	5.74	7.62
<b>Standard deviation</b>	8.30	0.26	6.74	0.83	1.52
<b>Coefficient of variation</b>	0.16	0.16	0.21	0.14	0.20
<b>Confidence interval (95%)</b>	20.63	0.65	16.74	2.06	3.78
<b>GCMS result</b>	53.60	0.00	32.90	5.79	7.71

**Table 6.6** Summary and statistical evaluation of all produced TLC plates. (Softwood; EASY version)

<b>Softwood TLC plates</b>	<b>Fatty acids</b>	<b>Resin acids</b>	<b>Sterols</b>	<b>Fatty alcohols</b>
<i>Unit</i>	%	%	%	%
1	29.82	31.46	30.79	7.93
2	48.84	23.73	21.20	6.23
3	35.94	41.74	16.73	5.59
<b>Mean</b>	38.20	32.31	22.90	6.58
<b>Standard deviation</b>	9.71	9.04	7.18	1.21
<b>Coefficient of variation</b>	0.25	0.28	0.31	0.18
<b>Confidence interval (95%)</b>	24.13	22.45	17.84	3.01
<b>GCMS result</b>	58.65	15.82	16.07	9.46

**Table 6.7** Summary and statistical evaluation of all produced TLC plates. (Hardwood; EASY version)

<b>Hardwood TLC plates</b>	<b>Fatty acids</b>	<b>Resin acids</b>	<b>Sterols</b>	<b>Fatty alcohols</b>
<i>Unit</i>	%	%	%	%
1	52.69	3.69	39.56	4.06
2	54.48	2.41	39.20	3.90
3	55.78	1.49	38.94	3.80
<b>Mean</b>	54.32	2.53	39.23	3.92
<b>Standard deviation</b>	1.55	1.10	0.31	0.13
<b>Coefficient of variation</b>	0.03	0.44	0.01	0.03
<b>Confidence interval (95%)</b>	3.84	2.74	0.78	0.33
<b>GCMS result</b>	54.01	5.12	33.35	7.52

# List of Figures

2.1	Chemical structure of cellulose . . . . .	5
2.2	Chemical structure of hemicellulose . . . . .	5
2.3	Phenylpropane units are the building block of lignin . . . . .	6
2.4	Chemical structure of significant pitch compounds: a) docosanol (fatty alcohol); b) oleic acid (fatty acid); c) sitosteryl linoleate (steryl ester); d) tristearin (triglyceride); e) stearic acid (fatty acid); f) linalool (terpenoid); g) abietic acid (resin acid); h) beta-sitosterol (sterols); i) phytan (terpene); j) betulin (heavy sterols) . . . . .	7
2.5	Structure of fatty acids and their behavior in water . . . . .	8
2.6	Negatively charged fatty acid micelles with encapsulated sterols, resin acids and fatty alcohols . . . . .	8
2.7	Milled cellulose fiber with outer fibrils . . . . .	12
2.8	Cellulose fiber in cross-section after the milling process - internal fibrillation	12
2.9	Curl - curvy cellulose fiber . . . . .	12
2.10	Kink - drastic change of direction of the fiber . . . . .	12
2.11	Cross-section of early and late wood fibers . . . . .	13
2.12	Theoretical and real bonding area of cellulose fibers . . . . .	13
2.13	Formation of hydrogen bonds between fibers - hydrogen atoms of the fiber (red); hydrogen atoms of water molecules (blue) . . . . .	14
2.14	Coulomb forces: Mechanism of attraction and repulsion [33] . . . . .	15
2.15	Capillary bridging between fibers [21] . . . . .	15
2.16	Van der Waals forces - interaction of atoms or molecules with shifted charges (dipoles) [34] . . . . .	15
2.17	Molecular bonding of cationic starch to cellulosic fibers; Acting coulomb forces (red marking) . . . . .	16
2.18	Differences in effect when using alum: a) desired effect (pitch adsorbed and fixed to fiber); b) to be avoided (pitch agglomerated) [40] . . . . .	17

2.19	MS chromatogram of industrial pitch with 1255 different components [3] . . .	18
2.20	Process of thin layer chromatography: a) Applying the mixture; b) put in eluent; c) start of substance separation; d) separation end; e) removing remaining eluent; f) evaluation . . . . .	19
2.21	Flow chart of 2D thin-layer chromatography with industrial pitch a) Apply pitch and starting with alkaline eluent b) end of the first round c) removing remaining eluent and restarting with acidic eluent and a 90 degree turn d) end of the second separation process e) removing remaining eluent f) coloring & evaluation . . . . .	20
2.22	Left: 1-dimensional TLC (top left and center) of the class components: abietic acid (A); beta-sitosterol (beta-S); stearic acid (S); mixture of compounds (M); docosanol (D). Right: 2D-TLC of all class components. [3] . . . . .	20
2.23	Determined regions of the component classes via peak method using model components . . . . .	21
2.24	Transfer of the spots from the PEAK tests to the industrial pitch sample . . .	21
3.1	Dried pitch sample from industrial paper mill . . . . .	25
3.2	Calibration cuvettes with different lugol filtrate concentrations - striking yellow color (dark = high concentration; light = low concentration) . . . . .	26
3.3	Produced laboratory sheet with over 30 agglomeration stains . . . . .	29
3.4	Location of the initial spot of the industrial pitch sample on the TLC plate (6.5cm * 6.5cm) for the 2D-TLC method (red circle) . . . . .	32
3.5	TLC experiment: TLC chamber with TLC plate inserted . . . . .	32
3.6	Chemical structure of Nile blue . . . . .	32
3.7	Finished TLC plate before coloring (left) and after applying the coloring agent (right) . . . . .	33
3.8	Upper LOD: Overfilling of the initial spot with sample - Tailing effect . . . . .	33
3.9	Lower LOD: too little sample applied - no visible spot recognizable . . . . .	33
3.10	Steps from the "IMFILL" function (Background: white pixel): Start screen (left); Procedure (center); Result (right); . . . . .	34
3.11	Steps of the "CLUSTERFILTER" function (Background: black pixel): Start picture (left); Classification (center-left); Filter step (center-right); Result (right);	34

3.12	Steps from the "PIXELKILL" function (Background: white pixel): Start picture (left); horizontal and vertical pixel detection (center-left); Elimination (center-right); Result (right) . . . . .	35
3.13	Steps from the "GAP FILLER" function (Background: white pixel): Start screen (left); Pixel search within a defined distance and in the same plane (center-left); Bridging and filling (center-right); Result (right) . . . . .	35
4.1	Starch retention experiments: mixing time: 1-2 min (two columns left); mixing time: 15-20 min (two columns center); mixing time: 15-20 sec (two columns right) . . . . .	37
4.2	Tensile index experiments: Comparison of aid substance combinations . . . . .	38
4.3	3D presentation principle to evaluate TLC spots . . . . .	39
4.4	TLC plate with sprayer stains . . . . .	39
4.5	TLC plate with a shifted fatty acid spot (red mark) . . . . .	40
4.6	Spot excerpt in JPG format . . . . .	41
4.7	Spot excerpt in TIF format . . . . .	41
4.8	Image from the first scan - scanning lamp not yet balanced (left); Image of the subsequent scanning process - intensity of the scanning lamp constant (right) . . . . .	41
4.9	TLC plate: peeling of the silica gel at the edges - caused by damage . . . . .	43
4.10	Review sections for a set, white frame; Division into 4 different queries (green, orange and gray must have a value of 255; yellow must have a value less than 250) . . . . .	44
4.11	Additional review sections for confirmation; Division into 4 different queries (green, orange, gray and yellow must have a value less than 250) . . . . .	44
4.12	Marking problem: overlapping of the set frames (left) and intensity falsification of the background by the second spot (center); Remedy: summarized marking (right) . . . . .	45
4.13	Marking process for two different thin-layer chromatography results: 2D-TLC - marking of the relevant area of the TLC plate - evaluation of multiple TLC plates possible (left); 1D-TLC - separate markings - same substance - only one TLC plate can be evaluated at the same time (right) . . . . .	45
4.14	Original image (a) with grayscale image (b) and the individual color channels (c = red; d = green; e = blue) . . . . .	46

4.15	Binarization of the images using Otsu’s method (a = grey; b = red; c = green; d = blue) of beta-sitosterol and docosanol: best result - green color channel (c)	47
4.16	Histograms of the color channels and the grayscale image (a = gray; b = red; c = green; d = blue) of beta-sitosterol and docosanol: Confirms that the green channel is the best choice . . . . .	47
4.17	Created masks: beta-sitosterol (left); docosanol (right); red frame for security against pixel loss through Otsu’s method . . . . .	48
4.18	3D view of the evaluation (EXACT version): initial image (top); beta-sitosterol spot (middle); Docosanol spot (bottom); separation via masks . . .	49
4.19	Binarization of the images using Otsu’s method (a = original; b = grey; c = red; d = green; e = blue) of fatty acids: best result - still green color channel (c)	50
4.20	Histograms of the color channels and the grayscale image (a = gray; b = red; c = green; d = blue) of fatty acids: green channel is the best choice for further operations . . . . .	50
4.21	Operation 1 to improve contrast: division into 4 quadrants (left); separate binarization of the squares (middle); re-assembling (right) . . . . .	50
4.22	Operation 2 for contrast enhancement: improvement of the transitions; division into 9 segments; again separate binarization of the transition segments .	51
4.23	Operation 3 for contrast enhancement: removal of the internal voids (a); Removing the surrounding collections of pixels (b); Reintroduction of the black pixels from operation 1 (c); application of Pixelkill (d); application of cluster filter (e); Application of Imfill (f); Adding border around the structure (g); Application of Imfill (h); Application of Gapfill (i); Comparison of the original image with the mask created for fatty acids . . . . .	52
4.24	3D view of the evaluation (EXACT version): initial image (top); fatty acid spot (bottom); separation via mask . . . . .	53
4.25	TLC plate with manual polygon spot selection of the EASY version . . . . .	54
4.26	Contrast manipulation: Steps to transform the image for easier calculation: Inversion (1); Contrast correction (2); Re-inversion (3) . . . . .	56
4.27	Manual contrast correction of the EASY version: original result (a); 10 % contrast correction ( recommended) (b); 20 % contrast correction (c); 30 % contrast correction (d) . . . . .	56

4.28	Calibration line with offset error in the small quantity range: stearic acid (EXACT version) . . . . .	57
4.29	Calibration line: stearic acid - comparison of all calibration attempts (EXACT version) . . . . .	58
4.30	UV scan: pure stearic acid spot (left); spot with stearic acid and abietic acid (right) . . . . .	58
4.31	Calibration line: pure stearic acid - exclusion of the first calibration attempt (EXACT version) . . . . .	59
4.32	Calibration line: beta-sitosterol (EXACT version) . . . . .	59
4.33	Calibration line: docosanol (EXACT version) . . . . .	59
4.34	Calibration line: beta-sitosterol (EASY version) . . . . .	60
4.35	Calibration line: docosanol (EASY version) . . . . .	60
4.36	Calibration line: data from all stearic acid experiments (EASY version) . . .	61
4.37	new process for determining the spots of stearic acid in combination with abietic acid: marking both spots together in the VIS image (a); switch to UV image (b); Marking of the abietic acid (dark spot) in the UV image (c); determination of the stearic acid signal by subtracting the abietic acid spot from the total spot . . . . .	62
4.38	Calibration line: stearic acid in the presence of abietic acid (EASY version) .	62
4.39	Calibration line: abietic acid with and without the presence of stearic acid (EASY version) . . . . .	62
4.40	TLC plate: with assigned substances to the spots . . . . .	63
4.41	Calibration line: betulin (EASY version) . . . . .	64
4.42	Separation of the IP1 sample using 2D-TLC: original image (left); after contrast correction (right); Identification of fatty acids (lower images), sterols and fatty alcohols (upper images) . . . . .	65
4.43	Comparison: EXACT version vs. GCMS analysis (IP1 sample) . . . . .	66
4.44	Separate substances on TLC plate: IP1 sample (left); IP2 sample (right) . . .	67
4.45	Scatterplot of EASY and EXACT version (IP1): Fatty alcohols, sterols and fatty acids combined with resin acids of 9 TLC plates are shown . . . . .	68
4.46	Scatterplot of EASY and EXACT version (IP2): Fatty alcohols, sterols and fatty acids combined with resin acids of 12 TLC plates are shown . . . . .	68

4.47	Comparison of all 2D-TLC results of the masses: 21 prepared TLC plates (IP1 sample) . . . . .	69
4.48	Comparison of IP1 and IP2 sample . . . . .	69
4.49	Comparison: (EASY version) IP1 and IP2 vs. GCMS analysis . . . . .	70
4.50	Comparison: EASY version vs. GCMS analysis (birch pitch sample) . . . . .	71
4.51	Comparison: EASY version vs. GCMS analysis (hardwood pitch sample) . . . . .	72
4.52	Comparison: EASY version vs. GCMS analysis (softwood pitch sample) . . . . .	72
6.1	TLC plate sample (birch) with evaluated individual spots . . . . .	77
6.2	TLC plate sample (IP1 & IP2) with evaluated individual spots . . . . .	78
6.3	TLC plate sample (softwood & hardwood) with evaluated individual spots . . . . .	79
6.4	Schematic flow diagram for a clear representation of the software operation of both versions . . . . .	80

## List of Tables

2.1	Composition of the cell wall in Central European hardwood and softwood . . . . .	3
2.2	Rf values in both directions from the 2D-TLC method of the substance classes [3] . . . . .	21
3.1	Starch retention trial setup . . . . .	24
3.2	Physical property measurements of the starch retention experiments . . . . .	28
3.3	Tensile index trial setup . . . . .	29
3.4	Amounts of chemicals in soy protein trials . . . . .	30
3.5	Physical property measurements of the soy protein trials . . . . .	30
3.6	Pitch classes with associated model components . . . . .	31
4.1	Questions about the definition of the problem definition of the EASY version . . . . .	53
4.2	Format template for pre-defined mass integration via EXCEL tables . . . . .	54
4.3	Comparison of the gradient values of the EXACT and EASY version . . . . .	63
4.4	Summarized slope values for further evaluation (EASY version) . . . . .	64
4.5	Determined mass values of the pitch classes from all experiments . . . . .	73
4.6	Yield of the analyzed spots compared to the amount applied . . . . .	73

6.1	Summary and statistical evaluation of all produced TLC plates. (IP1; EASY version) . . . . .	81
6.2	Summary and statistical evaluation of all produced TLC plates. (IP2; EASY version) . . . . .	82
6.3	Summary and statistical evaluation of all produced TLC plates. (IP1; EXACT version) . . . . .	82
6.4	Summary and statistical evaluation of all produced TLC plates. (IP2; EXACT version) . . . . .	83
6.5	Summary and statistical evaluation of all produced TLC plates. (Birch; EASY version) . . . . .	83
6.6	Summary and statistical evaluation of all produced TLC plates. (Softwood; EASY version) . . . . .	84
6.7	Summary and statistical evaluation of all produced TLC plates. (Hardwood; EASY version) . . . . .	84

# List of Abbreviations

**TLC** Thin layer chromatography

**2D-TLC** two dimensional thin layer chromatography

**A** Abietic acid

**B** Betulin

**beta-S** beta-Sitosterol

**D** Docosanol

**DFR** drainage freeness retention

**DPI** dots per inch

**GCMS** gas chromatography mass spectrometry

**FA** fatty acid

**HPTLC** High performance thin layer chromatography

**IP1** industrial pitch number 1

**IP2** industrial pitch number 2

**JPG** joint photographic group

**LOD** limit of detection

**M** mixture

**OA** Oleic acid

**RBA** relative binding area

**Rf** Retarding front

**S** Stearic acid

**TIF** tagged image file

**UBSK** unbleached softwood kraft pulp

**UV** ultraviolet scan

**VIS** visible light scan

# Bibliography

- [1] Martin A Hubbe, Orlando J Rojas, and Richard A Venditti. Control of tacky deposits on paper machines—a review. *Nordic Pulp and Paper Research Journal*, 21(2):154–171, 2006.
- [2] Anna Sundberg, Bjarne Holmbom, Stefan Willfoer, and Andrey Pranovich. Weakening of paper strength by wood resin. *Nordic Pulp and Paper Research Journal*, 15(1):46–53, 2000.
- [3] Werner Schlemmer, Melissa Egger, Madeline Dächert, Jussi Lahti, Markus Gschiel, Andrea Walzl, Erich Leitner, Stefan Spirk, and Ulrich Hirn. Rapid separation and quantitative analysis of complex lipophilic wood pulp extractive mixtures based on 2d thin layer chromatography. *ACS Sustainable Chemistry and Engineering*, 8(33):12534–12541, 2020.
- [4] William Edwin Hillis. *Wood extractives and their significance to the pulp and paper industries*. Academic press, 2014.
- [5] Roger C Pettersen. *The chemical composition of wood*. ACS Publications, 1984.
- [6] Anderson Guerra, Regis Mendonca, and Andre Ferraz. Molecular weight distribution of wood components extracted from pinus taeda biotreated by ceriporiopsis subvermispora. *Enzyme and Microbial Technology*, 33(1):12–18, 2003.
- [7] D McDonald, K Miles, and R Amiri. The nature of the mechanical pulping process. *Pulp and paper Canada*, 105(8):27–32, 2004.
- [8] Alan W Rudie, Joseph Morra, James M St Laurent, and Karen L Hickey. *The influence of wood and fiber properties in mechanical pulping*. 1993.
- [9] Eric O Fernandez and Raymond A Young. Properties of cellulose pulps from acidic and basic processes. *Cellulose*, 3(1):21–44, 1996.
- [10] Martin A Hubbe. Water and papermaking. 3. measures to clean up process water. *Paper Technol*, 48(3):23–30, 2007.
- [11] Krista Koljonen, Monika Oesterberg, Marjatta Kleen, Agneta Fuhrmann, and Per Steinius. Precipitation of lignin and extractives on kraft pulp: effect on surface chemistry,

- surface morphology and paper strength. *Cellulose*, 11(2):209–224, 2004.
- [12] Peder J Kleppe. Kraft pulping. *Tappi*, 53(1):35–47, 1970.
- [13] Martin A Hubbe, Richard A Venditti, and Orlando J Rojas. What happens to cellulosic fibers during papermaking and recycling? a review. *BioResources*, 2(4):739–788, 2007.
- [14] Josef S Gratzl and Chen-Loung Chen. Chemistry of pulping: lignin reactions. ACS Publications, 2000.
- [15] R. Gill. Chemical control of deposits : scopes and limitations. 1996.
- [16] Qingxian Miao, Liulian Huang, and Lihui Chen. Advances in the control of dissolved and colloidal substances present in papermaking processes: A brief review. *BioResources*, 8(1):1431–1455, 2013.
- [17] B.Sc. DI Roman Poschner. Influence of pitch on paper properties. Master’s thesis, TU Graz, 2020.
- [18] Gordon C. Chen Matthew A. Blazey, S. Allen Grimsely. Indicators for forecasting "pitch season". *Tappi Journal*, 2002.
- [19] Anna-Liisa Sihvonen, Kennngth Sundberg, Anna Sundberg, and Blame Holmhom. Stability and deposition tendency of colloidal wood resin. *Nordic Pulp and Paper Research Journal*, 13(1):64–67, 1998.
- [20] Gerard Murray, Karen Stack, Douglas S McLean, Wei Shen, and Gil Garnier. Dynamics of colloidal pitch adsorption at the solid–liquid interface by surface plasmon resonance. *Colloids and Surfaces A: Physicochemical and Engineering Aspects*, 341(1-3):127–133, 2009.
- [21] Peter A Kralchevsky and Kuniaki Nagayama. Capillary forces between colloidal particles. *Langmuir*, 10(1):23–36, 1994.
- [22] Martin A Hubbe, Anna Sundberg, Paulina Mocchiutti, Yonghao Ni, and Robert Pelton. Dissolved and colloidal substances (dcs) and the charge demand of papermaking process waters and suspensions: A review. *BioResources*, 7(4):6109–6193, 2012.
- [23] D. D. Dreisbach and D. Michalopoulos. Understanding the behavior of pitch in pulp and paper mills. *Tappi Journal*, 72:129–134, 1989.
- [24] Paivi Kokkonen, Antti Korpela, Anna Sundberg, and Bjarne Holmbom. Effects of different types of lipophilic extractives on paper properties. *Nordic Pulp and Paper Research Journal*, 17(4):382–386, 2002.
- [25] Per Tomas Larsson, Tom Lindstroem, Leif A Carlsson, and Christer Fellers. Fiber

- length and bonding effects on tensile strength and toughness of kraft paper. *Journal of Materials Science*, 53(4):3006–3015, 2018.
- [26] Ulrich Hirn and Robert Schennach. Comprehensive analysis of individual pulp fiber bonds quantifies the mechanisms of fiber bonding in paper. *Scientific reports*, 5(1):1–9, 2015.
- [27] Olli Joutsimo, Rolf Wathen, and Tarja Tamminen. Effects of fiber deformations on pulp sheet properties and fiber strength. *Paperi ja puu*, 87(6):392, 2005.
- [28] QQ Wang, JY Zhu, R Gleisner, TA Kuster, U Baxa, and SE McNeil. Morphological development of cellulose fibrils of a bleached eucalyptus pulp by mechanical fibrillation. *Cellulose*, 19(5):1631–1643, 2012.
- [29] Richard J Kerekes. Rheology of fibre suspensions in papermaking: An overview of recent research. *Nordic Pulp and Paper Research Journal*, 21(5):598, 2006.
- [30] RL Ellis and AW Rudie. Ideal fibers for pulp and paper products. In *Proceedings*, number 21, page 295. Louisiana State University, Division of Continuing Education, 1991.
- [31] Alexander Degen. *Wasserstoffbruecken als strukturbildendes Element -Synthese und Berechnung supramolekularer Komplexe*. PhD thesis, Johann Wolfgang Goethe-Universität in Frankfurt am Main, 2004.
- [32] Guenter Kelbg. Weitreichende zwischenmolekulare kräfte in der statistischen mechanik. *Annalen der Physik*, 464(3-4):159–167, 1962.
- [33] Dan S. Correnti. Mechanisms explaining coulomb’s electric force & lorentz’s magnetic force from a classical perspective. *Results in Physics*, 9:832 – 841, 2018.
- [34] H Margenau. Van der waals forces. *Reviews of Modern Physics*, 11(1):1, 1939.
- [35] Mohammadreza Kamali, Seyedeh Azadeh Alavi-Borazjani, Zahra Khodaparast, Mohammadreza Khalaj, Akram Jahanshahi, Elisabete Costa, and Isabel Capela. Additive and additive-free treatment technologies for pulp and paper mill effluents: advances, challenges and opportunities. *Water Resources and Industry*, 21:100109, 2019.
- [36] V Bobacka, J Näsman, N Kreutzman, and D Eklund. Adsorption of cationic starch onto peroxide-bleached tmp fibres: Influence of interfering wood substances. *Paperi ja puu*, 81(1):59–62, 1999.
- [37] Joseph A Maciaszek. Pulp and papermaking additive, aug 15 1978. US Patent 4,107,073.

- [38] Otto Wächter. Die hilfsmittel der modernen papiererzeugung. *Dauerhaftigkeit von Papier*, pages 68–90, 1980.
- [39] Edward Strazdins. The chemistry of alum in papermaking. *Tappi journal*, 69(4):111–114, 1986.
- [40] Anna Sundberg, Rainer Ekman, Bjerne Holmbom, Kenneth Sundberg, and Jeff Thornton. Interactions between dissolved and colloidal substances and a cationic fixing agent in mechanical pulp suspensions. *Nordic Pulp and Paper Research Journal*, 8(1):226–231, 1993.
- [41] Ana Gutierrez, Jose C del Rio, Maria Jesus Martinez, and Angel T Martinez. The biotechnological control of pitch in paper pulp manufacturing. *TRENDS in Biotechnology*, 19(9):340–348, 2001.
- [42] Ana Gutierrez, C Jose, and Angel T Martinez. Microbial and enzymatic control of pitch in the pulp and paper industry. *Applied microbiology and biotechnology*, 82(6):1005–1018, 2009.
- [43] Haoyu Jin, Lucian A Lucia, Orlando J Rojas, Martin A Hubbe, and Joel J Pawlak. Survey of soy protein flour as a novel dry strength agent for papermaking furnishes. *Journal of agricultural and food chemistry*, 60(39):9828–9833, 2012.
- [44] Ali H Tayeb, Martin A Hubbe, Pegah Tayeb, Lokendra Pal, and Orlando J Rojas. Soy proteins as a sustainable solution to strengthen recycled paper and reduce deposition of hydrophobic contaminants in papermaking: A bench and pilot-plant study. *ACS Sustainable Chemistry & Engineering*, 5(8):7211–7219, 2017.
- [45] Hans-Joachim Huebschmann. *Handbook of GC/MS*. Wiley Online Library, 2000.
- [46] Ana Gutierrez, Jose C Del Rio, Francisco J Gonzalez-Vila, and Francisco Martin. Analysis of lipophilic extractives from wood and pitch deposits by solid-phase extraction and gas chromatography. *Journal of chromatography A*, 823(1-2):449–455, 1998.
- [47] Joseph Sherma and Bernard Fried. *Handbook of thin-layer chromatography*, volume 89. CRC press, 2003.
- [48] M Sandstroem, MA Norborg, and A Ericsson. Applications of thin-layer chromatography to process control in the pulp and paper field. *Journal of Chromatography A*, 730(1-2):373–379, 1996.
- [49] Kay Fink, Richard E Cline, and Robert M Fink. Paper chromatography of several classes of compounds: correlated rf values in a variety of solvent systems. *Analytical*

- Chemistry*, 35(3):389–398, 1963.
- [50] Lumir Sommer. *Analytical absorption spectrophotometry in the visible and ultraviolet: the principles*. Elsevier, 2012.
- [51] Adam Chomicki, Piotr Slkazak, and Tadeusz H Dzido. Preliminary results for 2-d separation with high-performance thin-layer chromatography and pressurized planar electrochromatography. *Electrophoresis*, 30(21):3718–3725, 2009.
- [52] T Halkina and J Sherma. Use of the chromimage flatbed scanner for quantification of high-performance thin layer chromatograms in the visible and fluorescence-quenching modes. *Acta Chromatographica*, (17):250–260, 2006.
- [53] Mitchell E Johnson. Rapid, simple quantitation in thin-layer chromatography using a flatbed scanner. *Journal of Chemical Education*, 77(3):368, 2000.
- [54] Gregory K. Wallace. The jpeg still picture compression standard. *Commun. ACM*, 34(4):30–44, 1991.
- [55] Hiroshi Ijima and Masanori Yamaguchi. Quantification of carbohydrate based on scan image analysis for tlc technique compensating lack of spot overlaps. In *2016 IEEE International Conference on Imaging Systems and Techniques (IST)*, pages 515–519. IEEE, 2016.
- [56] Tinku Acharya. Integrated color interpolation and color space conversion algorithm from 8-bit bayer pattern rgb color space to 12-bit ycrCb color space, 2002. US Patent 6,392,699.
- [57] Dongju Liu and Jian Yu. Otsu method and k-means. In *2009 Ninth International Conference on Hybrid Intelligent Systems*, volume 1, pages 344–349. IEEE, 2009.
- [58] Sunil L Bangare, Amruta Dubal, Pallavi S Bangare, and ST Patil. Reviewing otsu’s method for image thresholding. *International Journal of Applied Engineering Research*, 10(9):21777–21783, 2015.